MIT
SEA
GRANT
PROGRAM

OCEAN ENGINEERING SUMMER LABORATORY 1976

Supervised by
A. Douglas Carmichael
Keatinge Keays
Donald A. Small

Massachusetts Institute of Technology
Cambridge, Massachusetts 02139

Report No. MITSG 77-22
November 1977

OCEAN ENGINEERING SUMMER LABORATORY 1976

Massachusetts Institute of Technology

and

Maine Maritime Academy

Prepared by students under the supervision of:

Professor A. Douglas Carmichael -- M.I.T.

Mr. Keatinge Keays -- M.I.T.

Professor Donald A. Small -- M.M.A.

Report No. MITSG 77-22

Index No. 77-122 Nnt

MASSACHUSETTS INSTITUTE OF TECHNOLOGY
Sea Grant Program

Administrative Statement

The Ocean Engineering Summer Laboratory provides students from the Massachusetts Institute of Technology and from the Maine Maritime Academy with the opportunity to apply theory acquired in the classroom to the actual design, construction, and operation of equipment in the marine environment. This report describes student projects completed during the summer of 1976. The projects included the use of wind and tidal currents to generate small amounts of electrical power, development of a pedal vehicle for scuba divers, construction of the dredge and dredge-handling equipment, a tethered grappling hook for use in the deep ocean, further development of a floating breakwater and the measurement of its efficiency, development of a Hall effect electronic compass for use in a small submersible, a meter for measuring line tensions, development of airlift for use in salvage, and some basic data acquisition on the action of compound catenaries. In addition, two biological projects were undertaken: an eel survey, and a scallop culture experiment.

Dean A. Horn
Director, 1977

Room 1-211 77 Massachusetts Avenue Cambridge, Massachusetts 02139 617, 253 7041

ACKNOWLEDGMENTS

This report describes the results of research done as part of the M.I.T. Sea Grant Program with support in part from the Office of Sea Grant in the National Oceanic and Atmospheric Administration, U.S. Department of Commerce, through grant number 04-6-158-44081, and from the Massachusetts Institute of Technology. The U.S. Government is authorized to produce and distribute reprints for governmental pupooses notwithstanding any copyright notation that may appear hereon.

Funding for the 1976 Ocean Engineering Summer Laboratory was provided by:

- NOAA, Office of National Sea Grant 04-6-158-44081
- Maine Maritime Academy
- Massachusetts Institute of Technology
- Undergraduate Research Opportunities Program, Massachusetts Institute of Technology
- Klapp and Poliak Scholarships, Massachusetts Institute of Technology
- Exxon Educational Foundation
- Dr. Buckminster Fuller, Breakwater Project

RELATED REPORTS

The following reports contain information concerning previous Summer Laboratories and are related to the projects described herein:

Cummings, Damon E. and David B. Wyman, OCEAN ENGINEERING SUMMER LABORATORY, SUMMER 1971, MITSG 72-3, NTIS COM-72-10327. Cambridge: Massachusetts Institute of Technology, October 1971. 191 pp., $4.00.

Keays, Keatinge, et al., HOLBROOK COVE SURVEY: A 1972 STUDENT SUMMER OCEAN ENGINEERING LABORATORY RESEARCH PROJECT. MITSG 72-19, NTIS COM-73-10621. Cambridge: Massachusetts Institute of Technology, December 1972. 88 pp., $3.00

Keays, Keatinge, et al., THE SEARCH FOR "DEFENCE" AND OTHER OCEAN ENGINEERING PROJECTS. MITSG 72-20, NTIS COM-73-10622. Cambridge: Massachusetts Institute of Technology, December 1972. 88 pp., $3.00.

Carmichael, A. Douglas and David B. Wyman. OCEAN ENGINEERING SUMMER LABORATORY, SUMMER 1973, MASSACHUSETTS INSTITUTE OF TECHNOLOGY AND MAINE MARITIME ACADEMY. MITSG 74-12, NTIS COM-74-10963/AS. Cambridge: Massachusetts Institute of Technology, February 1974, 166 pp. $4.00.

Carmichael, A. Douglas and David B. Wyman. OCEAN ENGINEERING SUMMER LABORATORY 1974, MASSACHUSETTS INSTITUTE OF TECHNOLOGY AND MAINE MARITIME ACADEMY. MITSG 75-12.

Carmichael, Douglas and David B. Wyman. OCEAN ENGINEERING SUMMER LABORATORY 1975. MITSG 76-3. Cambridge: MASSACHUSETTS INSTITUTE OF TECHNOLOGY, April 1976. 88 pp., $3.00.

The Sea Grant Information Center maintains an inventory of technical publications. We invite orders and inquiries to:

Sea Grant Information Center
M.I.T. Sea Grant Program
Room 5-331
Massachusetts Institute of Technology
77 Massachusetts Avenue
Cambridge, Massachusetts 02139

LIST OF PARTICIPANTS

- At Castine, Maine -

Massachusetts Institute of Technology

Lawrence E. Demar
Charles W. Jackson
David E. Mayer
Richard K. Mittleman
Keith W. Reid
Joseph H. Rice
Marianne Salomone
Bradley E. Schaefer
Michael H. Tobias
Meredith G. Warshaw

Instructing Staff:

Keatinge Keays
Herman S. Kunz
Arthur Baggeroer
Ira Dyer
Willard F. Searle

Graduate Student Staff:

James Slack

Maine Maritime Academy

Timothy Achorn
Kenneth Biebel
Steven B. Blatchely
Bradley S. Ducharme
Craig Ervin
Kevin Fitzpatrick
Leonard Gross
Edward Gustafson
David M. Jenkinson
Mark Kreider
James Lumsden
Michael Manning
James Molloy
Donald Pierce
Peter Scanlon
Gary M. Smith
Frederick Vogt
Frank M. Young

Instructing Staff:

Donald A. Small
Edgar Biggie
Groves E. Herrick

- At Cambridge, Massachusetts -

Massachusetts Institute of Technology

Edward M. Curtis III
Michael J. Saylor
John S. Kowalik

Instructing Staff:

A. Douglas Carmichael

TABLE OF CONTENTS

	Page
ADMINISTRATIVE STATEMENT	i
ACKNOWLEDGMENTS	ii
RELATED REPORTS	iii
LIST OF PARTICIPANTS	iv
TABLE OF CONTENTS	v
SUMMARY	vi
1.0 Introduction	1
2.0 Ocean Engineering Projects	2
2.1 Undercycle II	3
2.2 Buoy-Mounted, Electrical Generators	15
2.2.1 A Simple, Low-Cost, Windmill Generator	16
2.2.2 Tidal Current Electrical Generator Using a Savonius Rotor	25
2.3 A Controllable Grappling Hook	46
2.4 An Oceanographic Sampler Dredge Installation	54
2.4.1 Oceanographic Sampler Dredge	55
2.4.2 Sampler Dredge Handling Equipment	65
2.5 Construction and Test of a Portable Floating Breakwater	74
2.5.1 The Portable Floating Breakwater	75
2.5.2 The Efficiency of a Portable Breakwater	80
2.6 Hall Effect Electronic Compass for the Robot Submarine	89
2.7 Line Tension Meter	98
2.8 Mooring Research Project	108
2.9 Airlift Bags	122
3.0 Ocean Science Projects	126
3.1 An Eel Survey of the Bagaduce River	127
3.2 The Feasibility of Commercially Growing Deep Sea Scallops	134

SUMMARY

The 1976 Ocean Engineering Summer Laboratory is the sixth in a series of undergraduate laboratories that was initiated in 1971. The laboratory is intended to provide undergraduates with an opportunity to undertake a meaningful project in an ocean environment. The descriptions of the student projects are contained in this report, and they are fourteen in number. The undercycle, buoy-mounted windmill, and floating breakwater are continuations of projects initiated in earlier summer laboratories.

A listing of the projects, the student participants, and a brief summary is included in the table below.

Proj. No.	Proj. Title	Participants	Summary
2.1	Undercycle II	E. Curtis III	Development and testing of a pedal vehicle for scuba divers which was originally designed and built in 1975.
2.2.1	Simple, Low-Cost, Windmill Generator	S. Blatchely D. Jenkinson F. Young	A small electrical generating windmill was designed and constructed.
2.2.2	Tidal Current Electrical Generator Using a Savonius Rotor		A small generating device using a Savonius rotor driven by the tidal currents was designed and constructed and limited testing was accomplished.
2.3	A Controllable Grappling Hook	J. Kowalik	A controllable tethered grappling hook to recover a lost camera in the deep ocean was designed and constructed.
2.4.1	Oceanographic Sampler Dredge	K. Fitzpatrick M. Kreider M. Manning P. Scanlon	A heavy-duty shallow water oceanographic bottom sampler dredge was designed, constructed and tested.
2.4.2	Sampler Dredge Handling Equipment	D. Mayer M. Tobias	An Australian "Rocket-Launcher Scallop Tipper" was designed and built for use with the oceanographic sampler dredge.
2.5.1	The Portable Floating Breakwater	K. Biebel	The floating breakwater constructed and modified in previous summer laboratories was modified, reassembled, and deployed.

Proj. No.	Proj. Title	Participants	Summary
2.5.2	Efficiency of a Portable Breakwater	B. Schaefer	The efficiency of the portable breakwater was measured, utilizing spar buoys and a movie camera.
2.6	Hall Effect Electronic Compass for the Robot Submarine	M. Saylor	A compass utilizing the "Hall effect" was designed, constructed, and tested. It is intended for use in a small submersible constructed in earlier ocean engineering summer laboratories.
2.7	Line Tension Meter	C. Ervin J. Lumsden	A meter for measuring the tension in manila or synthetic lines was designed and built.
2.8	Mooring Research Project	R. Mittleman K. Reid J. Rice	A conventional mooring leg consisting of a compound catenary and spring buoy was deployed and data were obtained.
2.9	Airlift Bags	T. Achorn E. Gustafson	Airlift bags for use in salvage were designed and assembled and subjected to a limited amount of testing.
3.1	An Eel Survey of Bagaduce River	B. Ducharme G. Smith F. Vogt	An experimental study of the eel population in the Bagaduce River was attempted.
3.2	Feasibility of Commercially Growing Deep Sea Scallops	L. Gross D. Pierce	An experimental and economic study of the feasibility of growing and marketing deep sea scallops was accomplished.

1.0 INTRODUCTION

The Ocean Engineering Summer Laboratory provides undergraduate students with an opportunity to design and build equipment for use in an ocean environment and then to test the devices in that environment. For the most part, the students have had relatively little experience in engineering design and are afforded a period of about four weeks in which to select, design, and construct their device. The finishing touches and the peripheral arrangements, for example, devising the mooring, as well as the testing consume a second four-week period. This pattern is true for those students who conducted their tests in Castine, Maine. Those involved in the testing in the Cambridge, Massachusetts, area were more advanced students and had longer periods in which to design and construct their devices.

Due to the relative inexperience of the students and the time and other constraints, the equipment does not always operate successfully. The modest successes which are achieved are an adequate reward, although the occasional "Eureka" response is that which causes the instructors to return year after year.

In addition to the projects, a series of evening lectures including motion pictures featuring ocean engineering topics was conducted. Many of the students participated in a scuba diving class and qualified for NAUI certificates.

Professor Ira Dyer conducted a lecture and demonstration on the principles of underwater acoustics and Professor Arthur Baggeroer introduced the students to the theory and practice of seismic profiling.

Although these activities are not reflected in the subsequent pages of this report, they were an integral part of the experience designed to introduce aspiring ocean engineers to the environment that will dictate the details of their solutions.

2.0 OCEAN ENGINEERING PROJECTS

2.1 UNDERCYCLE II

At present, underwater transportation for the scuba diver is limited to swimming with the use of rubber fins, or the use of electrically-powered propulsion units. Another alternative, analogous to a bicycle used for land transportation, would be a man-powered vehicle for underwater use. Such a vehicle would be of value if it increased the diver's range of operation and speed, while providing an acceptable level of maneuverability. In addition, it might also offer the diver a capability for carrying gear and/or a payload of some kind.

A vehicle of this sort, Undercycle I, was designed, built, and tested for the 1975 Summer Laboratory. The development and testing of the vehicle was continued during the 1976 Summer Laboratory in order to improve Undercycle I's structural reliability and maneuvering characteristics. The modified vehicle was renamed Undercycle II.

Background

Undercycle I was a pedaled vehicle, consisting of a rectangular frame approximately 7 feet long and 2 feet wide, constructed from 1-1/2 inch (inside diameter) PVC pipe and pipe fittings, a gearbox and propeller mounted aft, and two individually operated forward diving planes which serve as control surfaces (see Figure 2.1.1). The diver lies prone on a 12-inch diameter plywood disk mounted at waist level on the frame and "flies" the vehicle by pedaling and manipulating the diving planes. Turns are accomplished by rolling in much the same manner as an airplane. Because of the difficulty expected in underwater pedaling, especially for a diver encumbered with a wet suit, the gear ratio and propeller characteristics were chosen to allow a slower pedaling cadence than that of a cyclist on land. The resulting design used a large (18-inch diameter) three-bladed propeller and a 4:1 gear ratio, giving an ideal propeller speed of 155 rpm for a diver developing one-tenth horsepower.

Testing a Undercycle I revealed problems associated with the structural reliability of the vehicle, the use of a sealed gearbox, and a lack of stability which led to difficulties in maneuvering. The structural problems, which were the result of higher-than-expected forces and torques developed during pedaling, included shearing of various connections and excessive twisting of the gearbox about its attachment to the vehicle frame. The problem with the sealed gearbox was avoided by allowing it to flood, while sacrificing a significant amount of buoyancy and increasing the rate of corrosion of the gears. The lack of stability resulted from the torque developed by the large propeller operating at low rpm, causing the entire craft to roll. While the roll could be corrected by use of the control surfaces, this greatly reduced the range of vehicle maneuverability. One solution was proposed to this problem: the

THE UNDERCYCLE

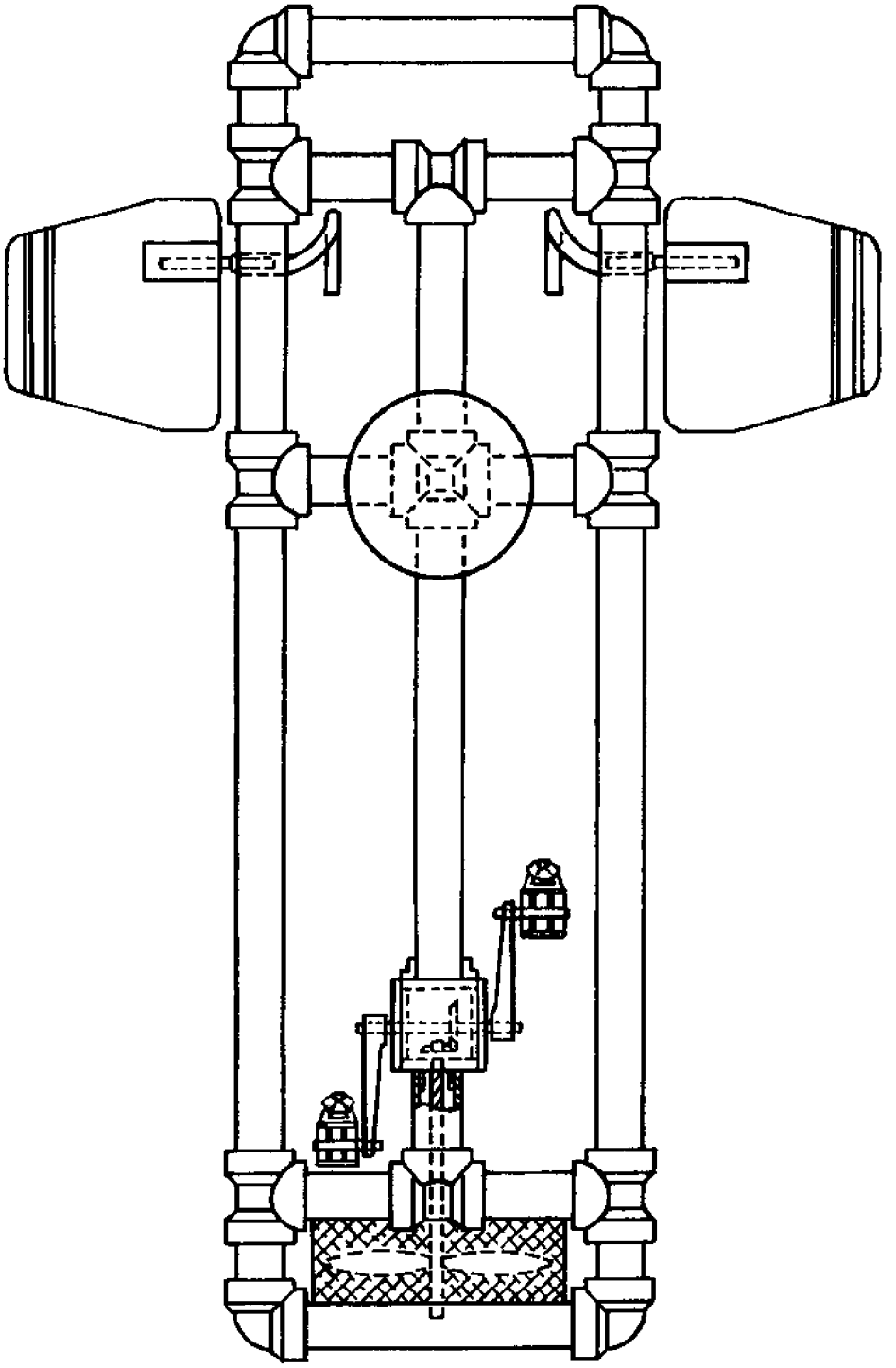

FIGURE 2.1.1

addition of a weight keel of perhaps 20 pounds attached amidships below the diver.

It was therefore proposed to continue to develop the Undercycle concept by correcting the above-mentioned problems. Three phases of work were planned: construction and testing of a model of Undercycle I in order to gain a better understanding of the rolling characteristic and test solutions for eliminating it; structural analysis of components in which critical torques, bending and shearing forces were expected to develop so that modifications might be designed; and application of the results to the actual vehicle followed by testing.

Model Testing

A small rubber-band-powered model of Undercycle I was constructed on a scale of 1:9, based on the ratio of the diameter of a conveniently-sized propeller to the diameter of Undercycle I's propeller. A similarly scaled model figure was strapped to the model to simulate a diver wearing scuba gear. For the first series of tests the control surfaces of the model were fixed in the neutral position. The model was ballasted to match Undercycle I as closely as possible, and tested in a tank 7 feet long, 3 feet wide, and 2 feet deep.

With the control surfaces fixed, the model exhibited the same tendency to roll experienced in the tests of Undercycle I. Counterclockwise rotation of the propeller produced a clockwise rotation of the model. This tendency was exaggerated in the model due to the higher speed of propeller rotation produced by the rubber band motor.

Two solutions to this rolling characteristic were tested with the model. The first used a weight of lead shot attached to the bottom of the propeller shroud with a compensating amount of buoyant material attached to the top of the shroud. This configuration was expected to move the model's center of gravity below its center of rotation so that a restoring moment would be developed when the model began to roll. The proper amount of weight required to eliminate roll was determined by trial and error. Use of the weight resulted in stable test runs with the model tipped at an angle of approximately 15°. Attachment of the weight and buoyant material on an axis approximately 15° from the vertical resulted in stable runs with the model on an even keel, though at rest it was tipped approximately 15°.

The second solution used a keel attached below the center of gravity and a compensating amount of buoyant material attached to the frame directly above the keel. The results achieved were similar to those found using the first solution.

Additional tests were then run with the control surfaces fixed in a variety of positions, in order to determine the maneuvering characteristics of the model. The tests were run

with no correction for roll, as well as with each of the two compensating devices attached. It was found that, due to the tendency of the model to roll in the clockwise direction, turns to the right were easier to accomplish than turns to the left, but often resulted in overturning if too much angle was applied to the control surface. After some modification of the model, it was also found that, if the control surfaces were independently manipulated in two axes of rotation, slightly improved maneuvering characteristics could be achieved.

The second series of tests yielded somewhat limited results because any chosen configuration of the control surfaces remained fixed for the entire test run. Continuous independent manipulation of the control surfaces during the maneuver would have allowed better simulation of the maneuvering characteristics of the Undercycle. However, the tests did show that correction of the roll characteristic would significantly increase the Undercycle's maneuverability.

Structural Analysis

Structural analysis of various components of the Undercycle was undertaken using the same design criteria as the original design with the exception that a less conservative value of 0.6 horsepower was used for evaluation of the forces and torques developed by pedaling. The first components examined were the crankshaft and propeller shaft. The applied torque on these shafts was evaluated using the 0.6 horsepower value and a crank rpm of 40; the applied torque was found to be 945 lbf in. Since the bicycle cranks used on the Undercycle provide a lever arm of 6-1/2 inches, 945 lbf in of torque is equivalent to a 150 lbf applied by the diver to the pedals. It was assumed that this force varies sinusoidally with an average value of 150 lbf. The maximum expected force for design purposes would therefore be 235 lbf.

The maximum expected shearing stress in twist on these shafts was calculated to be 31,865 psi for the crankshaft and 62,236 psi for the propeller shaft. For the brass crankshaft used in the Undercycle I gearbox, this shear stress exceeded the proportional limit of 20,000 psi. This indicated that a higher strength, i.e., steel, crankshaft should be used. For the propeller shaft, the shearing stress exceeded the proportional limit for a mild steel like the drill rod used in Undercycle I, so substitution of a higher strength material was also indicated for this component.

In addition, the bending stresses developed in the crankshaft were studied. With a design force of 235 lbf applied to the pedals, the force on the 4-inch diameter bevel gear was found to be 764 lbf. For the 5-1/2-inch crankshaft used in Undercycle I, supported by bearings 2 inches on either side of the centrally located bevel gear, the maximum expected bending moment was found to be 764 in. lbf. The maximum bending stress was found to be 31,875 psi, almost identical to the maximum expected shearing stress.

The problem of the gearbox twisting about its attachment to the vehicle frame was also examined. For Undercycle I, the gearbox was rigidly attached only to the forward frame member which is 30 inches in length. Since the angle of twist of a thin-walled tube is directly proportional to the length of the tube, this angle could be reduced to less than 1/3 of the Undercycle I value if the gearbox was rigidly attached to both the 30-inch forward frame member and the 10-inch aft frame member. The contribution of the transverse frame members to which the fore and aft frame members are attached to the gearbox twist through bending of the transverse members was found to be about 40 times larger than that required to twist the fore and aft longitudinal members. It was concluded that anchoring the gearbox to both the fore and aft frame members would provide adequate resistance to twisting.

Design and Construction Modifications

The Gearbox

In order to minimize corrosion of the crankshaft and gears, and to provide additional buoyancy, it was decided to construct a sealed gearbox. A section of 4-1/2-inch I.D. aluminum pipe was chosen for the housing with endcaps to be machined from 5/8-inch aluminum plate. This thickness was required to allow seating for teflon crankshaft bearings and rubber O-rings, which were designed to provide static seals at the endcaps and rotary seals around the crankshaft and propeller shaft. Dimensions of the gearbox were controlled by the size of the bevel and pinion gears.

Since the structural analysis of the brass crankshaft used in Undercycle I had shown it to be weak in both shear and bending, an attempt was made to use a bicycle crankshaft, machined to accept the bevel gear, O-ring seals, and teflon bearings. However, bicycle crankshafts are manufactured of hardened steel, and could not be machined with the facilities available to the laboratory. A crankshaft of slightly longer dimensions than the bicycle crankshaft, made of mild steel, was then designed and machined for the Undercycle II gearbox.

In order to correct one more possible source of mechanical failure in the gearbox, a support was designed to fix the pinion gear in position against motions which might result from the thrust developed by the propeller (Figure 2.1.2). The support consisted of a section of 1-1/2-inch aluminum rod passing through the gearbox along the axis of the propeller shaft. The ends of the rod protruded 1-1/2 inches aft and 1 inch forward of the gearbox housing. Welds were to be made around both these protrusions through the gearbox housing. The rod was designed in one piece, machined to allow clearance for the bevel gear and crankshaft and to enclose the pinion gear on three sides. At the same time, the end of the propeller shaft to which the pinion gear is attached would be fixed in position relative to the bevel gear by means of flanged teflon bearings in the sup-

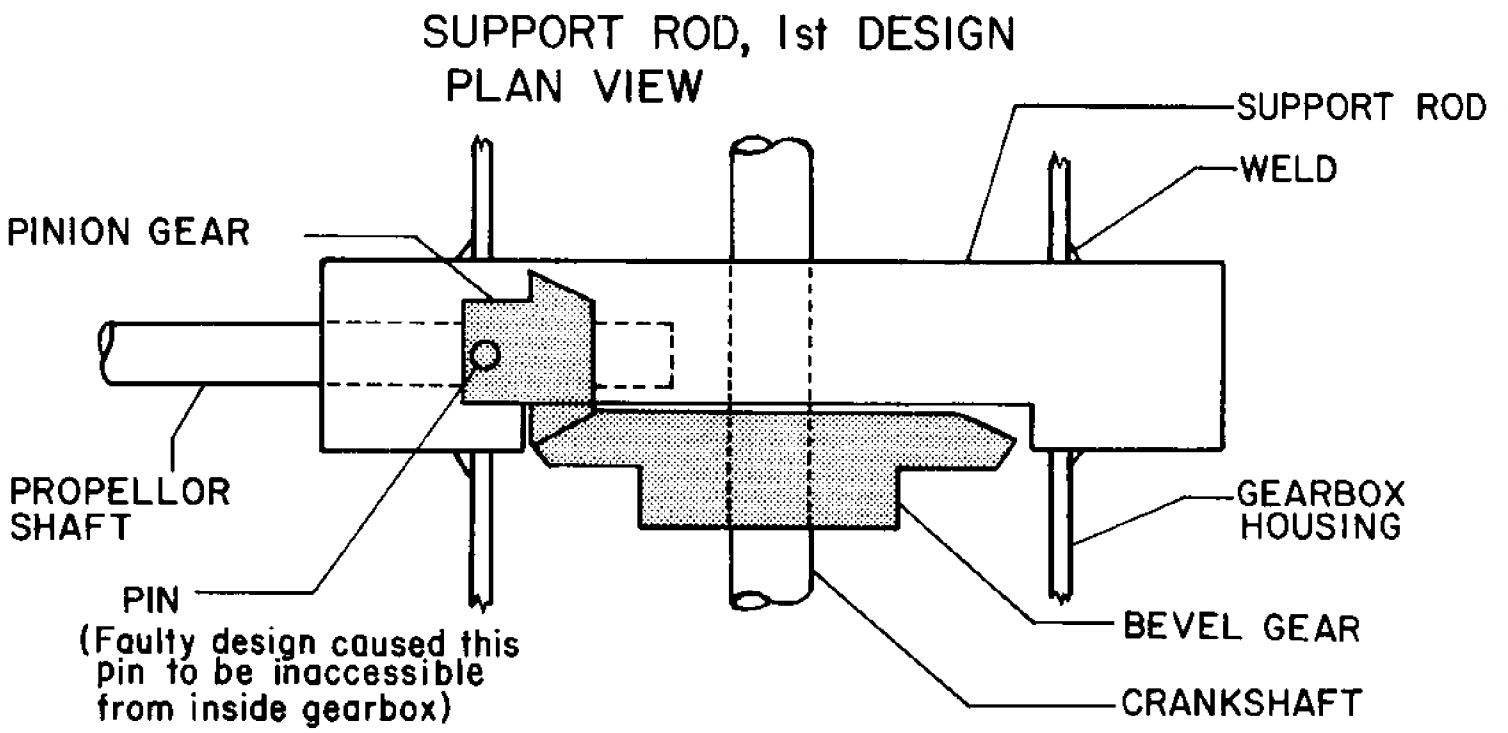

FIGURE 2

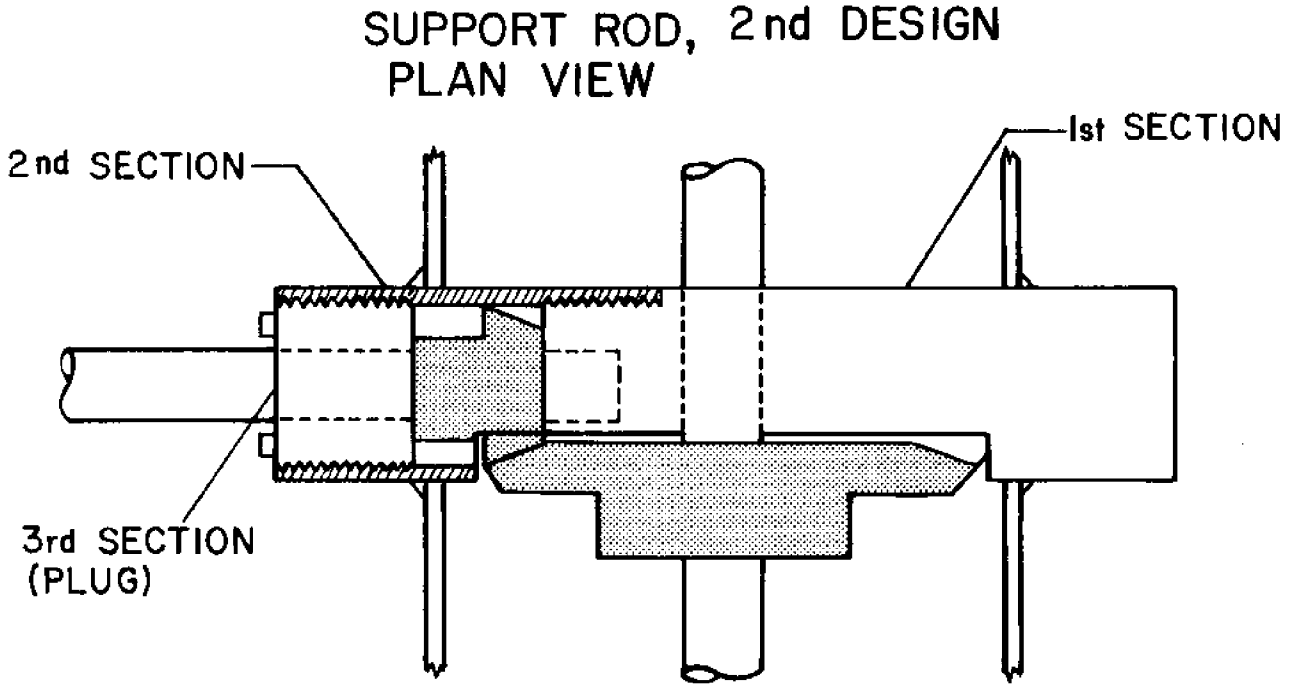

FIGURE 2.1.2

port rod. Clearance would be left to allow removal of the pinion gear from the inside of the gearbox for lubrication and maintenance purposes.

When the various components of the gearbox were assembled, it was found that the dimensions of the gearbox housing did not allow the direct access to the pinion gear which had been assumed in the first design. To correct this error, the support rod was redesigned in three threaded sections (Figure 2.1.2). One of the sections was salvaged from the forward part of the first rod and a second was machined to thread into it, making up a rod of the same length as the original design. This assembly was then welded to the gearbox housing. Access to the pinion gear was allowed through the hollow aft end of the second section. The third section of the rod was a plug which threaded into the second section, trapping the pinion gear and propeller shaft between two flanged teflon bearings.

The addition of the support rod to the gearbox also allowed rigid attachment of the gearbox to the frame both fore and aft where the protruding portions of the rod fit into the PVC frame members. A 1/4-inch bolt passing through the joint was used for the forward connection, while four machine screws were used for the aft connection since the propeller shaft prevented use of a bolt.

One further problem was encountered in construction of the gearbox. The welding of the support rod sections to the gearbox housing resulted in distortion of the shape of the housing. Although the distortion was small, it prevented the proper fitting of the endcaps to the housing. This was corrected as much as possible by brute force bending of the housing back to its original shape, but did not result in a perfect fit for the endcaps.

Control Surfaces

As a result of the model tests, the attachment of the control surfaces to the vehicle frame was also modified to allow rotation about two axes (Figure 2.1.3). For each control surface, a PVC "T" joint was machined to allow the 1-1/2-inch PVC tubing of the frame to pass freely through it. The joint was fixed in place at the point of attachment of the control surface, but allowed to rotate about the axis of the frame member. The short shaft connecting the control surface to the handgrip was passed through the lower part of the "T", leaving the control surface free to rotate about two orthogonal axes. As in the model tests, it was hoped that this modification would result in a greater range of maneuverability.

Other Modifications

Additional modifications to Undercycle I included substitution of 1/4-inch bolts for cotter pins at all frame connections not glued together. This allowed easier assembly and

"T" JOINT ROTATIONAL AXES

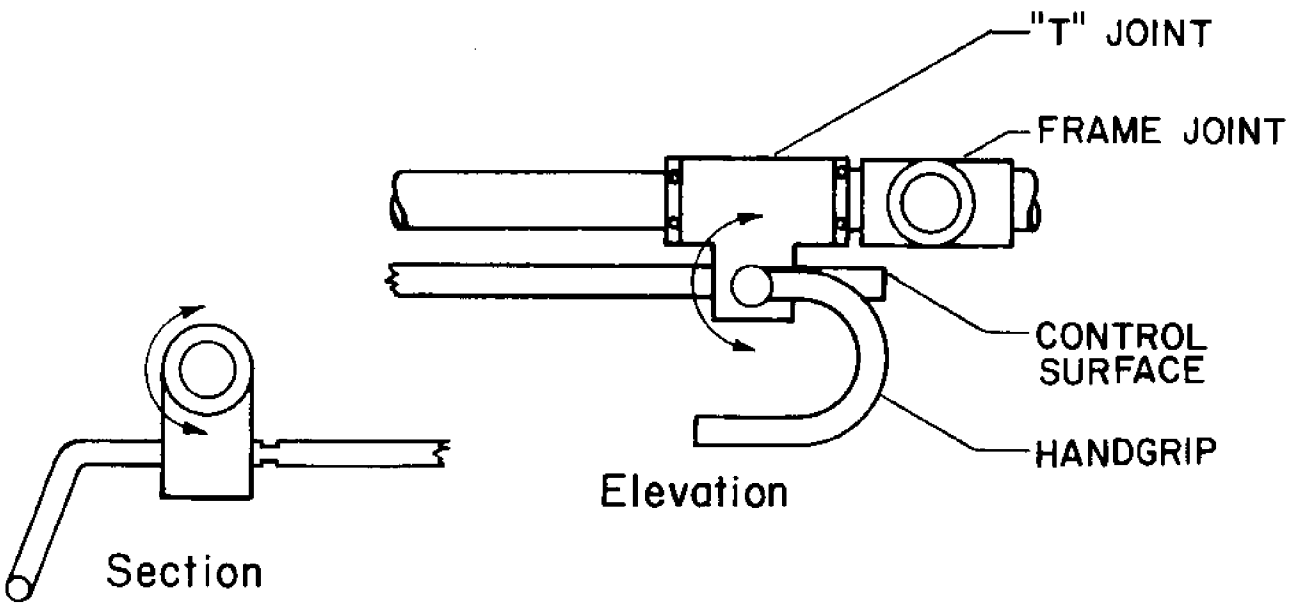

FIGURE 2.1.3

disassembly of the vehicle for transportation purposes. A 1/2-inch stainless steel propeller shaft was substituted for the 1/2-inch drill rod which had been severely corroded during testing in seawater. A 1/4-inch bolt and a 1/8-inch steel pin were substituted for the cotter pin and aluminum pin used to attach the bevel and pinion gears to their shafts.

The Testing Program

Buoyancy and Initial Testing

The first tests of Undercycle II were conducted in a swimming pool to find the proper amount of buoyancy necessary to hold the vehicle slightly positively buoyant. Most of the frame tubes were filled with a rigid styrofoam and additional styrofoam was added at the rear of the vehicle to achieve the proper trim.

Test runs were then made with the diver using mask and snorkel. The control surfaces were allowed to rotate about two axes for the first tests. Once the diver became accustomed to operating the vehicle, it was decided to limit the control surfaces to their more conventional single axis of rotation because they tended to "flop" uncontrollably, making it even more difficult to maneuver.

The first series of tests showed an improvement in structural reliability over Undercycle I. No problems were encountered with joint connections or gearbox components during these or any of the subsequent tests. A small amount of leakage occurred in the gearbox, due primarily to the imperfect fit of the endcaps. As the O-rings of the rotary seals became worn in later tests, they also contributed to this leakage. This occurred after about 10 hours of testing.

The first of the tests also bore out the results of the early model tests; Undercycle II was difficult to steer along a straight line without use of the control surfaces to correct for the propeller torque. It was also found to be impossible to turn the vehicle within the confines of the pool without overturning.

Addition of Keel

It was decided to try the keel solution tested with the model to improve the vehicle maneuvering characteristics. One advantage of the keel over the addition of weight to the propeller shroud was the added point of support it would provide when the vehicle was out of the water. The keel was constructed of 3 sections of one-inch O.D. PVC pipe projecting 13 inches below the frame. Thin pieces of sheet lead were wrapped around the horizontal tube (Figure 2.1.4). The proper weight of lead required was determined by trial and error test runs in the pool.

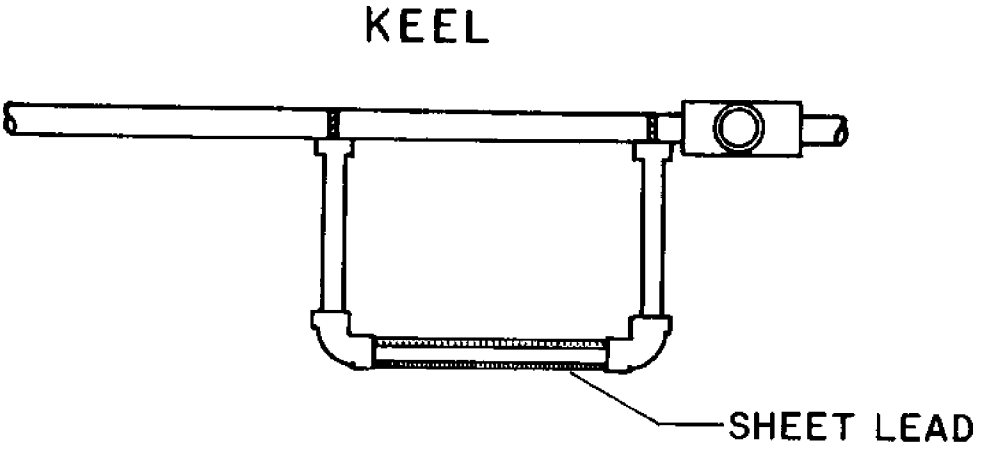

FIGURE 2.1.4.

When the proper weight was applied, Undercycle II was found to handle with greatly improved maneuvering characteristics. Turns with a radius of approximately 20 feet were achieved by first opposing the control surfaces to turn the vehicle on its side, then angling both surfaces in the direction of the turn, and opposing them again when the turn was completed. Without the addition of the weighted keel, Undercycle II would not have been stable on its side, and would have overturned.

Application of Dihedral to Control Surfaces

A series of tests were then run with the control surfaces set at approximately 15° of dihedral, which was achieved by rotating the "T" joints to the proper angle and fixing them with cotter pins. This modification allowed some improvement in climbing and diving characteristics, but the turning characteristics were impaired. It was found to be much harder to turn the vehicle on its side because at this amount of dihedral the control surfaces acted like rudders as well as diving planes, which decreased their efficiency when the control surfaces were opposed for a turn. The angle of dihedral was then decreased to about 5° for the next series of tests.

Testing with Scuba Gear

A day of final testing of Undercycle II was conducted at Lake Cochituate with a diver wearing scuba gear. Preparation for the tests included the change in control surface dihedral and replacement of worn O-rings on all seals with new O-rings.

The only conclusive result of these tests was a new problem with vehicle stability. The same tendency to overturn when turns were attempted was experienced as had occurred with no keel attached. It was concluded that the additional weight of the scuba tank above the diver changed the center of gravity of the vehicle enough that the weight of the keel no longer provided an adequate restoring moment.

The lack of visibility in Lake Cochituate was also found to be a significant problem in these tests. The murkiness of the water caused the diver to lose his orientation almost immediately so that it was impossible to accurately judge the performance of the vehicle in terms of speed or maneuvering characteristics.

Conclusions and Recommendations

The maneuvering characteristics achieved in the pool with the diver using mask and snorkel were judged to be acceptable for a vehicle of this type. Adjustment of the weight of the keel should allow this same amount of maneuverability for a diver using scuba gear. While this level of maneuverability is limited compared to that of a diver swimming with fins, it would be adequate to perform the function of underwater point-to-point transportation.

The other criteria for vehicle acceptability included in the introduction were not as thoroughly evaluated in the testing program as vehicle maneuverability. Use of mask and snorkel was found to be excessively tiring for the diver so that the range allowed by Undercycle II could not be reliably determined. The straight-line speed was judged comparable to the speed of a swimming diver for an equal exertion of energy. However, the 4:1 gear ratio did not allow a great deal of variation in pedaling speed. Further testing of Undercycle II should include trials with alternative gear ratios.

Another limitation of Undercycle II is the loss of buoyancy caused by compression of the styrofoam when the vehicle is used at any significant depth. Some modification allowing control of buoyancy by the diver or by an automatic sensing device would be necessary if Undercycle II is to be used to aid a diver in performing any useful tasks underwater.

2.2 BUOY-MOUNTED, ELECTRICAL GENERATORS

2.2.1 A SIMPLE, LOW-COST WINDMILL GENERATOR

The purpose of this project is to demonstrate that a windmill can be constructed and used to power an electrical device. Many buoys located in this country's waterways use small batteries and diesel-powered chargers to power their lights, horns, etc. The diesel power plants must be periodically supplied with fuel as well as maintenance. A small wind generator could replace the high-maintenance diesel-charging system, thereby potentially reducing the cost and complexity of the buoy systems while eliminating the need for fuel.

Background

In the 1975 MMA/MIT summer laboratory, a light-construction, low-cost windmill was built to drive a small alternator. While it proved to be somewhat of a success, it was damaged beyond repair before its performance characteristics could be measured. In the 1976 MMA/MIT laboratory another more sturdily built windmill was constructed in order to obtain necessary data concerning the windmill's efficiency and torque characteristics. The design of the windmill was basically that of its predecessor, the most noticeable changes being increased ruggedness of both blades and rotor supports. Since the failure of the 1975 windmill lay in the failure of a blade guy wire, it was decided that improvements could be made by increasing the gauge of the metal used for blades and employing a more fatigue-resistant type of stainless steel wire.

It was also hoped that the efficiency of the windmill could be improved by changing the aerodynamic characteristics of the rotor. The 1975 rotor was designed with the blades mounted in the hub at a 45-degree angle to the rotor axis and an angle of 75 degrees at the tips of the blades. The 1976 windmill was first constructed with these same angles and tested. A new rotor was then designed and built with a 30-degree angle at the hub and a 75-degree angle at the blade tips. By observing a better performance and a higher RPM, it was determined that the efficiency of the latter design exceeded that of the former.

Construction of the Windmill and Support Structure

The first phase of construction was the flotation structure for the windmill. In the 1975 windmill design a small plastic, foam and wood raft was used to support the windmill. This year a small fiberglass boat was used, resulting in improved capability for recording data from the windmill while aboard. The boat (see Figures 2.2.1.1 and 2.2.1.2) is of fiberglass construction, 11'4" long and five feet wide with a fiberglass cover enclosing the inner sections. On the after section of the boat two triangular, vertical fins of 1/2" plywood and 15 square feet in area were erected. These vanes were sufficient to keep the boat pointed into winds of five knots and above, even in a three-knot tidal current.

BLADE ANGLES RELATIVE TO WINDMILL SHAFT:
45° TIP
75° ROOT

SCALE 1" = 1'

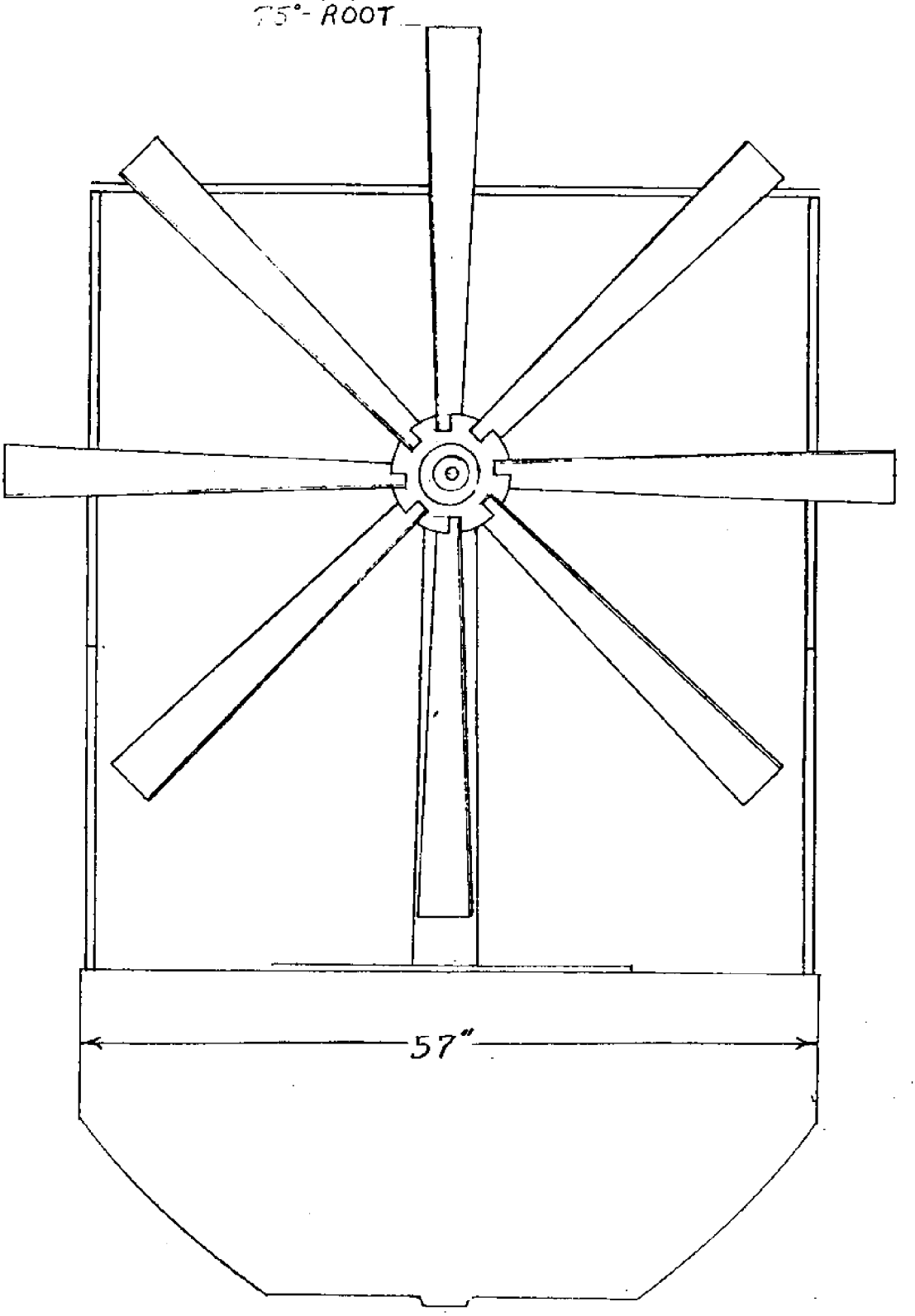

MID-SECTION FRONT VIEW

Figure 2.2.1.1

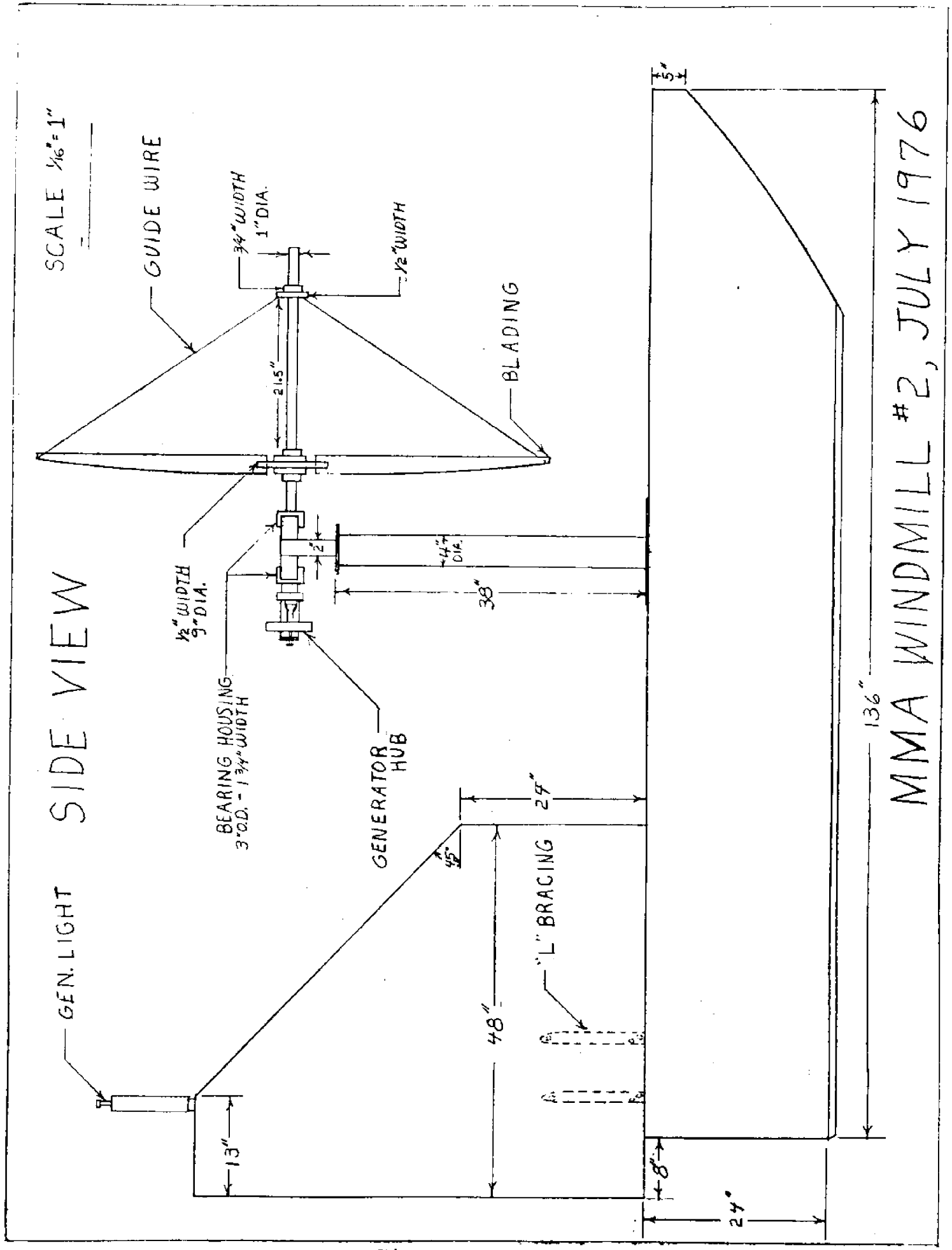
MMA WINDMILL #2, JULY 1976
SCALE 1/16" = 1"
SIDE VIEW
GUIDE WIRE
BLADING
GEN. LIGHT
BEARING HOUSING
3" O.D. - 1 3/4" WIDTH
GENERATOR HUB
"L" BRACING
3/4" WIDTH
1" DIA.
1/2" WIDTH
1/2" WIDTH
9" DIA.
21.5"
2"
4 1/2" DIA.
38"
29"
45°
48"
13"
136"
5"
8"
24"

Figure 2.2.1.2

A complete diagram and dimensions of the fins are given in Figure 2.2.1.2. A small light, powered by a generator attached to the windmill, was connected between the two vanes and supported by a 1-1/2"-wide piece of wood.

The main support of the windmill was a 4"-diameter, 3'4"-length of pipe connected to a 18" by 13" steel plate at the base. The upper part of the pipe contained an 8" by 6" plate to support the bearing housings. The basic difference between the construction of the 1975 and 1976 supporting structures was that the latter was of increased weight and of more rigid construction.

In designing the eight windmill blades, it was decided to use the same type of blade design incorporated in the 1975 windmill utilizing a heavier gauge of metal. Eight galvanized sheet steel blades were used. The blades were of a 0.032" thickness, 30" in length and were bent at the leading edges, increasing their thickness and thus their aerodynamic capabilities, giving a constant chord of 3-3/4". The blades were then bent 1" from this leading edge to incorporate a small camber that ran the entire length of the blade. It was found that by using a pipe longer than each blade secured to the working vise, each blade could be easily cambered by simply bending it around the pipe.

Each blade was bolted to a 9"-diameter, 3/4" plywood hub. The hub contained 8 mounting cuts to hold the 8 windmill blades. These cuts were angled to fixed blade geometric angles at 45 degrees to the rotor axis at the hub and 75 degrees at the blade tips. The tip angles were controlled by guy wires as well as by the cuts on the hub.

The 9" hub was then fastened to two 4" plastic PVC flanges. A 1" diameter hole was centered in the hub to accommodate an aluminum shaft. The PVC flanges were then secured to the aluminum shaft by drilling the flange and the aluminum shaft to incorporate a 1/4" bolt. In any future design, aluminum flanges should be constructed to achieve a much more precise fit to the plywood hub and the aluminum drive-shaft. The entire aluminum shaft was supported by a bearing housing with tandem sleeves.

The bearing housings were machined from 3"-diameter soft steel, round stock. Using a boring bar, the sleeve was bored out to an inside diameter of 2-3/8". Upon completion of the bearing housings using a pair of set screws for each bearing. It was found that this method of securing bearings was inadequate. In future designs the bearings should be pressed into the housings after the housings have been welded to their supporting brackets. Additional brackets were used to house the Sturmey-Archer bicycle "Dynohub" that was used as a load. Figure 2.2.1.2 shows the overall structural layout of the system.

The rotor blades were supported by 0.054"-diameter guy wires that ran from the tip of each blade to a 4"-inch PVC flange located on the aluminum shaft 2-1/2" in front of the wooden

hub. By varying tension on these wires via turnbuckles, both the coning of the rotor and the tip angles of the individual blades could be controlled. For the construction of the guy wires only four turnbuckles were used to angle the eight blades. This method of using one turnbuckle for each pair of blades proved inadequate. In the final construction eight turnbuckles were used to improve the adjusting characteristics of the windmill blades. It was found that using the eight guy wires led to a satisfactorily precise control of tip angle. In future designs some sort of measuring apparatus might be constructed so that the exact twist can be achieved for each windmill blade.

The second phase of the project was to test the windmill. Upon completion of construction, the apparatus was towed to a point approximately 100 yards astern of the Training Vessel and anchored, utilizing a 3-point mooring system and a 300-lb anchor. A four-man team was needed to obtain the data--one man transmitting windspeeds from a shoreside anemometer, one man recording them aboard the launch, and two aboard the float, one measuring RPMs and the other torque readings. For the RPM readings a tachometer which read directly from the spinning shaft was used. For the torque a Prony brake was employed. At given times the windspeed, torque and RPMs were recorded and thus data were obtained from which the calculations for efficiency and tip speed ratio could be made. Having measured the torque and RPMs at zero load and at various loads in 8- to 15-knot winds, it was calculated that for a combination of four sets of figures that the efficiency for the windmill was about 57 percent, and the blade speed tip ratio was approximately 2.

The efficiency of the windmill and its bearings was computed to be approximately 57 percent at optimum load and a windspeed of 12-1/2 MPH. This efficiency is computed as a percentage of the maximum power available to a windmill; thus a 100 percent efficient windmill would still utilize only 16/27 of the kinetic energy contained in the wind.

Efficiency was calculated as:

$$\eta = \frac{\text{useful power output}}{\text{total power available}} = \frac{\tau(n)\ 2\pi/60}{0.364\ V^3 A}$$

where

τ = torque (Newton-meters)

n = RPM

V = airspeed (meters/sec)

A = rotor disc area (meters^2)

The 57 percent efficiency implies that the windmill was extracting approximately (57)(16/27) = 34 percent of the total kinetic energy in the wind.

ROTOR RPM VS INCIDENT WIND SPEED

(No load)

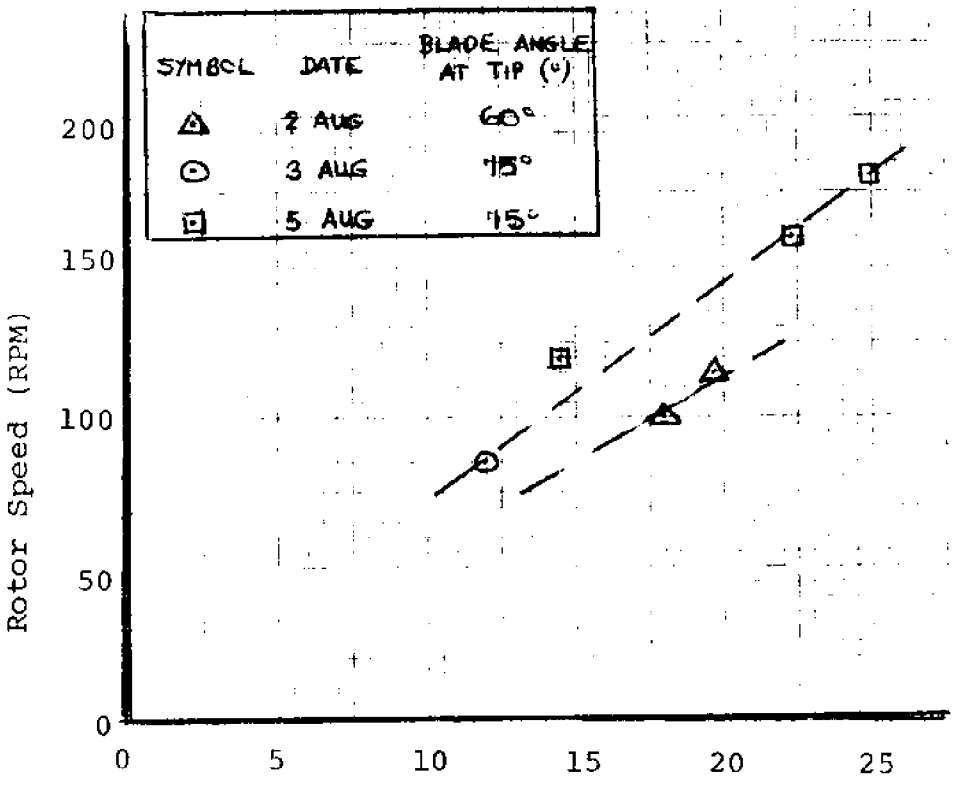

ROTOR MECHANICAL OUTPUT VS ROTOR TORQUE

(Varying RPM)

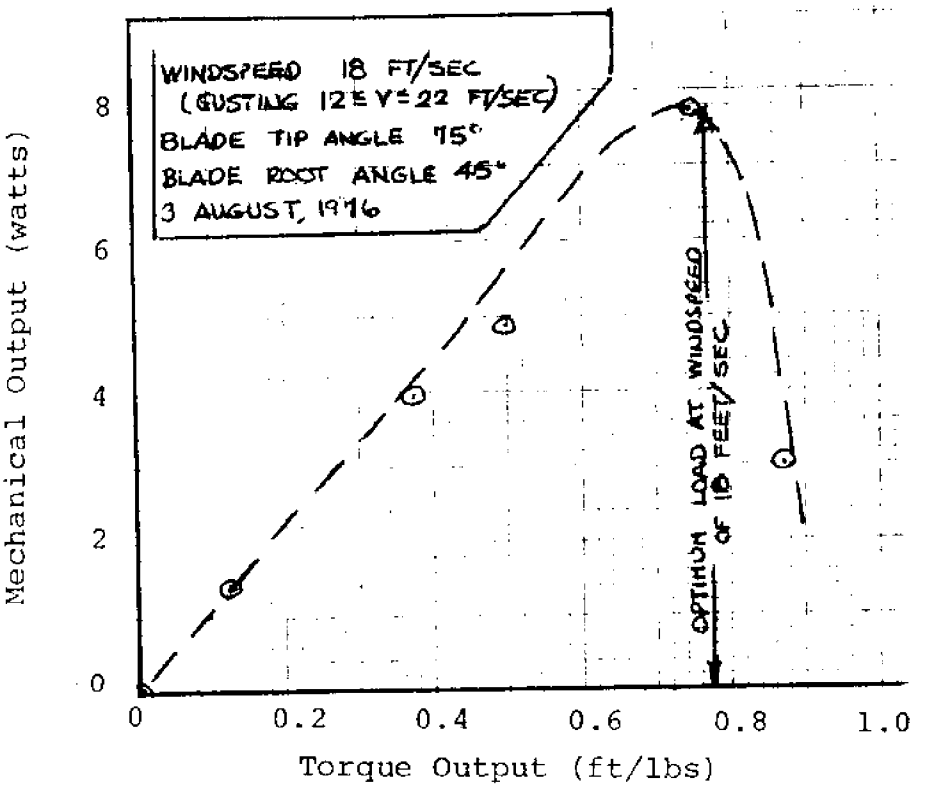

FIGURE 2.2.1.3

TIP SPEED RATIO VS INCIDENT WIND SPEED

MMA Windmill #2 - No Load

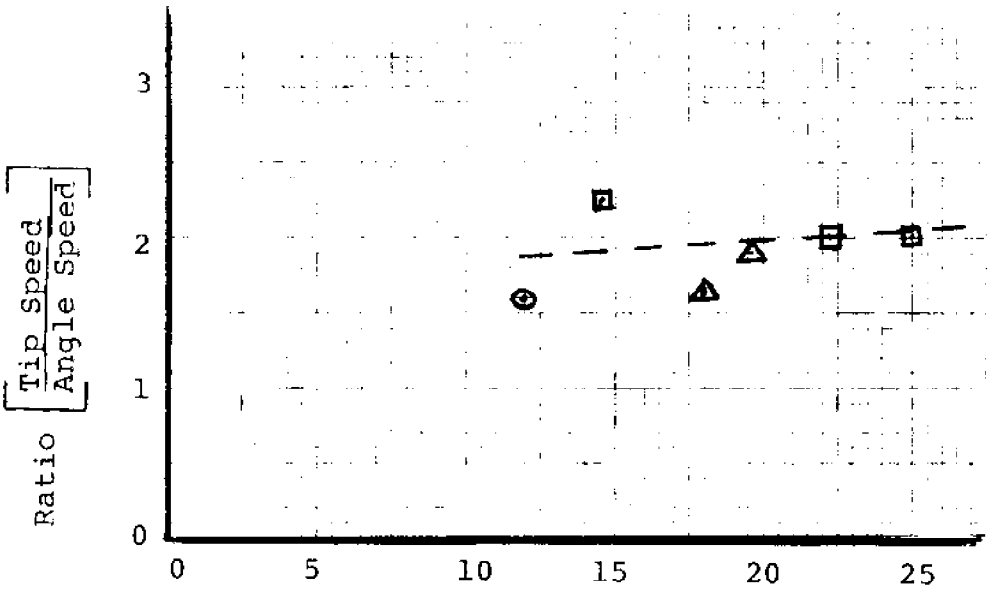

ROTOR TIP SPEED VS INCIDENT WIND SPEED

MMA Windmill #2 - No Load

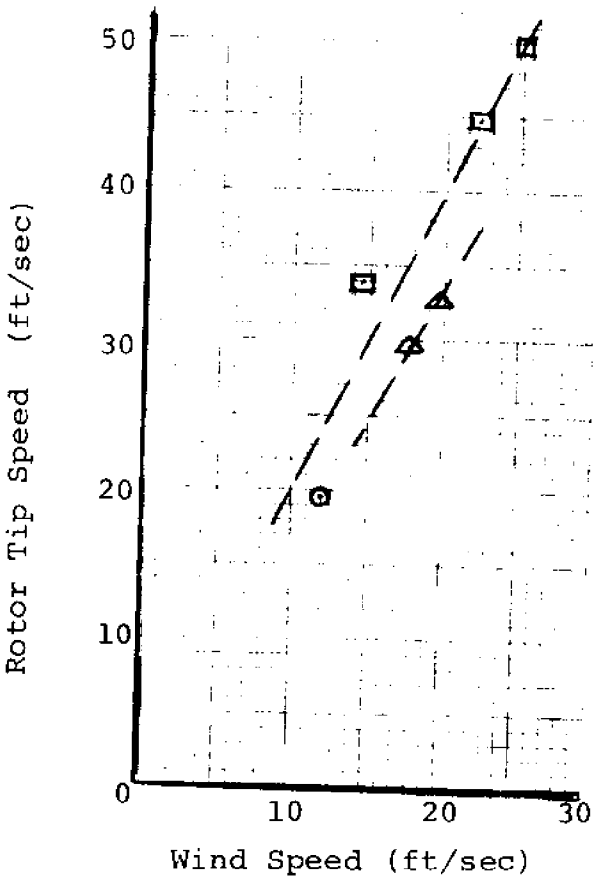

Legend

Symbol	Tip Angle	Date
△	60°	8/2
⊙	75°	8/3
⊡	75°	8/5

FIGURE 2.2.1.4

The weak link in this calculation is the estimated windspeed which was recorded on an anemometer nearly 200 meters from the position of the windmill. As efficiency depends on V^3, a small error in V would lead to a large error in efficiency.

The computed value compares well with typical values for other types of windmills:

2-Blade High Speed - 70%

American Multibladed - 51%

Dutch 4-Bladed - 27%

MMA 8-Bladed - 57%

The plotted data are contained in Figures 2.2.1.3 and 2.2.1.4.

Conclusions

The experiments on the windmill revealed:

Efficiency at optimum load was about 55 percent of that of a "perfect" windmill;

The tip speed ratio at optimum load was approximately 2;

The windmill performed well at windspeeds of 5 to 20 knots with no indication of malfunction over a period of 10 days.

Recommendations for Future Experiments

1. Unsealed bearings should be used in order that they may be lubricated.

2. A slightly lighter-gauge metal might be used for blades.

3. A brake and a thrust bearing should be mounted.

4. Blades should be more deeply inserted into the hub for better support and perhaps a better material could be used for the hub.

5. The windmill should be statically and dynamically balanced.

6. The base of the windmill should pivot instead of relying on the boat. A round buoy with a shackle on the bottom and a windvane located behind the rotor might also be employed.

7. Leading edges of the blades should be bent at the place of purchase.

8. Bearings should be pressed into the bearing sleeves after the sleeves have been welded to the supports. Do NOT use set screws to secure them. The bearings should have been pressed onto the shaft.

9. Some type of portable anemometer should be employed so as to take the data directly on site.

2.2.2 TIDAL CURRENT ELECTRICAL GENERATOR USING A SAVONIUS ROTOR

The purpose of the project was to design and construct a system that was capable of generating and storing electrical energy for continuous self-sustaining operation of electrical devices and small enough to be mounted on a buoy.

Background

There were two options available as a power source for an electrical generator: tidal current and wind. Both had been attempted in previous Summer Labs with little success. Tidal current was selected this year when it was realized that for a given Savonius area (the projected area of the rotor normal to the flow, i.e., length multiplied by diameter and power output the ratio of required air velocity to the required water velocity is approximately 9:1.

Tidal currents of three to four knots for seven hours a day occur in waters near Castine, Maine. This would mean the equivalent of 27- to 36-knot winds, which appeared unlikely to occur. Even if it proved more efficient to use the wind, the tidal currents could be depended upon four times per day to charge the battery, while the wind could be calm for long periods of time. Not only would the wind-powered buoy be inoperative for longer periods of time, but it would also have to be built to withstand very high wind velocities. The tidal currents could be depended upon to remain within a working range for a good portion of the day. Later, it was found to be impracticable to moor the buoy in the three- to four-knot currents so it was necessary to work in the Bagaduce River's one- to one-and-a-half-knot currents. Even though this cut the power available from the current by a factor of 27 and put the equivalent wind velocities into a more workable range, it was decided to continue with the current-powered system.

The Generator

A bicycle rim alternator, a bicycle hub alternator, and an automobile alternator were candidates for the electrical power generator.

Several tests were performed on each alternator to determine which would be most suitable for the project. The first test, a comparison of power output versus load, found each alternator's internal resistance and thus its most efficient load. That load was used in the subsequent test (see Figure 2.2.2.1). Each alternator was driven at a constant speed during this test, the small bicycle alternators by an electric drill, and the larger automobile alternator by a metal machine lathe.

The bicycle rim alternator required several thousand RPM in order to generate a usable amount of power. This speed was considered unattainable for all practical purposes, so no further tests were conducted on this alternator.

FIGURE 2.2.2.1

ALTERNATOR TEST FOR INTERNAL RESISTANCE

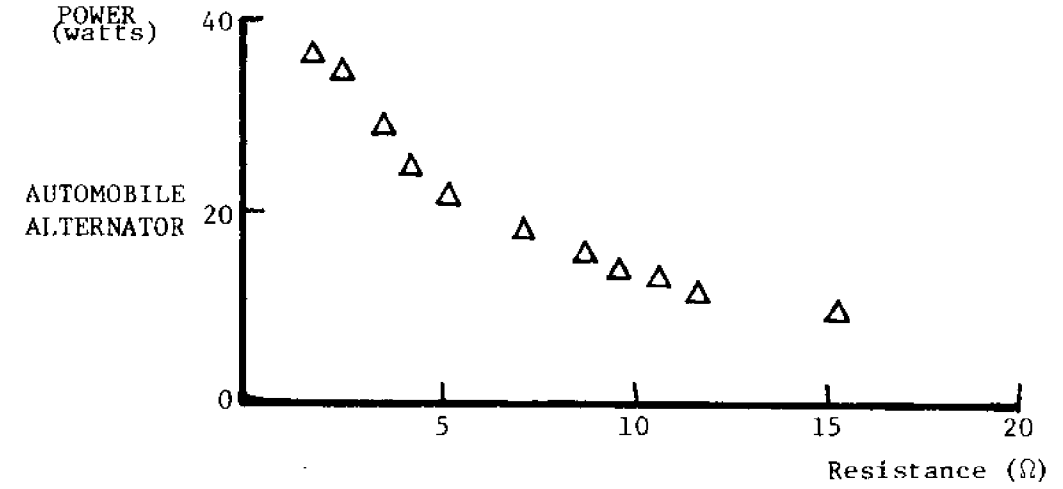

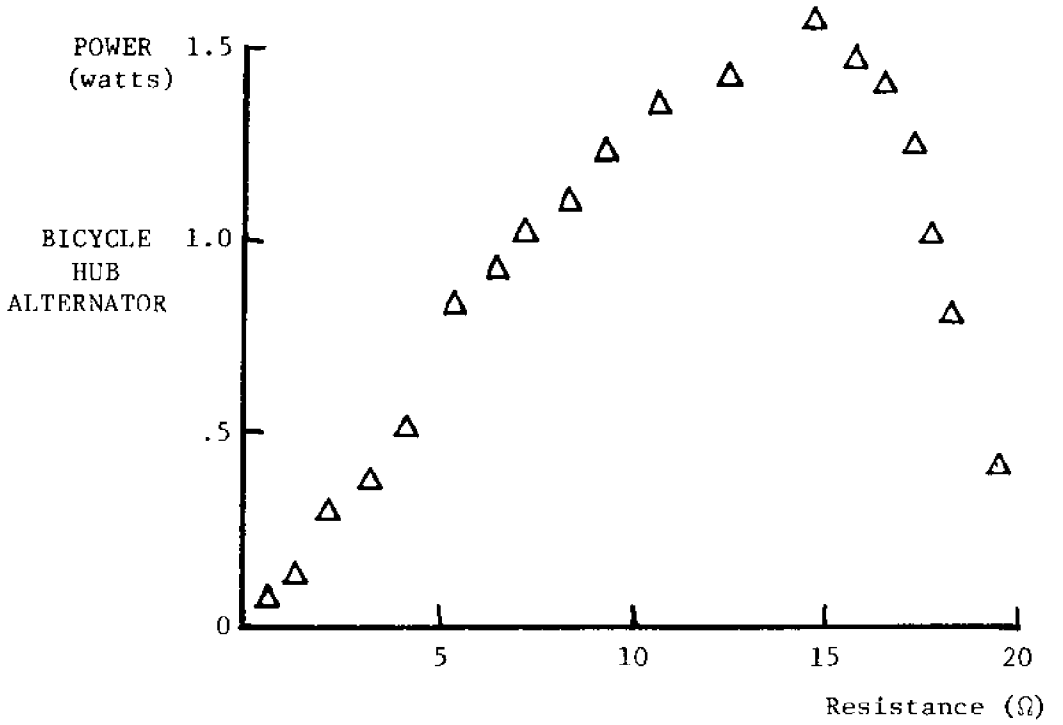

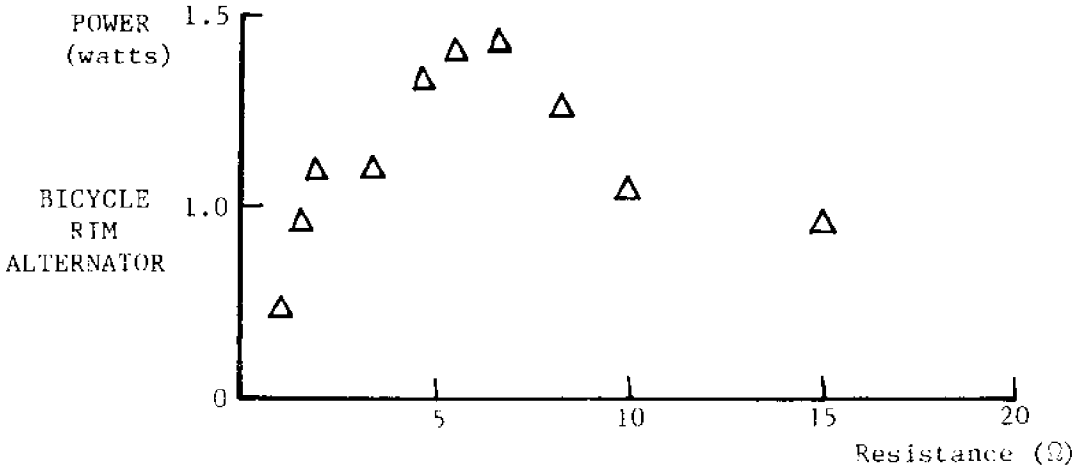

The next test performed was a comparison of power output versus RPM. Based upon the power provided by the alternator and the approximate efficiencies in the system, the rotor size was determined.

The last test determined the torque required to turn the alternators at given speeds. Both tests were conducted on a metal machining lathe using a spring scale on two different lever arms to measure torque. These tests helped determine the necessary rotor size.

Figure 2.2.2.2 shows the torque and output power versus the RPM characteristics of the two alternators. Although the automobile alternator delivered more power than the hub alternator, it would require a prohibitively large rotor to drive it. From all of these data, it was concluded that the hub alternator would be the best choice.

The Rotor

The impeller used was a Savonius rotor. It was chosen in favor of a propeller for several reasons:

1) A propeller must be very precisely machined in order to work efficiently, while an S-rotor is relatively easy to manufacture.

2) An S-rotor will operate in low water velocities.

3) A propeller is more likely to get fouled with seaweed, debris, etc.

4) An S-rotor is omnidirectional while a propeller would have to be able to turn with the current.

5) An S-rotor has a vertical shaft which would allow the generator to be above water without right-angle gearing, and eliminate the need for a pressure-proof, waterproof housing.

Because of the relative ease of construction of the S-rotor it was possible to make small prototype rotors for testing to determine design parameters.

None of the available literature specified what the optimal separation between the two blades should be. A small rotor with movable blades was made and tested in a tank with a one-knot current. The RPM and torque were measured for several different separations. It was found that the rotor delivered the most power when the ratio of the distance between the inner edges of the blades to the radius of the blades equaled 0.75, as shown in Figure 2.2.2.3.

Because of its shape, a Savonius rotor does not turn smoothly, but slows down and delivers less torque when at certain

FIGURE 2.2.2.2

BICYCLE HUB ALTERNATOR

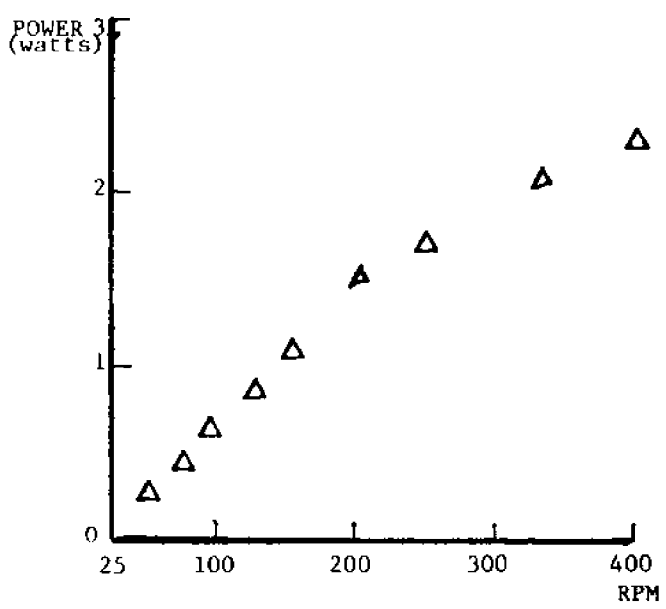

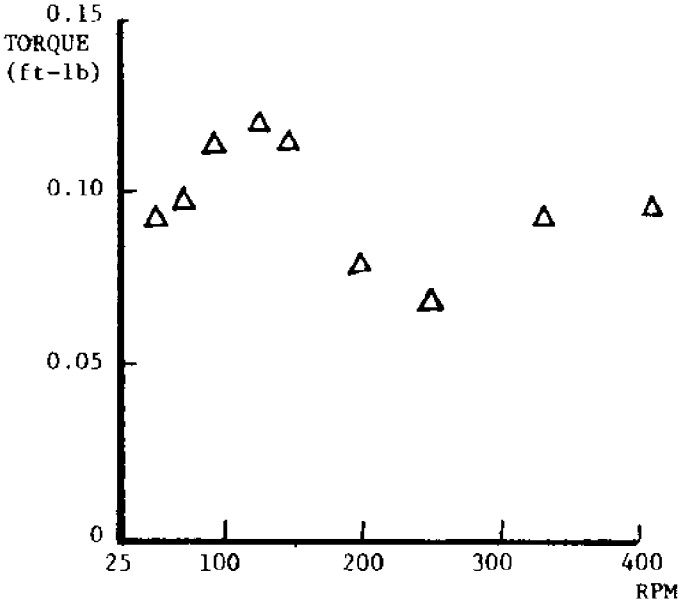

AUTOMOBILE ALTERNATOR

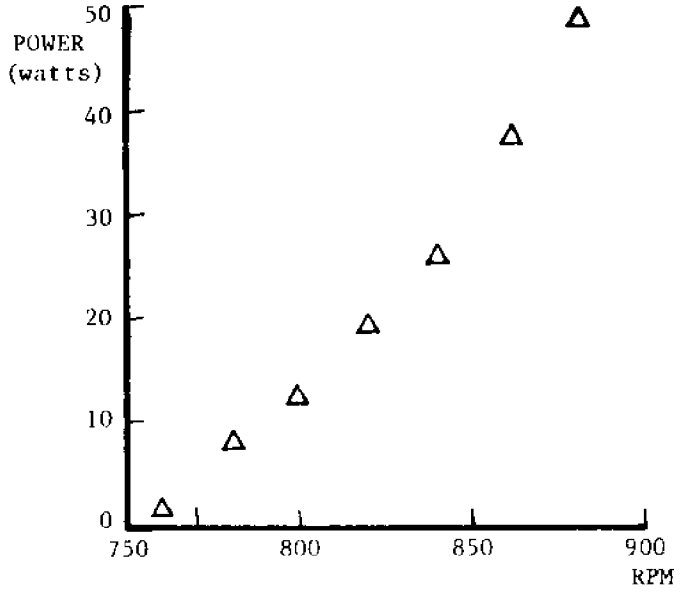

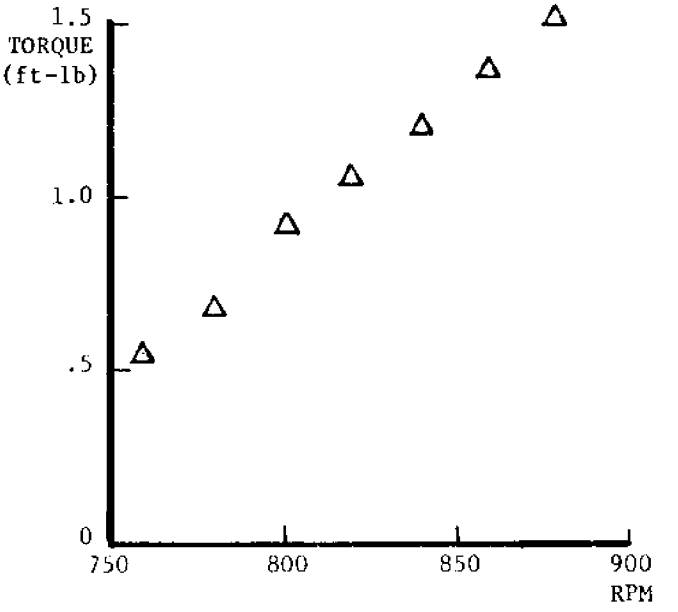

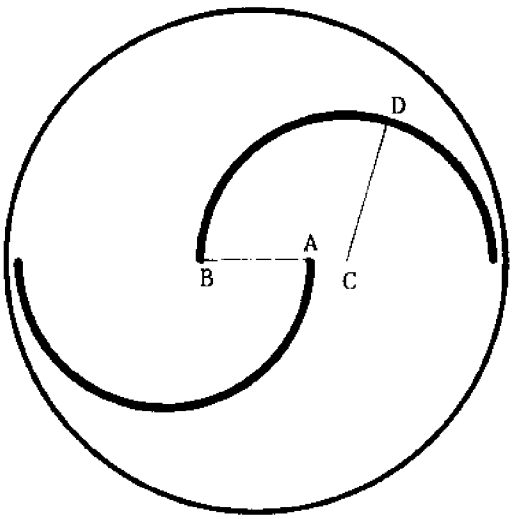

FIGURE 2.2.2.3

SPACING OF ROTOR BLADES $\frac{\overline{AB}}{\overline{CD}} = 0.75$

angles to the current (see Figure 2.2.2.4). To allow the impeller to rotate more smoothly, two S-rotors were put together with the blades oriented at a 90°-angle.

To determine the characteristics of the Savonius rotor, a small prototype impeller was built and tested in a propeller tank at water velocities ranging from 1.91 to 6.09 knots. From the data on rotor torque--RPM, length, diameter and water velocity--a "dimensionless" efficiency curve was plotted to determine the optimum design parameters.

The efficiency, η, is the ratio of power delivered by the rotor to the power available from the water. This was plotted against J, the ratio of the water speed to the tip speed of the rotor (see Figure 2.2.2.5).

Given:

n = rotational frequency of rotor
τ = torque delivered by rotor
ρ = density of water
v = velocity of water
d = rotor diameter
l = rotor length

Then:

$$\eta = \frac{2\pi n\tau}{\frac{1}{2}\rho v^3 dl}$$

$$J = \frac{V}{\pi nd}$$

Knowing J at peak efficiency and the water velocity that was expected, the rotor diameter necessary to achieve a particular frequency of rotation could be calculated. Given the diameter and efficiency, it was possible to determine torque per unit length of the rotor. Using diameter and efficiency, the length required for a desired power output could be determined.

The Assembly

Rotor Size Selection

After having completed the bench tests of the hub alternator and propeller tank tests of the Savonius rotor, the size of the final rotor could be determined. Setting a goal of one watt delivered to the battery, the 4" x 7" test rotor had the RPM and torque to drive the hub alternator directly at three knots. This would not be possible at one-knot currents unless another shape rotor was used. Based upon the results plotted in Figure 2.2.2.4, the ratio of the waterflow velocity to tip speed of the rotor was determined to be 0.90 when the Savonius was operating most efficiently. To get one watt out of the hub alternator, about 200 RPM were required. For direct drive at one knot this would have meant a rotor diameter of less than an inch! For intercepting a useful water volume, an impractically long rotor would be required and the Savonius behavior at such small radii was unknown. The obvious solution was gearing. This would permit a well-proportioned rotor to be used, linking the high-torque, low-RPM rotor with the low torque, higher RPM alternator.

A 15 percent combined efficiency of rotor and gear box was

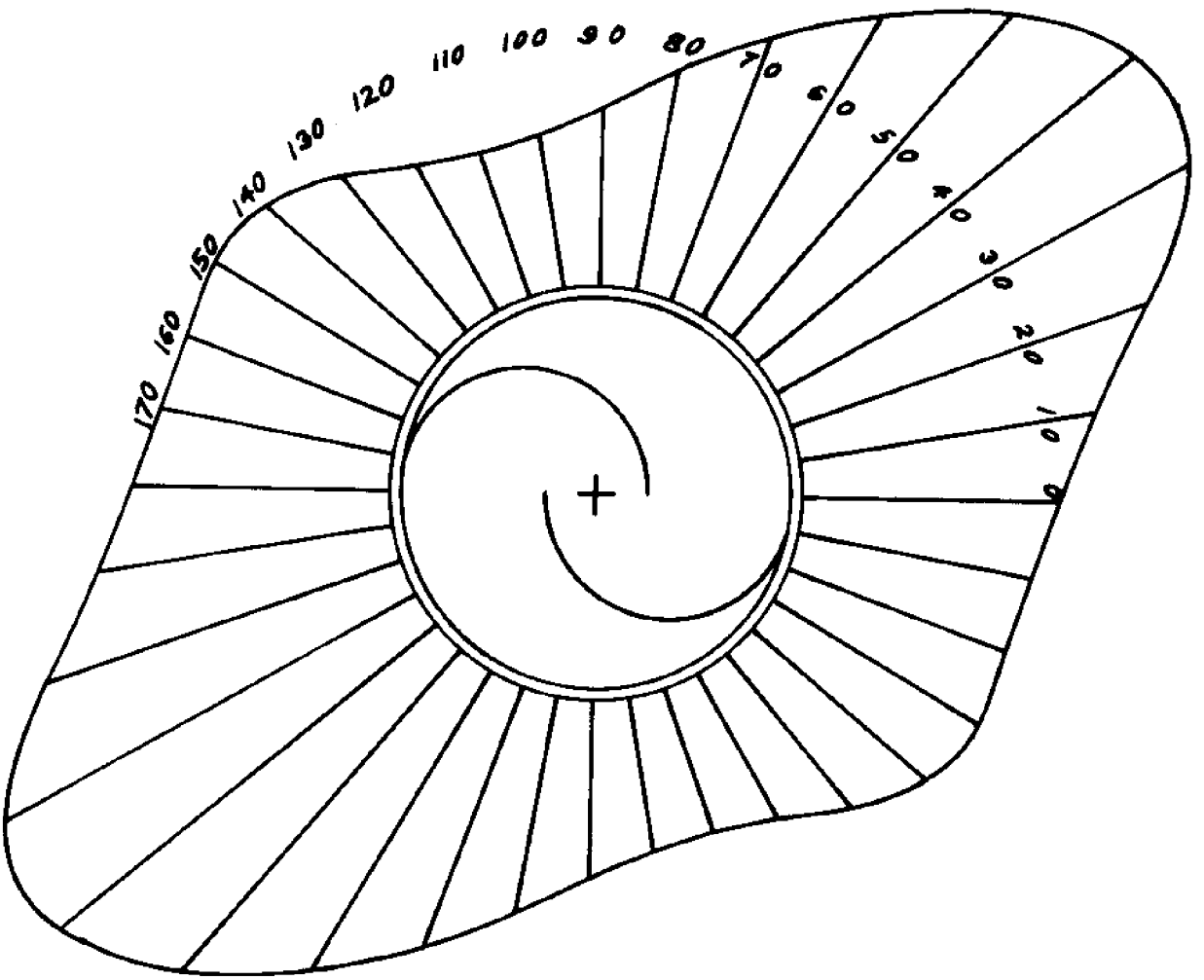

FIGURE 2.2.2.4

POLAR CURVE OF TORQUE
ON SAVONIUS ROTOR BLADES

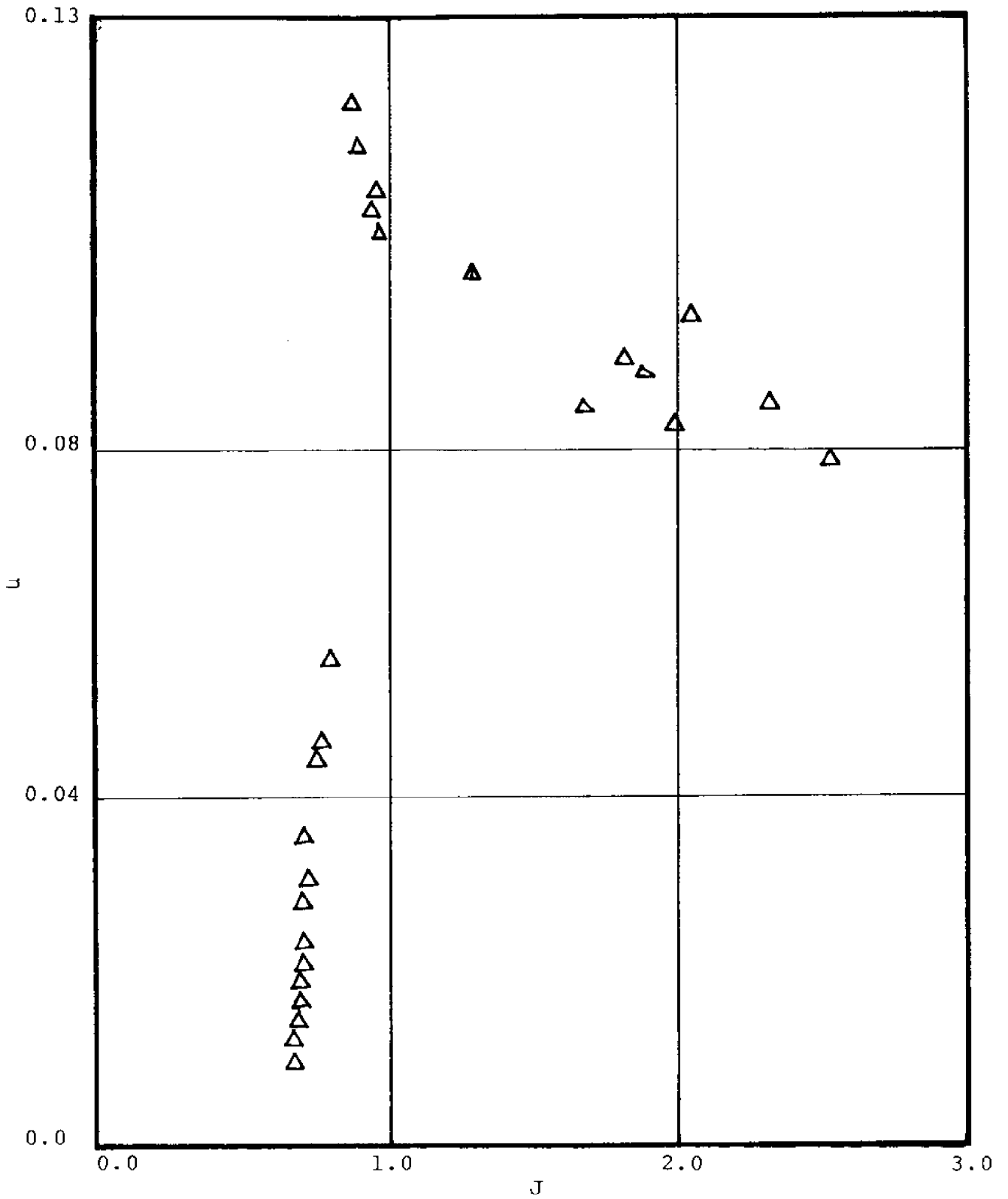

FIGURE 2.2.2.5

EFFICIENCY CURVE FOR SMALL PROTOTYPE ROTOR

assumed. The smaller rotor was 13 percent efficient, but its blades were thick in relation to rotor diameter (1/4" thick, 7" diameter). Its efficiency is plotted in Figure 2.2.2.5. It was planned to build the larger rotor out of sheet steel so the blades would be much thinner (less than 1/8" for a 16" diameter). It was also thought that edge effects would be less noticeable on the larger rotor. It was thought that the rotor would be 30 percent efficient, but gearing was expected to decrease the total efficiency by half.

Test data showed about 25 percent efficiency of generator and rectifier. From this the Savonius area could be calculated. The energy available in a moving incompressible fluid is $\frac{1}{2}\rho Av^3$, where ρ is the density of the fluid; A, the area being captured; and v, the undisturbed fluid velocity. In seawater (ρ = 1.99 slugs/ft^3) at one knot (1.69 ft/sec) the power available is 6.43 watts/ft^2 rotor area. Assuming one watt of power, the blade area must be:

$$(1 \text{ watt desired})\underset{\text{mech. effic.}}{(1/.15)}\underset{\text{elect. effic.}}{(1/.25)}(1 \text{ ft}^2/6.43 \text{ watts}) = 4.14 \text{ ft}^2$$

A list of rotor dimensions could now be made: a wide, short rotor with a large gear ratio, or a thin, tall rotor with a smaller gear ratio. A 10.5 : 1 gear ratio with a 40"-long rotor of diameter 16" was chosen.

The Gear Box

Construction of the gear box was straightforward and time-consuming. The increase was 2-stage: 3.5 : 1, then 3.0 : 1. Teflon thrust bearings and ball bearings were also used. The box viewed from the side is shown in Figure 2.2.2.6. For protection, the gear box, generator, and battery were housed in a waterproof plywood box.

The Buoy

The elements of the buoy system had to be constructed to fulfill several requirements.

The rotor shaft had to be kept aligned with the gear box while the drag of the rotor was causing a bending moment on the rotor shaft. The shaft needed to be supported as close to the rotor as possible with a bearing. This lower bearing was mounted in the end of a piece of 1" PVC pipe (see Figure 2.2.2.6). Using the data taken from the tests in the propeller tunnel at M.I.T., the drag coefficient was determined to be about 0.34 for a Savonius rotor with the resultant force directed 30° off the direction of the current.

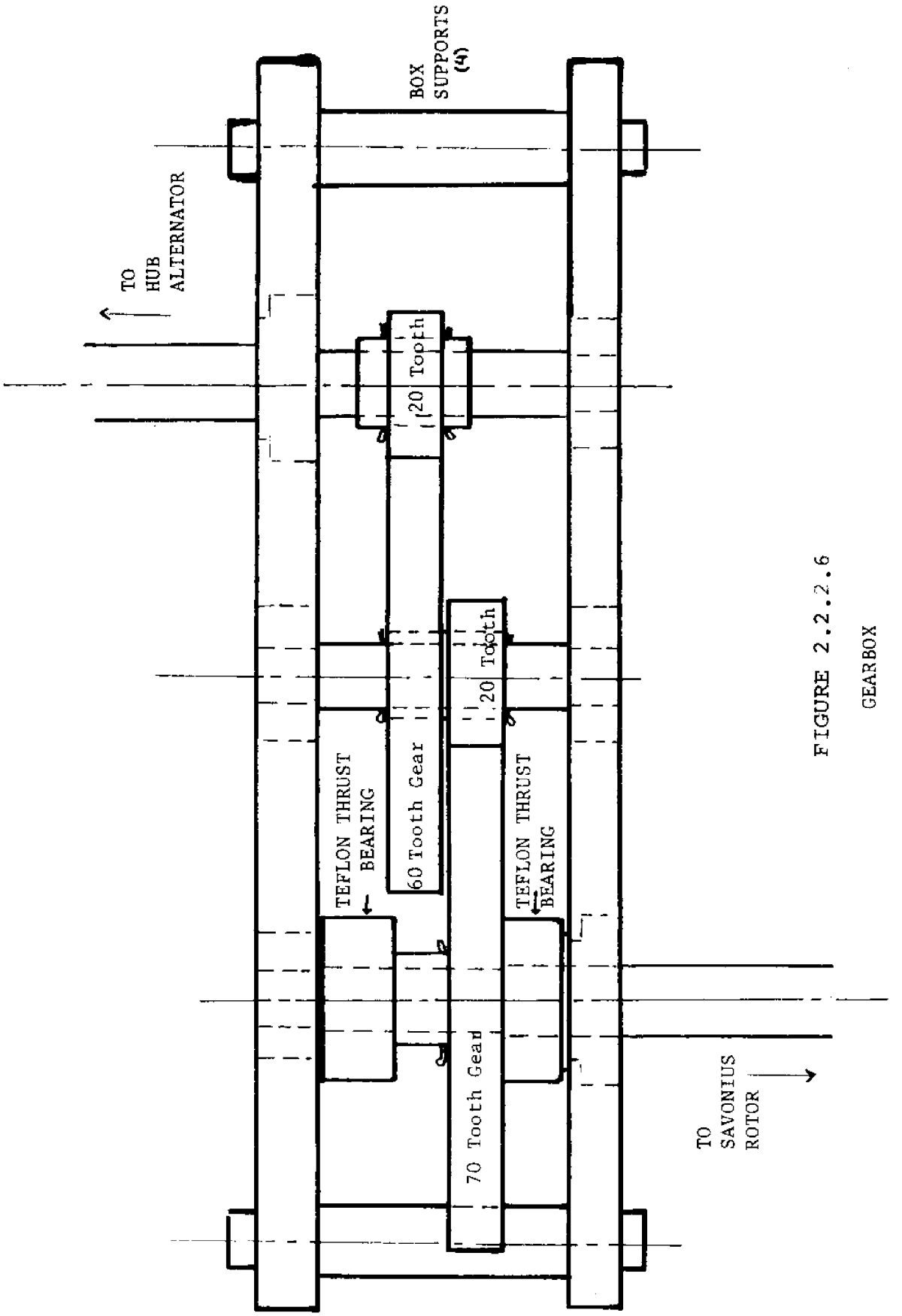

FIGURE 2.2.2.6

GEARBOX

$$F_{drag} = 1/2(.34)(\rho \text{ water})(v^2)(A)$$

ρ water = density of water
v = velocity of the flow
A = area of rotor

The 16" x 40" rotor in a 1.5-knot current experiences a ten-lb drag force. The bending of the shaft was calculated, knowing its radius and the modulus of elasticity using simple beam theory.

u = displacement of the shaft
x = distance along the shaft
M = bending moment
E = modulus of elasticity
I = moment of inertia of the cross-sectional area of the shaft

For a 1/2" 316 stainless steel rod, as shown in Figure 2.2.2.6 ($E = 28 \times 10^6$ psi), the maximum transverse displacement inside the PVC pipe was found to be 1/4" (see addendum at the end of this section). This is extreme, but not unacceptable. To keep the lower bearing in line, the PVC pipe was fitted with a flange which was bolted through the plywood gear box housing to the gear box. The PVC pipe was stayed to the buoy frame with 1/8" stainless steel wire and turnbuckles.

The components of the generating system had to be protected from the sea water. The rotor, constructed of rolled sheet steel, was painted with epoxy sealer and paint. The shaft was made of 316 stainless steel which resists corrosion in salt water. Since the bearing at the bottom of the PVC pipe was submerged, teflon was used; thus the water acted as a lubricant. The gear box, alternator, and circuitry were placed in a sealed plywood box above the water level. A Garlock oil seal was placed in the top of the PVC pipe so the sea water would not enter the plywood box through the shaft hole.

The buoy had to maintain the system nearly upright against the drag on the rotor and the motion of the waves. It also had to support the rotor at least three feet below the water surface and the gear box and circuitry above the water surface. The buoyancy also had to be great enough to support the weight of a person on the buoy accomplishing any maintenance or adjustment. A spar buoy was considered. Mooring at the center of drag would eliminate heeling and keep the water flow normal to the rotor shaft. However, since its buoyancy is critical, it would require adjustment while deploying and render on-site repairs difficult. It was rejected in favor of a float arrangement. A block-shaped float with a large, square water plane area would permit the assembly to ride the waves with a minimum of tipping. This also meant that the base of the PVC pipe could be further stabilized by guying it to the frame of the flotation at the surface. The buoy was built as shown in Figure 2.2.2.7.

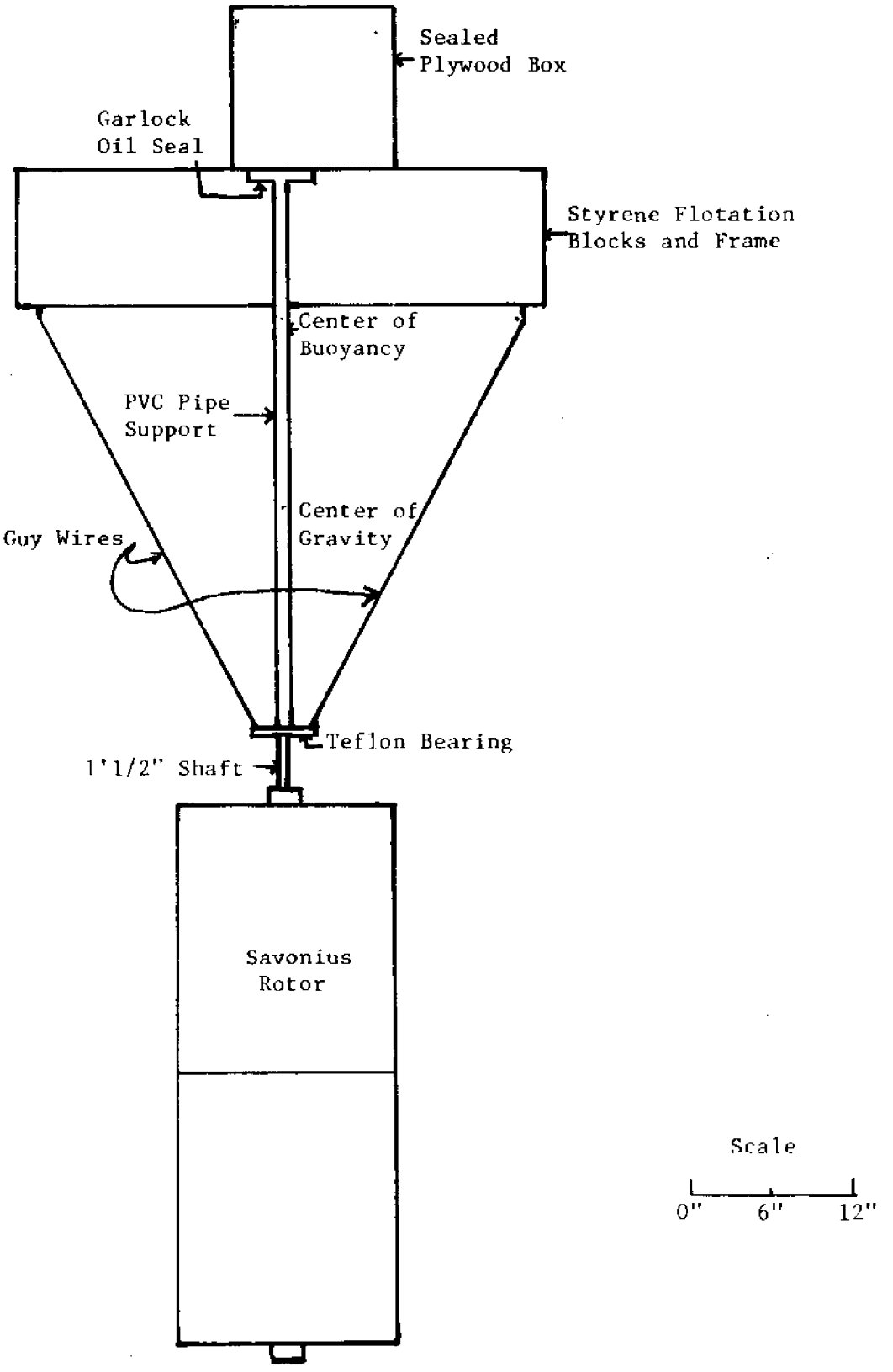

FIGURE 2.2.2.7

DIAGRAM OF BUOY DESIGN

The buoyancy needed for the 120-lb system was provided by two styrene blocks 10" x 19" x 44". This allowed the buoy to sink only 2" in the water and only about 3" more with a person sitting on it. The righting moment is determined by the height of the metacenter above the center of gravity ($\overline{GM}$) as given below:

$$\overline{GM} = \overline{KB} - \overline{KG} + \frac{I}{V}$$

$$M_{righting} \quad W_{total} \times \overline{GM} \times \sin \theta$$

I = moment of inertia of the waterplane area
V = total volume of water displaced by buoy
$\overline{KB}$ = distance of center of buoyancy is above base of buoy flotation
$\overline{KG}$ = distance of center of gravity is above base of buoy flotation
W_{total} = total weight of buoy
θ = angle of pitch (restricted to small angles)

For the buoy as designed, $M_{righting}$ = 10,050 in.-lbs/radian, and $\overline{GM}$ = 84" which meant that the buoy would tip 2° in a 1.5-knot current. This is equivalent to about a two-inch trim which is quite acceptable. The period of pitching (T) can also be calculated to determine if it is near the three- to four-second period of the waves.

$$T = 2\pi \left(\frac{I}{(\overline{BG})(W_{tot}+W_{ap})} \right)^{1/2}$$

$\overline{BG} = \overline{KB} - \overline{KG}$
I = total moment of inertia of buoy about the $\overline{KG}$
W_{ap} = apparent weight which must be added (= displacement of water)

The calculated period for the buoy system is about 1-2/3 seconds. The large size of the waterplane area and the damping of the rotor lessens any wave frequency problems.

The buoy system required a mooring that would keep the whole buoy from rotating, keep the mooring lines out of the rotor, and keep the buoy from being pulled underwater by the currents or tide. It was decided that spring buoys would be used because they solved two problems; they would keep the mooring lines clear of the rotor, and also not transmit vertical forces from the mooring line to the main buoy. A two-point mooring was all that was needed to keep the buoy from spinning (see Figure 2.2.2.8). Polypropylene line was used so that the mooring lines would float and stay clear of the rotor.

The Electrical Circuit

The electrical circuit that was installed in the buoy was one that provided full wave D.C. rectification in order to charge a six-volt battery (see Figure 2.2.2.9). For the towing

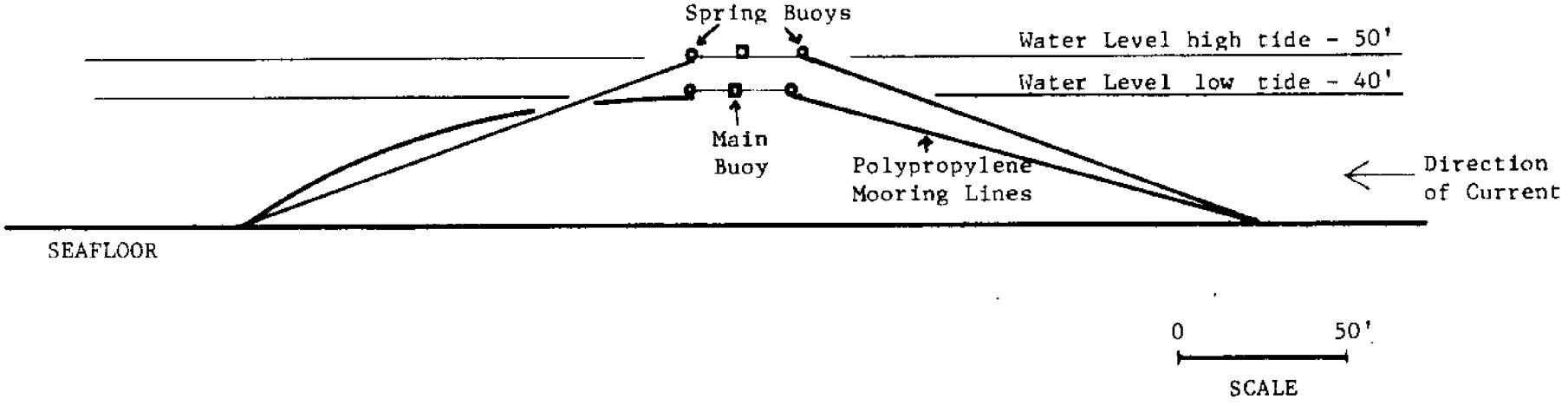

FIGURE 2.2.2.8

DIAGRAM OF MOORING SYSTEM

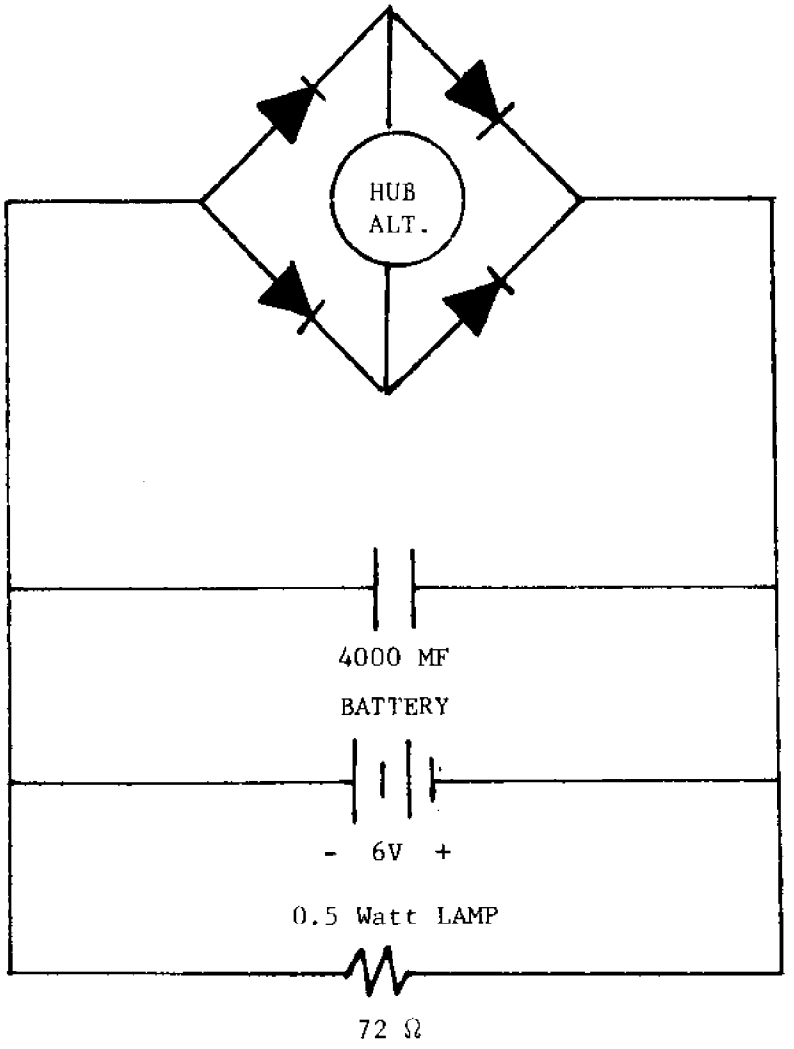

FIGURE 2.2.2.9

BATTERY CHARGING CIRCUIT

test, the battery-charging circuit was replaced with a purely resistive circuit. Two meters were connected in this circuit in order to measure the voltage across and the current through the bulb (see Figure 2.2.2.10).

Water Velocity Measurements

Measuring the water velocity posed a problem because the surface speed of the water could differ from the velocity at rotor depth. In order to measure the velocity of the water turning the rotor, a "chip log" was constructed. It consisted of a triangular piece of wood that was weighted at the bottom and attached to a length of twine that had knots at 5-foot intervals. To measure water velocity, the chip log was lowered into the water and allowed to run out with the current for a set time period. The wood piece stayed approximately two feet below the surface, perpendicular to the current. This method was estimated to be accurate to within ± 10%, which was adequate.

Results

The buoy was moored in an area that was expected to have 1- to 1.5-knot currents. The area did not have the expected currents, but that was discovered too late to find a better area. Instead of relocating the buoy, it was towed behind a small boat while the water speed relative to the boat was measured with the chip log. The electrical current and the voltage across the bulb were also measured. From these data, power output versus water velocity was plotted (see Figure 2.2.2.11). Later a spot was found with a 1.5-knot current and the system was able to generate 1.02 watts (3.4 volts, 0.30 amperes).

Conclusions

The efficiency calculations used to determine rotor size and design speed were proven correct since the device worked, delivering the expected wattage in the designed flow.

The large rotor did seem to have a better efficiency than the much smaller test rotor; the edge-effects may have been significant in the smaller rotor. Gear box and rotor combined efficiency was 15% as predicted.

The output of the alternator was very similar to that forecast from the lathe tests.

The mooring site selection is important and should not be left to the end, nor should the visual observations of so-called "experts" be taken literally. Water velocity tests should be made at a likely site.

A greater efficiency could be obtained from the generator by charging a battery (i.e., at voltages higher than across a purely resistive lamp). This can be seen in Figure 2.2.2.12. If the voltage is raised along lines A or B (voltage versus amper-

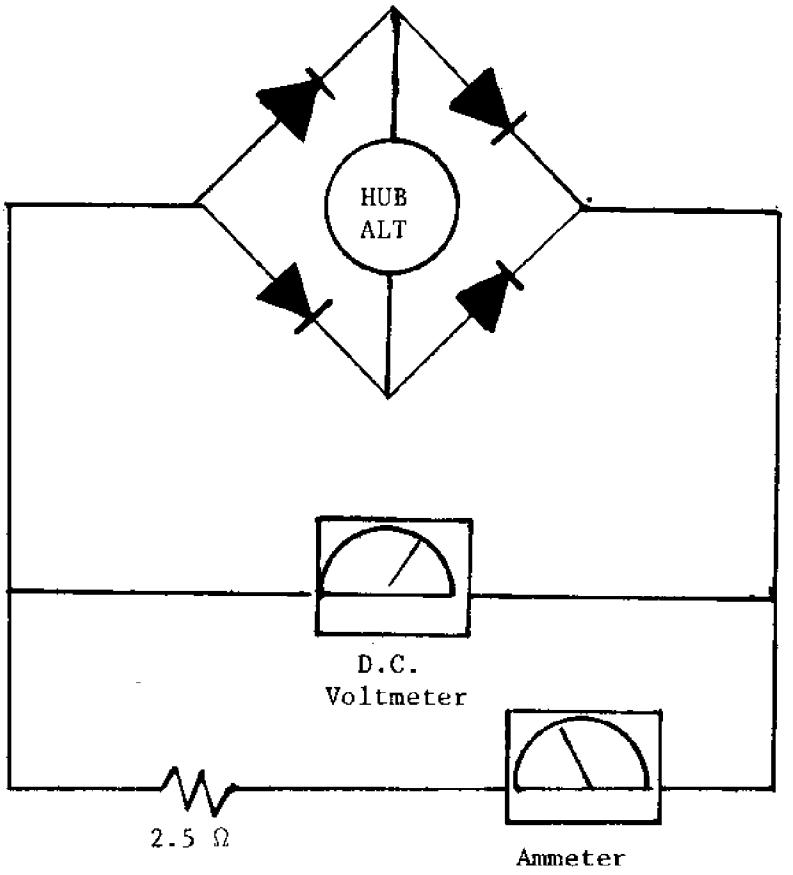

FIGURE 2.2.2.10

TOWING TEST CIRCUIT

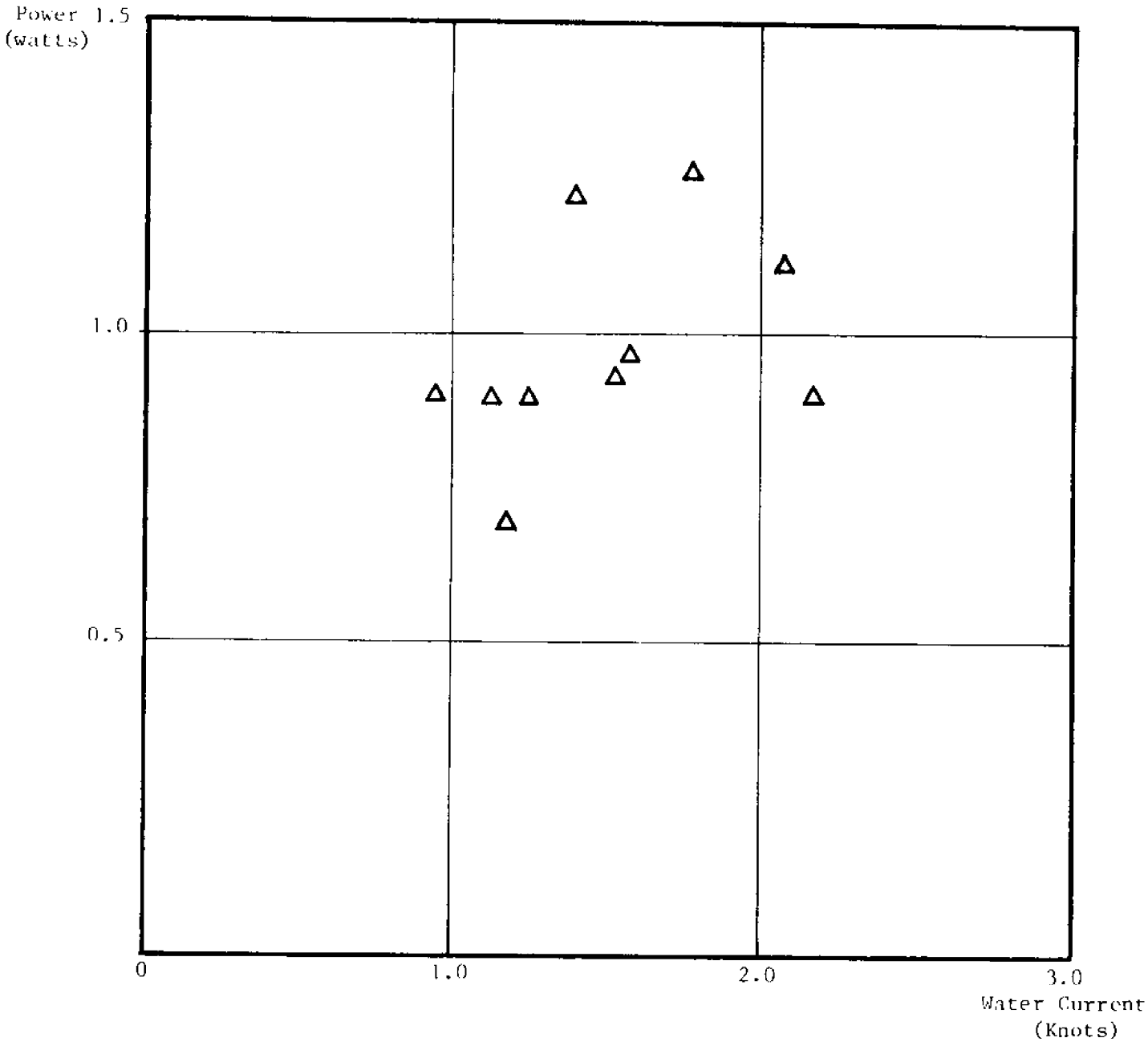

FIGURE 2.2.2.11

POWER OUTPUT VS WATER CURRENT IN TOWING TEST

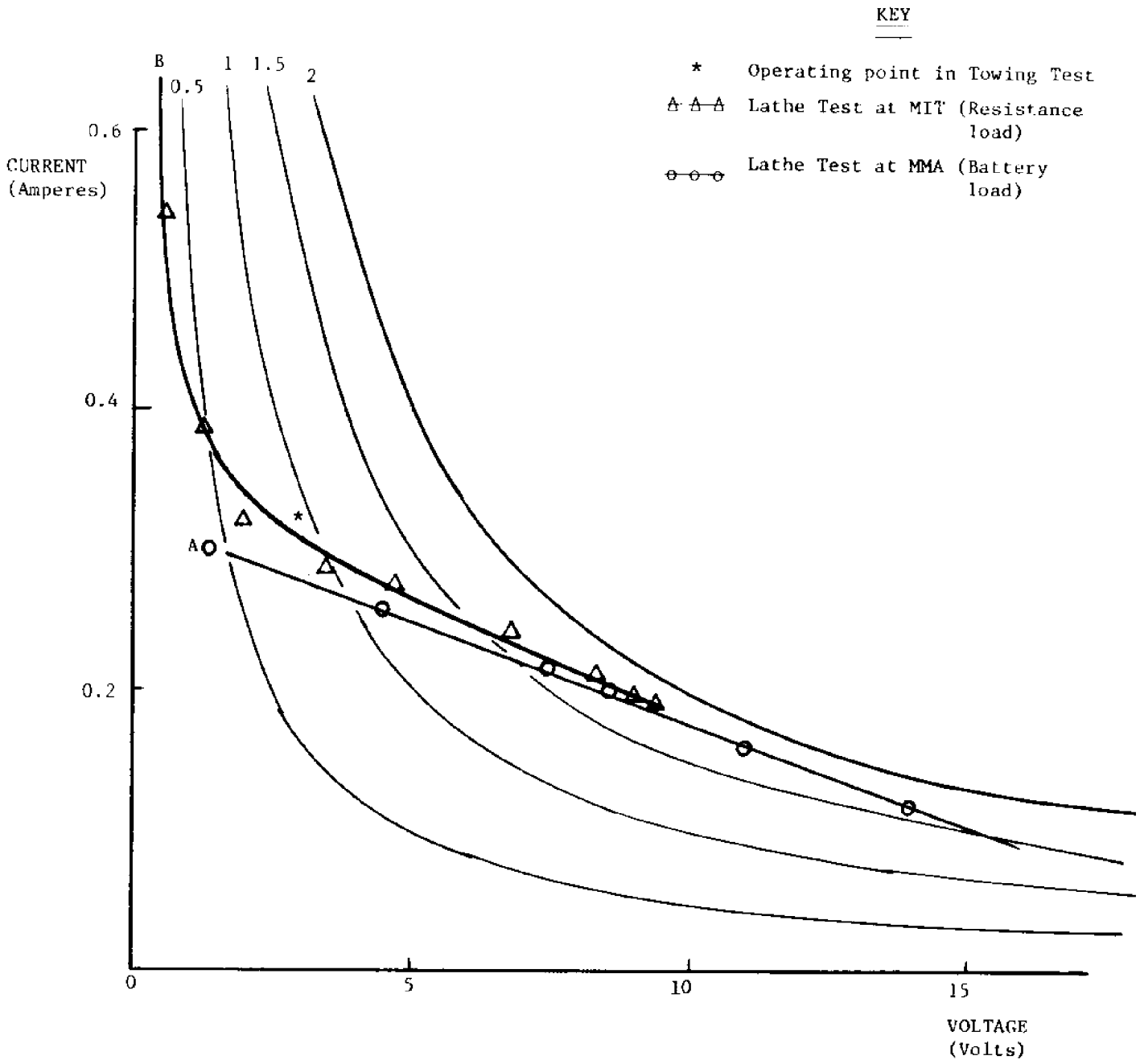

FIGURE 2.2.2.12

age characteristic lines of hub alternator), the total ouput rises and reaches a maximum around 10 V, and 1.75 watts (numbered hyperbolas are lines of equal power).

The power data test was not extensive enough to establish a reliable relationship between water velocity and power generated. At two knots the rotor efficiency may have been impaired because of an increase ratio of water velocity to rotor tip speed as the alternator and gear box resisted higher RPM.

Recommendations

Water velocity tests should be used to determine a mooring site before any design or construction begins. It is recommended that a battery be used to improve generator efficiency. More extensive tests should be conducted on the relationship of power output to water velocity. The rotor-buoy assembly proved effective and might be used for further study.

ADDENDUM TO SECTION 2.2.2

The shaft displacement calculations are based upon the well-known result

$$\frac{M}{EI} = \frac{d^2u}{dx^2} \tag{1}$$

E and I are constants for the metal shaft, and M is linearly varying over the rod inside the PVC. It is maximum at the lower teflon bearing where $M = F_{drag} \cdot L$ (L is the distance between the teflon bearing and the center of drag of the rotor). The moment at the top bearing is zero. Thus if we set up a coordinate system with origin at the teflon bearing with $x = \ell$ at the top bearing

$$M = (F_{drag} \cdot L)\left(\frac{\ell - x}{\ell}\right) \tag{2}$$

Substituting

$$\frac{F_{drag} \cdot L \cdot}{EI\ell}(\ell - x) = \frac{d^2w}{dx^2} \tag{3}$$

Integrating once

$$\frac{F \cdot L}{EI\ell}\left(\ell x - \frac{x^2}{2} + C_1\right) = \frac{du}{dx} \tag{4}$$

Integrating again

$$\frac{F \cdot L}{EI\ell}\left(\frac{1}{2}\ell x^2 - \frac{1}{6}x^3 + C_1 x + C_2\right) \tag{5}$$

We know that the bearings are fixed so $u(0) = u(\ell) = 0$. Therefore, $C_1 = -\ell^2/3$ and $C_2 = 0$ so Equation (5) becomes

$$u(x) = \frac{F \cdot L}{EI\ell}\left(\frac{1}{2}\ell x^2 - \frac{1}{6}x^3 \frac{\ell^2 x}{3}\right) \tag{6}$$

setting $du/dx = 0$ in Equation (4). The maximum displacement occurs at $x = (1-\sqrt{3}/3)\ell$ at which point $u = -0.69\ F \cdot L \cdot \ell^2$.

2.3 A CONTROLLABLE GRAPPLING HOOK

Objects dropped in the ocean are often very difficult to retrieve, even in comparatively shallow water. The difficulties are compounded with depth and in ocean currents. The project described here was prompted by the loss of an expensive camera. It was realized that the conditions of the loss were unique, but that a device to satisfy this particular need would have wider applications.

Background

In 1973, while photographing the sunken battleship MONITOR, the Duke University research vessel EASTWARD lost a camera sled and camera equipment belonging to "Doc" Edgerton of M.I.T. on the battleship. "Doc" Edgerton was interested in what could be done to design and construct a device which would be capable of recovering the lost equipment and the valuable photographs it contained.

The MONITOR lies on the bottom of the ocean off Cape Hatteras, Virginia, in 220 feet of water. There is a steady current of about two knots. Of the many possible salvage methods which could be used, this particular situation made most impossible. The two-knot current would make recovery of the sled by scuba divers too difficult and dangerous to be worthwhile. Hard-hat divers would not be able to approach the MONITOR because the ship has been declared a national historic landmark, and is protected from destruction. A hard-hat diver could damage part of the fragile wreck in his attempt to recover the camera sled. A conventional grappling hook, dragged haphazardly in hopes of blindly snagging the sled, would be prohibited because it would most certainly be damaging. A fourth possibility would be to have a small manned submarine, such as the ALVIN, make a descent to the MONITOR to recover the sled. This would be prohibitively expensive unless the ALVIN were being used to explore the wreck and the recovery of the camera sled was undertaken as an incidental.

It was decided that a remotely controllable grappling hook would be designed and constructed to be the solution to this problem. The hook would have to be able to be maneuvered to attach itself to the camera sled and bring it to the surface. This device would be able to be used in many similar situations and be an inexpensive, safe and efficient method of recovery.

Design Considerations

There were many considerations in deciding how this retrieval system was to be designed. The hook would have to be capable of carrying a load of about 250 pounds (approximately the weight of the camera sled) and would have to be viewable from the surface as it was being maneuvered into position.

A device which could move 250 pounds would have to be quite

powerful and therefore rather large. This would create maneuvering problems. It was decided that, instead of having a large, independent device which could retrieve objects itself, a small tethered device could be used. This would attach itself to the camera sled, and both the hook and the sled would be brought to the surface by the tether.

The hook was to be suspended on a 15-foot tether from a television camera (Figure 2.3.1). The camera and sufficient lighting would be in waterproof housings. Having the television camera viewing the whole recovery area was thought to be better than having the camera positioned near the hook where its view would be limited. The operator of the hook controls would view the progress of the hook as it maneuvered into position. Once the hook was engaged, the whole system would be winched to the surface with its prize.

In order to maneuver the hook, a small vehicle was designed to which the hook would be attached. The vehicle was designed as small as possible to maximize maneuverability and to minimize drag and power consumption. It was designed to be mobile in all directions--ahead-astern, up-down, and transversely.

The limit to the smallest size the vehicle could be depended upon the smallest motor which was able to overcome the drag of the tether (including the control wires), the vehicle itself, and the hook. The velocity of the vehicle was 3 knots which gave a forward velocity of 1 knot when moving against a 2-knot current.

In order to minimize the drag of the tether, it was necessary to use the thinnest possible cable which could sustain the weight of the vehicle and the object being recovered. Kevlar plastic cable, manufactured by DuPont, was selected because of its high tensile strength. A 1/8-inch diameter is able to withstand 1,000 pounds, four times as much as the expected load. The control wires for the motors, when wrapped around the support cable, would double the effective diameter of the tether to 1/4 inch.

The drag of the tether was calculated to be approximately 10 lbf. Half of this would be at each end of the cable so the vehicle would experience about 5 lbf from the drag of the cable.

The hook itself was made of 1/4-inch diameter stainless steel rod, two feet long. The drag of the hook was calculated as about 1/5 lbf.

The drag calculations for the vehicle body were based on the previous calculation of the drag of the robot submarine. The robot vehicle was 7 feet long and 15 inches in diameter. The profile of the vehicle was the same as the profile of the robot. Drag is proportional to the velocity squared and the dimensions squared. The dimensions of the vehicle were one-quarter those of the robot sub. The drag on the robot was

THE RECOVERY SYSTEM

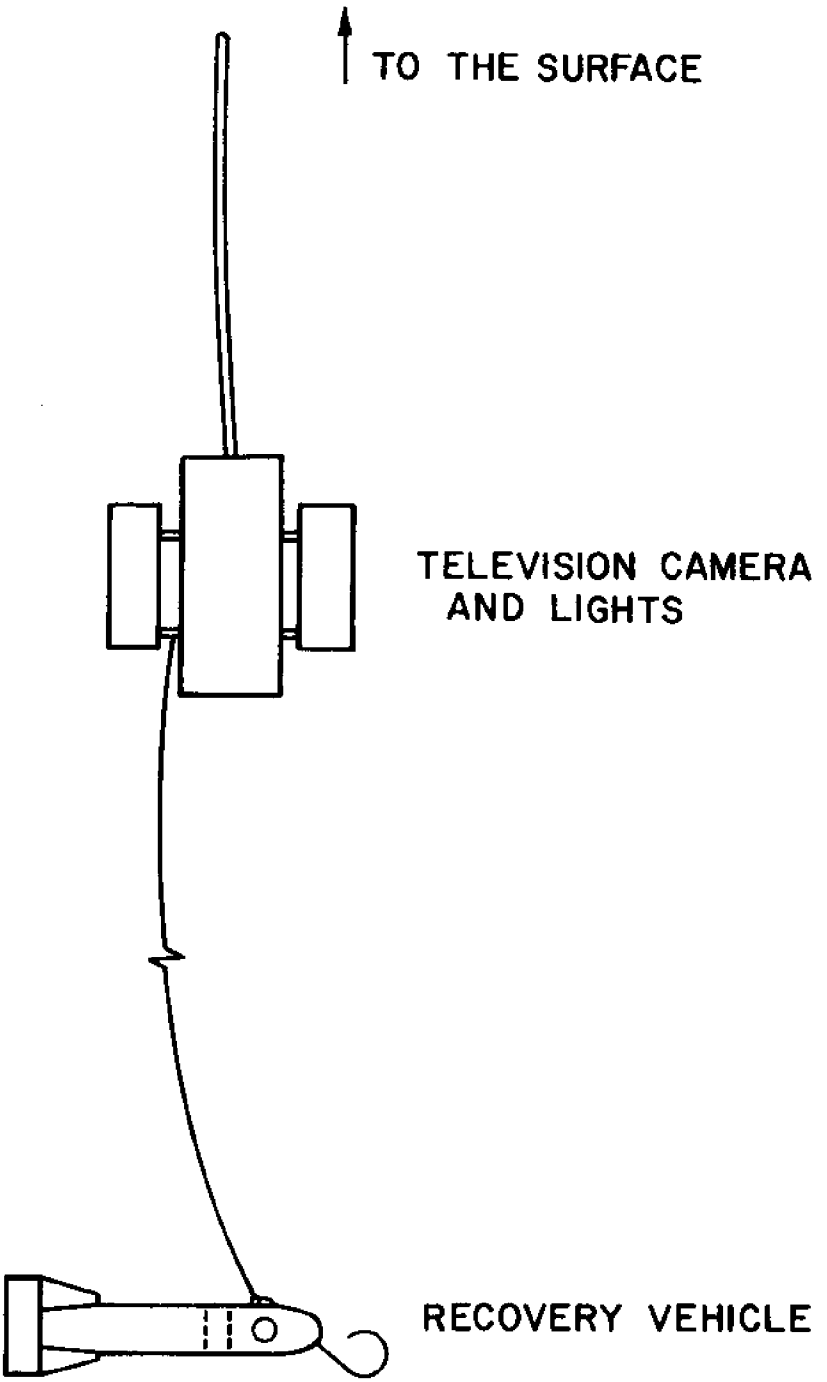

FIGURE 2.3.1

6 pounds at its maximum velocity of 2.8 knots. Hence the drag of the vehicle was calculated as 0.5 lbf.

The total drag on the vehicle at 3 knots is about 7 pounds. A small waterproof trolling motor was chosen for the vehicle. This motor was advertised as providing 7 pounds of thrust, enough to overcome the drag.

One of the design criteria was that the vehicle was to be very maneuverable so that it could be gently guided to its target. It had to be capable of ahead-astern, up-down, and lateral motion. The main propulsion motor was to supply ahead-astern movement. For the other directions, two methods of propulsion were considered--waterjets and conventional propeller thrusters. It was decided that conventional propeller thrusters would offer fewer design and construction difficulties. It was also decided to use 2 thrusters, one for vertical movement and the other for lateral movement.

The thrusters consisted of high-speed d.c. motors in waterproof housings. They were located in holes passing through the body of the vehicle, centered so they would force water past themselves through the holes. The vehicle moved in a direction opposite to the water flow.

The vertical thruster was mounted near the center of the vehicle to keep it as level as possible while moving up and down. The lateral thruster was installed forward of the vertical thruster so that it would give a moment to the vehicle which would cause it to be pivoted around its center of gravity. The amount of thrust produced by each thruster at 1,000 rpm was found to be 1-1/4 pounds.

The vehicle was designed so that its motors could be operated with a 12-volt battery, if necessary. All three motors were continuous duty reversible d.c. motors. The main propulsion motors could be operated at any voltage up to 28 volts.

Preliminary controls consist of three switches, each of which controls one motor. Plans for variable speed controls have been designed, but not constructed.

Fabrication

The body of the vehicle was made from wood to provide buoyancy and to permit the intricate motor installation. Basswood was used because of its fine grain and resistance to swelling when exposed to water. Pieces were glued together, and the profile was turned on a wood lathe. The rear was bored out for the main propulsion motor and the two holes for the thrusters were bored. Supports were constructed from basswood for the thrusters. These were affixed inside the holes so the thrusters would be centered in the holes. Another hole was drilled at an angle through the nose of the body of the vehicle to attach the hook (Figure 2.3.2).

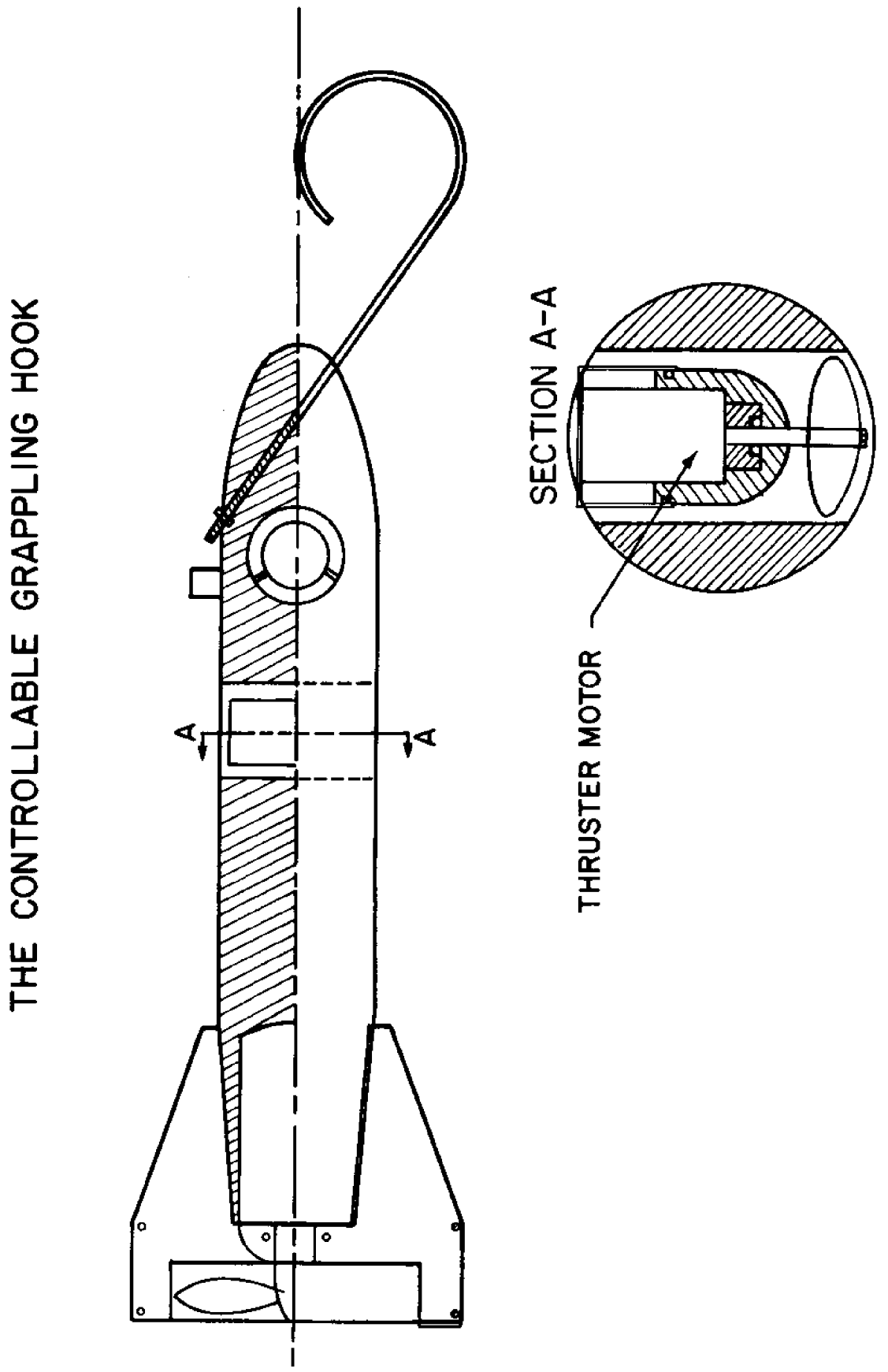
THE CONTROLLABLE GRAPPLING HOOK
A
A
SECTION A-A
THRUSTER MOTOR

FIGURE 2.3.2

The hook was formed from 1/4-inch diameter stainless steel rod. The radius of the curved portion of the hook was 3 inches. It was threaded for 6 inches along the length of the shank so it could be attached to the vehicle body with nuts and be used as the attachment point of the tether. This was the load-bearing part of the vehicle, the part that attached the object of recovery to the tether cable.

The rear of the vehicle body was tapered to reduce the resistance. Here were attached four aluminum fins. These fins provided stability for the sub and also retained the main propulsion motor. An inch-wide ring of aluminum was fastened to the fins. It surrounded the propeller to protect it.

The thrusters posed an interesting design problem. It was decided that small, high RPM d.c. motors housed in waterproof housings would be an adequate solution. The propeller shaft extended from the housing through a dynamic O-ring seal. The housings were two-piece. The bases were made from copper pipe-end caps. The tops were made from PVC plastic, turned to size on a metal lathe. It was streamlined and equipped with 2 O-ring seals, a static seal where the top joined the bottom, and a dynamic seal for the propeller shaft. The motor leads were passed through small holes in the housing tops and cemented into place.

The propeller shafts were turned from a 1/4-inch stainless rod. The surface was polished to a mirror finish. One end was drilled to force-fit on the motor shaft; the other end was threaded so the propeller could be fastened on with a nut.

Both the shafts and the motor housing tops were difficult to construct. The friction of the dynamic seal had to be minimized so the thrusters would put out sufficient RPM's. This required small O-rings which made machining to tight tolerances difficult.

Once the motors had been prepared, they were positioned in the vehicle body. Their leads were connected to an 8-prong plug jack epoxied to the vehicle body behind the upper part of the hook shank. The leads were epoxied flush with the surface of the vehicle body to minimize drag. Enough slack was left to allow access to the motors so they could be repaired or replaced if necessary. The main propulsion motor was held in place by the fin assembly, and the thrusters were held in place with small pieces of PVC bolted to the vehicle which prevented their removal.

Testing

Once the motors, hook and fin structure were in place, the sub had to be ballasted. It had to be slightly negatively buoyant so it would lie in the camera's view while at rest in calm water. Ballasting was done by recessing portions of the body and epoxying lead in the voids. The vehicle displaced about

1/4 cubic foot so it had to weigh about 8 pounds. This allowed for plenty of ballast located so the sub would tend to remain horizontal and not roll.

The completed vehicle consists of the two directional thrusters, the main propulsion motor, the fins, the hook and the body. In tank tests all three motors performed well. The vertical thruster tended to raise the nose of the vehicle higher than the rear.

The thruster housings were tested for their waterproofness. Keeping the motors dry was critical because any leakage of salt water into the motor would cause electrical short circuits and corrosion. The housings were tested by creating a vacuum inside, submerging the thruster in water, and running the motor for a few minutes. Visual inspection was all that was needed to tell if there had been any leaks. The vacuum was used to increase the pressure drop across the seal. Leaks would be more likely under higher pressures. The main motor, encased in its own sealed housing, was assumed to be waterproof.

The vehicle has not been completed. Reballasting is necessary so the sub will be negatively buoyant in salt water since the vehicle was tested in fresh water. The thrusters, which operated well, tended to be more powerful in one direction than the other. This is due to the shape of the motor housing, and the different efficiencies of the propeller when rotated in opposite directions. This did not affect the performance of the vehicle to any noticeable degree.

The main motor moves the vehicle swiftly and surely. There is no indication of instability with the main motor running; the vehicle moves straight ahead without veering to right or left. There is slight rolling to one side due to motor torque, however, but this does not affect performance adversely. The vehicle is operable and does perform its designed function. It is easy and almost fun to operate.

Future Developments

Before the vehicle is used in the ocean, it must be tested further to make sure it is waterproof and can withstand the pressures of water, at least 225 ft (100 psi). The vehicle, as it was designed and built, could possibly fail under the high pressures of great depths. The high pressure would have many effects on the vehicle. It could compress the wooden body, changing the density and therefore the buoyancy of the vehicle. The thrusters, tested under an effective depth of 33 feet, would probably still be effective. The higher pressure would increase the pressure of the O-ring on the propeller shaft, decreasing its rotation and making maneuvering a little more slow. The motor's slower speed could be counteracted by increasing the voltage across the motors, giving them more power. The major concern with the high pressure, however, is the main propulsion motor. The motor was purchased already waterproofed, but its seals and housing were designed by its manufacturer to

withstand low pressures. If a high pressure test resulted in the failure of the dynamic seal, the motor would have to be modified to have a more effective seal. This would require a substantial amount of work with extensive modification of the fin structure, which holds the main motor in place.

Once the vehicle is seaworthy, the next step would be to test the vehicle's behavior when it is operated in currents in order to gain more knowledge as to how it responds in all possible situations.

A final preparation before the actual operation of the vehicle would be to arrange a "dry run" of the entire system, both the vehicle and the television viewing system. This final preparation would decide if the whole system is operable. It is possible that the operator of the vehicle would not be able to get it in view of the television camera, especially in swift currents. This would occur because the operator would not know the orientation of the vehicle when it was out of view of the camera. However, with no power to the propulsion motors and thrusters, the vehicle should be facing the center of the television view.

2.4 AN OCEANOGRAPHIC SAMPLER DREDGE INSTALLATION

2.4.1 OCEANOGRAPHIC SAMPLER DREDGE

There are various ways of collecting animals and plants from shallow ocean bottoms: from scuba diving and collecting samples by hand through use of electric fields to scare, attract or stun. The most practical method in normal situations is by the use of the bottom sampler dredge towed at low speeds behind a small boat.

Background

Bottom sampler dredges are used extensively by the Oceanography Department at the Maine Maritime Academy. The dredges used to date have been only partly satisfactory, being either too cumbersome and easily entangled, or too flimsy and too light to keep good contact with the bottom. With the growth of oceanographic and ocean engineering programs at MMA, there arose a need for more robust dredges of improved design. During this project two candidate dredges were constructed.

Design Considerations

A primary design consideration was the terrain encountered along the Maine coastline, and particularly in the Bagaduce River and nearby Penobscot Bay. The bottom is generally mud or silt with frequent rocks and large boulders. The ability of a dredge to survive collisions with such rocks and boulders, and to glance over or around them readily was critical.

Before designing the sampler dredge, it was necessary to run tests on the existing MMA sampler dredge. The dredge had a light stainless steel frame with a fibrous net. The bridle consisted of a one-meter chain connected to the forward end of the dredge. Connected to the chain was a 75-meter nylon tow rope. Testing of the sampler dredge was held in four different locations, each of which had different bottom terrains.

The Academy's 20-horsepower outboard utility boat, SPIDER, was used as the towboat. All tests were conducted at depths of approximately 10 meters. These tests showed:

1. At three knots the dredge was too light to reach bottom.

2. At speeds slow enough for the dredge to operate properly (two knots or less), control of the boat was lost.

3. In the typical two-knot currents in the Bagaduce, it was not possible to keep the dredge on the bottom even with the towboat and dredge stationary.

4. The mesh on the dredge nets was too fine. On a typical run so much mud collected that the net ripped due to lack of support and strength.

As a result of these tests it was decided that any improved sampler dredge must have a heavier, more rigid frame than the existing dredge, and that its net must be both stronger and more evenly supported.

In addition to the requirement for a self-freeing capability on a boulder-strewn bottom, the new dredge was further required to

(1) Be readily adaptable to collection of samples of various sizes, from tiny shrimp and fish through large sea cucumbers;

(2) Be capable of maintaining contact with the bottom at drag speeds of at least three to four knots relative to the water;

(3) Be light enough submerged to be retrievable by a hand winch on a small boat;

(4) Be compact and light enough ashore to be readily transported and positioned by no more than two people;

(5) Be inexpensive and simple in design and construction, readily maintained and repaired by students alone, and

(6) Be designed without special parts.

Two types of dredges (see Figures 2.4.1.1 and 2.4.1.2) were chosen for construction and test. The first was a strengthened version of the existing type of dredge used at MMA, while the second was an adaptation of the Cape Town (Day) Dredge.

Technical Description

Construction

In the design of the first new sampler dredge, the original shape of the MMA dredge was maintained with a few minor alterations. As shown in Figure 2.4.1.1, the height of the dredge is 8" with a width of 26". This is smaller than the original sampler dredge due to the heavier construction. This size reduction was required because the sampler dredge must be handled by a hand winch. The design included two sled-like runners separated by three supporting members beneath the dredge. The first member is located at the bottom of the mouth, and is the heaviest of the three as it is expected to carry most of the load. It is located 20-1/2" aft of the forward end. The second member is located at the top of the mouth. It is of relatively lighter construction placed 10" aft from the forward end. The third member, used solely for stiffness and support, consists of a rod located between the upper runners 33-1/2" aft of the forward end.

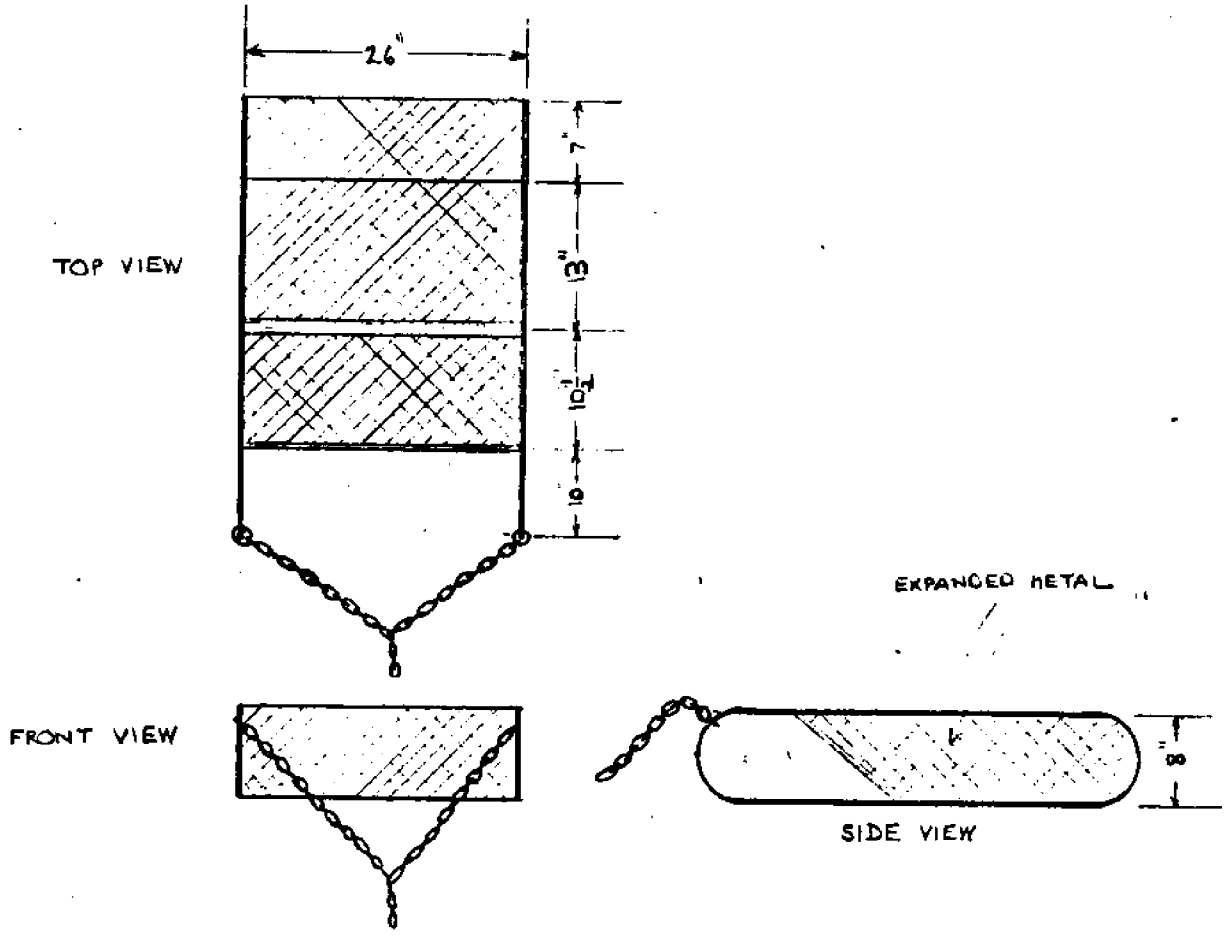

1 inch = $\frac{1}{16}$ inch

NAME	DRAWING	CLASS	DR. #	DATE
MARK KREIDER & PETE SCANLON	SAMPLER BOTTOM DRAG	SUMMER LAB.	1	27 JULY 76

Figure 2.4.1.1

SKETCH NUMBER 2
CAPE TOWN (DAY) DREDGE

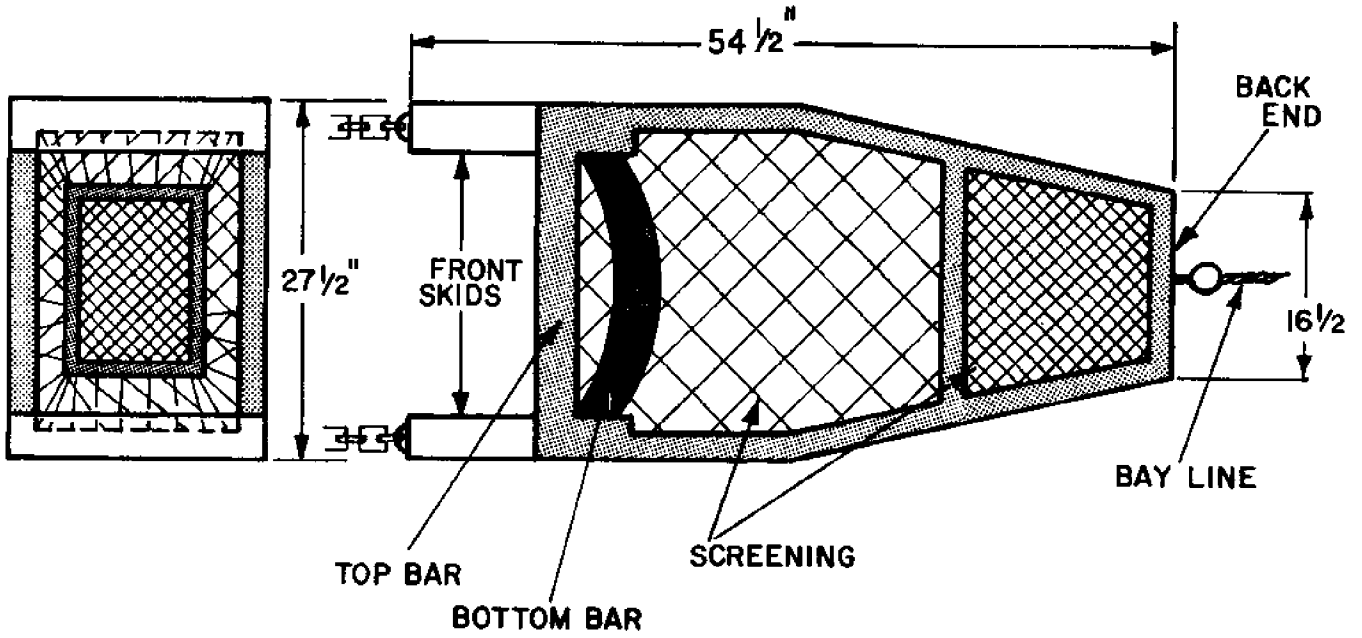

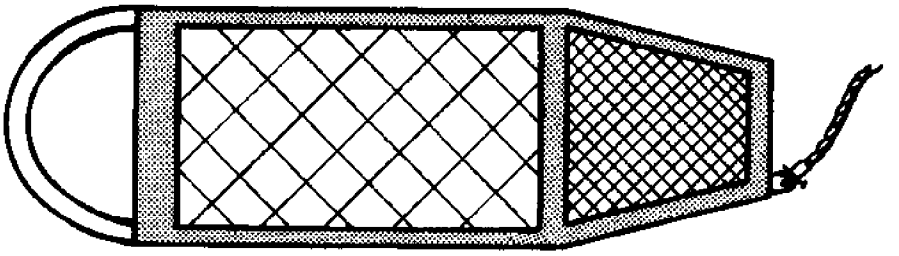

FIGURE 2.4.2.

Attached around the outside of the runners from the bottom of the mouth, aft to the top of the mouth, expanded metal was attached for support of the fiber net. It is necessary to include the expanded metal so that even a flexible fine-mesh net will not tear in use. The net fits inside the expanded metal and attaches around the mouth of the dredge. Nets may be interchanged by removing the nuts and bolts that hold the net to the mouth.

The design for the bridle may take several forms. In order that the dredge function properly, it must remain flat on the bottom. Organisms disturbed by the bottom of the mouth have a tendency to swim upward. By swimming upward, they will be trapped by the overhanging upper mouth and will remain in the net. The bridle must be situated so that, under most angles of pull, the dredge will remain flat and right side up. This is accomplished by designing a sliding portion of the forward runners. A rod, 1/4 inch in diameter, is attached to both the 180° bends on the forward runners (refer to Figure 2.4.1.1). A two-meter chain is shackled on to each sliding portion, free to move as the angle of the towline changes. The towline is attached to the chain bridle.

Several possibilities for bridle attachment were examined. The first is to have an equalizing bridle. In this attachment the towline is able to move along the length of the chain to compensate for the turning of the dredge. The second is to solidly attach the towline to the bridle. This was decided to be the better of the two for our purposes because normally the sampler dredge is pulled in a straight line. This method was used in our tests of the new dredge.

The design of the runners has a significant effect on the operation of the sampler dredge. They are constructed so as to tend to free the dredge in case of a snag (rocks, foreign objects, etc.). The action of the dredge when snagged is to bound over the obstruction. This is the reason for the 180° turn on the ends of the runners. As force increases on the dredge, the line tension will shift to the curved runner ends. Thus, any further tension will have a tendency to lift the drag over the object and to right the dredge when clear as long as the towline remains in tension.

The attachment of the expanded metal is by stainless steel clamps. The expanded metal is attached to the upper mouth and bent back and around to the lower mouth. Side strips of expanded metal are attached to the sides of the drag. One-inch bar stock is welded between the upper and lower runners for the attachment of the side strips.

Attachment of the expanded metal by welding was first attempted, but it was not feasible. The weld caused melting of the expanded metal. The second method was to braze the expanded metal. This failed as well because the surfaces would not hold the brazing.

In the operation of the sampler dredge, it is important that the net remain inside the cage of the dredge. There is a tendency for the net to float out. It is recommended that the after end of the net be lashed to the cage with twine. The speed of the tow should be approximately two or three knots. A hand winch should be used when raising or lowering the dredge.

The basic frame of that second, Cape Town-type dredge was welded together, then heated and bent to obtain the required shape. Since 1" x 1/8" x 1" angle iron was used, special care had to be taken when heating and bending so as not to crack or weaken the steel. After the basic frame had been assembled, strength members were added to the top and sides to prevent the possibility of the dredge being deformed when towed over rough bottoms. After the strengthening members were added, the mild steel skids (see Figure 2.4.1.2) were cut and formed to size. These skids were formed into a semicircular shape and were welded to the front end of the dredge. The depth of the skids had to match that of the front end of the dredge so that there would be a close fit to make it possible for welding. Special attention was given to the design of the selection of the lower front section of the dredge which transmits most of the dragging force. A half-inch diameter cylindrical base was used. It was heated and formed to shape so as to fit the already constructed frame. This bottom forward piece (see Figure 2.4.1.1) was set back further than the top forward piece so that, when dragging along the bottom, samples having a tendency to be shot straight up by the dredge are captured instead by the overhanging edge rather than missing the dredge altogether.

Screening was chosen for the dredge because of its light weight and the ease of procuring various sizes for the purpose. The screening that was chosen was 1/4" mesh for the after section and 1/2" mesh for the forward section. The reason for the coarse screening forward and the fine screening aft is that, when towing the dredge along the bottom, the samples have a tendency to stay in the middle of the dredge, while in the forward section they are pushed to the back and sides toward the end. Also, with coarse screening at the forward end a good portion of the mud will filter through allowing more time for towing. The screening is held within the frame by 1/2" x 1/2" pieces of mild steel which are bolted to the frame holding the screening in place. A steel handle was welded on the back of the dredge to facilitate dumping the samples onto the deck.

The chain bridle is attached to the two front skids and brought to a point three feet ahead of the dredge. From this point a single line is fixed and led to the boat to complete the towing process.

Tests

The two dredges were each tested against the existing dredge over both muddy and rocky bottoms. In each case, the dredges were hauled over a 100-meter distance at a depth of approximate-

ly 10 meters. Each dredge was connected to the 34-foot inboard towboat via a 20-meter line.

Each of the new dredges proved superior to the existing dredge. While the Cape Town-type dredge appeared marginally superior, the limited number of tests run were insufficient to demonstrate this conclusively. Further tests are planned as part of the regular oceanography program at MMA for Autumn 1976.

Table 2.4.1.1 summarizes the results of the comparison between the old dredge and the first of the new dredges, which was most similar in shape to the original. As the table indicates, the new dredge was markedly superior to the existing dredge. It can be towed faster, thus enabling more samples to be gathered in a given time. It can be used in a wide variety of depth and current conditions because of its greater weight. Finally, its stronger construction allows it to be used effectively on the bottom environment that would damage the existing dredge.

A further test was run on the new dredge alone to determine its characteristics without the fiber net as, for example, in the collection of larger organisms such as sea urchins and sea cucumbers. In this configuration, the drag was successfully towed at speeds of up to five knots over a boulder-strewn bottom. The dredge encountered several objects so large as to momentarily stop the towboat (a 34-footer); after freeing itself (presumably by glancing over or around the obstruction), the dredge was undamaged and the collection of samples continued.

In the only direct comparison of the two new dredges, the Cape Town type appeared to be better suited to towing against strong currents, exhibiting less tendency to bounce off the bottom in three- to five-knot currents. Further, the Cape Town dredge showed significantly less tendency to capsize in use. As noted previously, more tests will be required to find whether these preliminary results are indicative of true superiority. The sample-gathering abilities of the two new dredges appeared roughly comparable.

Conclusions and Recommendations

The results of the above study indicate:

- The new dredges performed satisfactorily, successfully collecting a large variety of samples under both muddy and rocky conditions.
- The new dredges were superior to the existing dredge in ability to reach bottom in rapid currents, in ruggedness, and in ability to operate while filled with mud.
- There appears to be no significant advantage of one new dredge over the other. Limited evidence suggests that the Cape Town (Day) Dredge may have less tendency to capsize in use.

Table 2.4.1.1

Results of Comparison Tests of New and Old Sampler Dredges

Test #	Bottom	Current	Drag Speed	Results (existing dredge)	Results (new dredge)
1	Hard	2 knots	2 knots against current (4 kn total)	Dredge did not touch bottom. No samples collected	Dredge on bottom for full 100 meters. Collected over 75 identifiable individuals including: sea urchins scallops flounder starfish shrimp hermit crabs crabs
2	Soft	1 knot	1 knot against current (total speed 2 kn)	Dredge on bottom for full 100 meters. Collected much mud and the net ripped	Dredge on bottom for full 100 meters. After mud was sieved through the net, the following were collected: 1 bottle several sea urchins 1 starfish

Table 2.4.1.2

Technical Description
(Sample Dredge)

The specifications of the Cape Town (Day) Dredge built to this project are as follows:

	Front	Back
Width	27-1/2"	16-1/2"
Depth	15-1/2"	11-1/4"
Length Overall	54-1/2"	
Weight	60 lbs	
Winch	Hand winch on PANTHALASS with a capacity of 200 lbs	
Manpower Required	Winch operator and two men on deck	
Material - frame	Mild steel angle iron 1" x 1/8" x 1"	
screening	1/2", 1/4"; 1/2" forward, 1/4" aft	
chain	6' of 1/2" links for the bridles	
Speed for towing	Less than 1 kn or drift	
Wire at/meter depth	2:1	
Suggested fishing time	20-25 min	
Special comments	This device works well and can be used in reasonably rough weather	

See Figure 2.4.1.2

- The additional weight of the new dredges compared to the old dredge (new: 50 pounds; old: 15 pounds) makes them more difficult to handle ashore, but is insignificant in use. Further, use of mild steel in the new dredges in place of the stainless of the existing dredge will require increased maintenance of corrosion protection.

Time ran out before several important points were resolved. Tests in the following areas are recommended:

- Methods of attaching expanded metal to the dredge framework should be carefully evaluated. (Welding, theoretically a good choice, did not work in practice.)

- Tests should be conducted on the effects of different types of bridles (stationary, equalizing, etc.) as applied to the two dredges and various bottom and towing conditions.

- Further comparison tests between the two types of dredge, including underwater observation of the dredges in operation.

Acknowledgments

The authors wish to thank the following people for their assistance:

Professor John Barlow for his assistance with the early designing stages.

Captain Willard F. Searle who introduced us to several types of bridles which were very useful.

Mr. Groves E. Herrick whose advice and supervision were invaluable.

2.4.2 SAMPLER DREDGE HANDLING EQUIPMENT

The focus of this project was the construction of a handling device to be mounted on the stern deck of the 34-foot MMA work boat PANTHALASS, for a small experimental dredge used to collect specimens of marine life (Figure 2.4.2.1).

Background

The dredge had previously been deployed from a davit on the side of the boat. The idea for a different method of deployment came from magazine articles on Australian scallop fisheries. There, fishermen have devised a dredge-handling device operating over the stern of a boat rather than amidships, using scallop dredges greatly resembling the MMA dredge. The dredge is under greater control than when handled from a boom, and it has been found to require fewer men to empty a dredge. The purpose was therefore to adapt the Australian concept to the dredge and boat.

Construction

Drawings of the Australian "rocket launcher scallop tipper" are shown in Figure 2.4.2.2. A warp, running from a winch on the fishing vessel to the dredge in the water, passes over a sheave on the top of the handling device. The winch lifts a rigid dredge vertically out of the water until the dredge hits stops on the tipper. Continued pulling on the warp causes the device to tip, rotating about a pivot point until dredge and tipper are inclined at a 45 degree angle with the horizontal. In this dumping position, the contents of the drag spill out onto the deck for collection. (The dimensions of the tipper are designed so that it will not tip until the dredge, in its vertical ascent, hits the stops on the handling device.) Upon letting up on the winch, the tipper and dredge then rotate back to the vertical position from which the dredge can again be lowered into the water.

Stress calculations indicated that 1"-diameter steel pipe would be of sufficient strength for expected static loads, and sections of this material were welded together to form the handling device (see Figure 2.4.2.3). It was mounted on the stern deck of PANTHALASS atop a plywood platform which distributed the vertical load. The completed assembly is shown in Figure 2.4.2.4. The afterdeck was shored up with vertical 3/4"-plywood sheets to prevent its failure should the dredge become caught on rocks and the handling device have experienced forces approaching the 1-1/2-ton breaking strength of the warp.

Operation

The operation of the handling device was tested under a variety of circumstances, including actual dredging in mud flats near Castine, Maine. The clam population of New England is none the worse for that particular escapade. (The experimental dredge is still in the experimental stage.) The dredge handler worked, though a number of problems required occasional manhand-

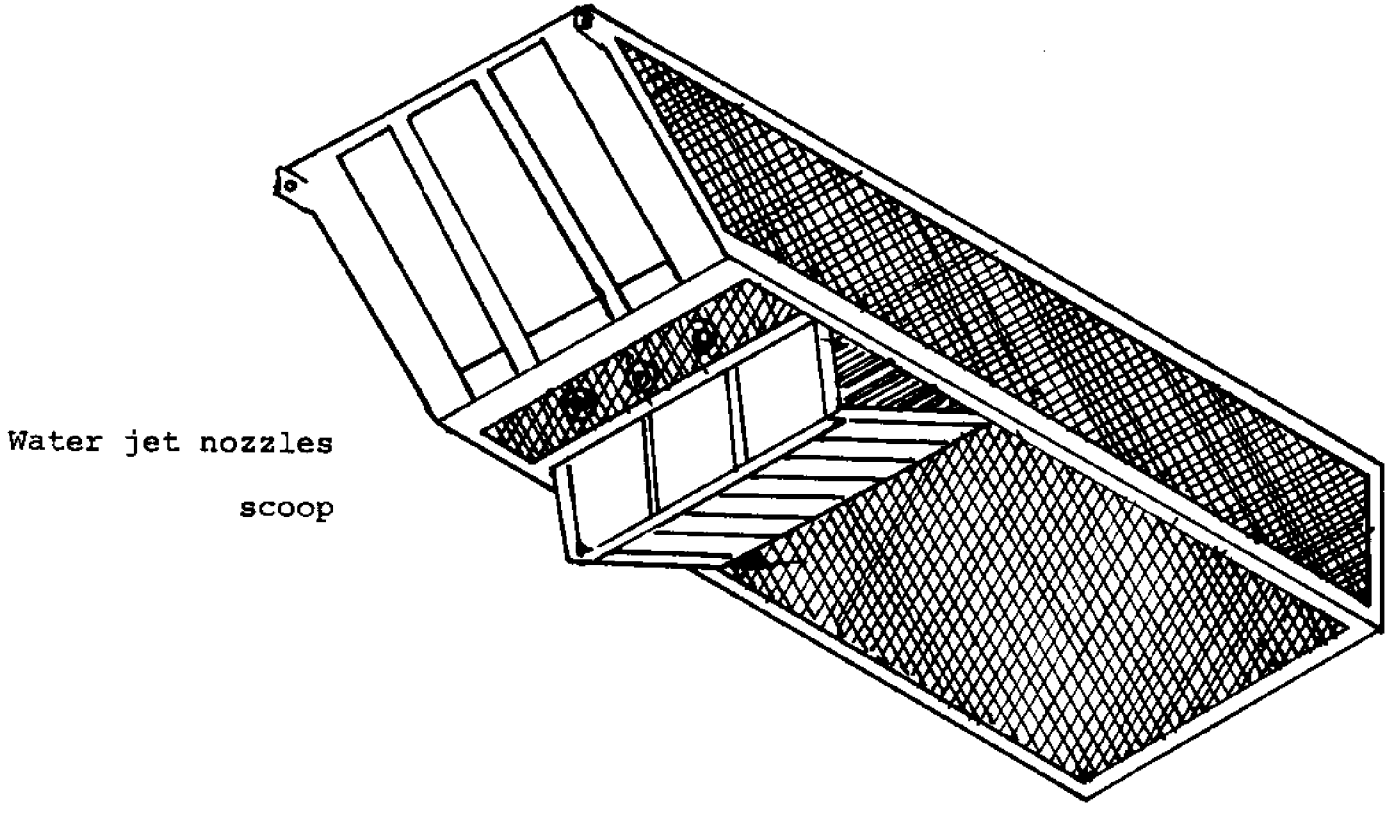

Figure 2.4.2.1

Isometric View of Experimental Hydraulic Dredge Scale 1 : 10

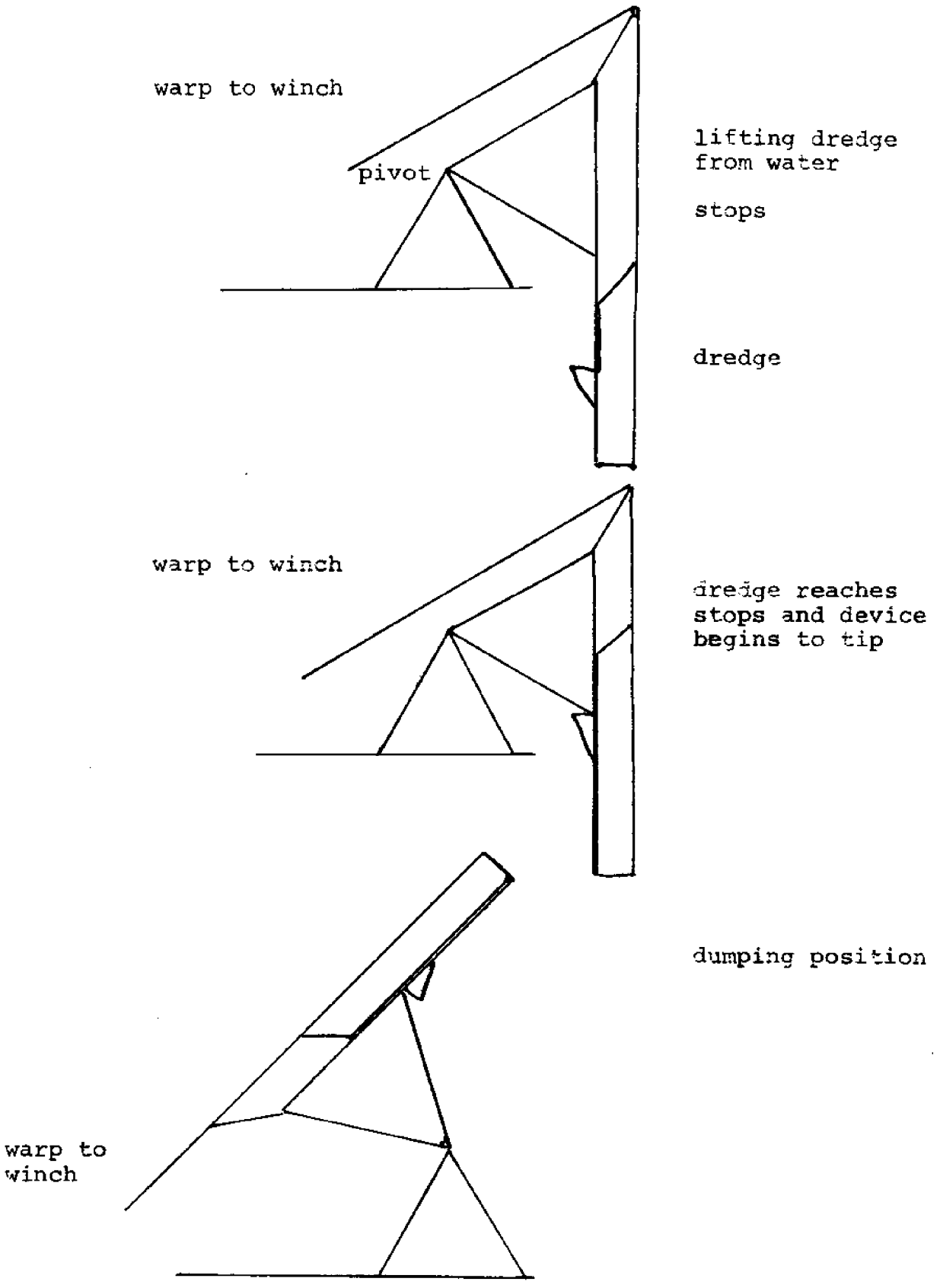

Figure 2.4.2.2

Operation of Dredge Handling Device

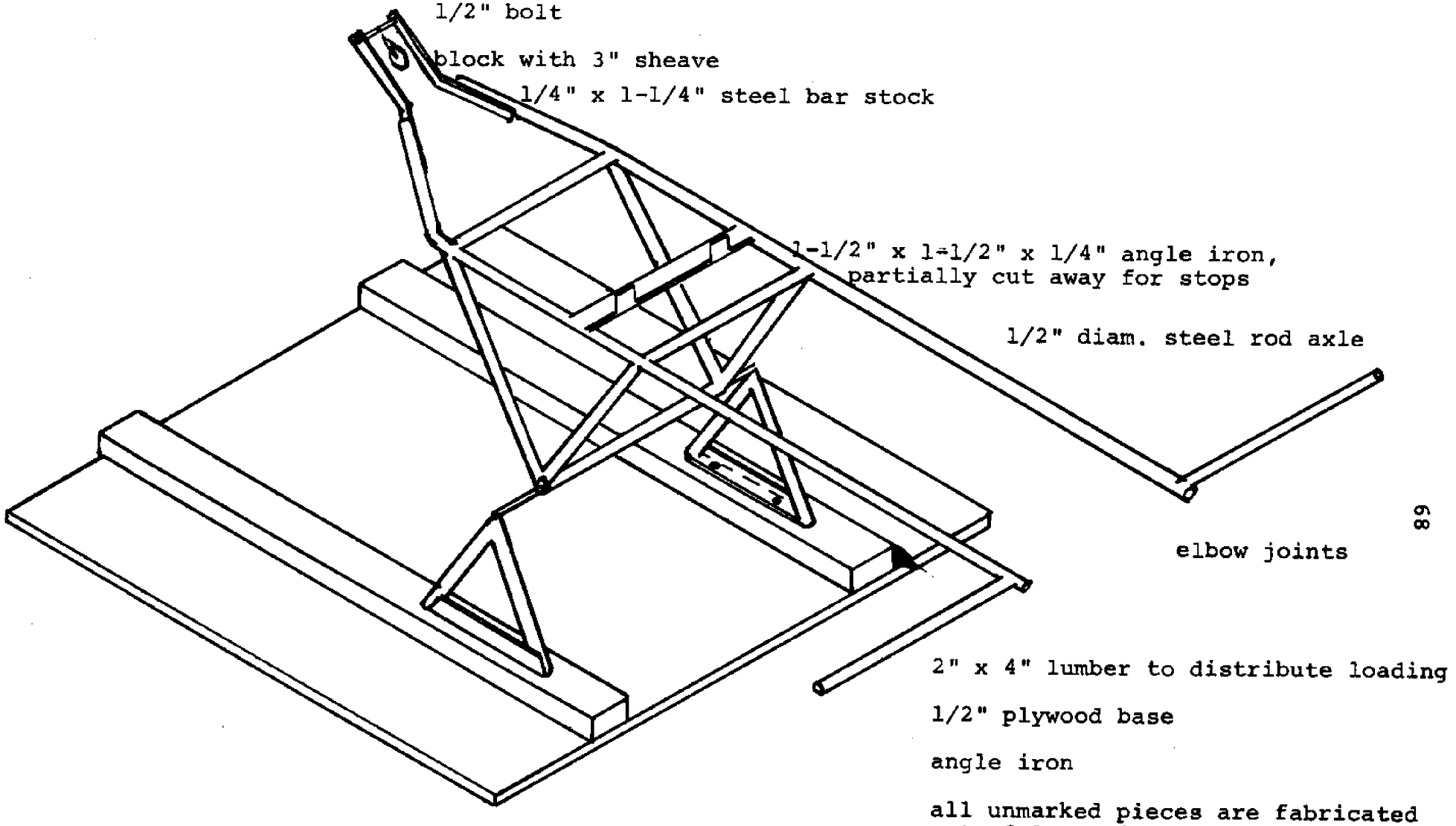

Figure 2.4.2.3

Isometric View of Dredge Handling Device. Scale 1 : 12

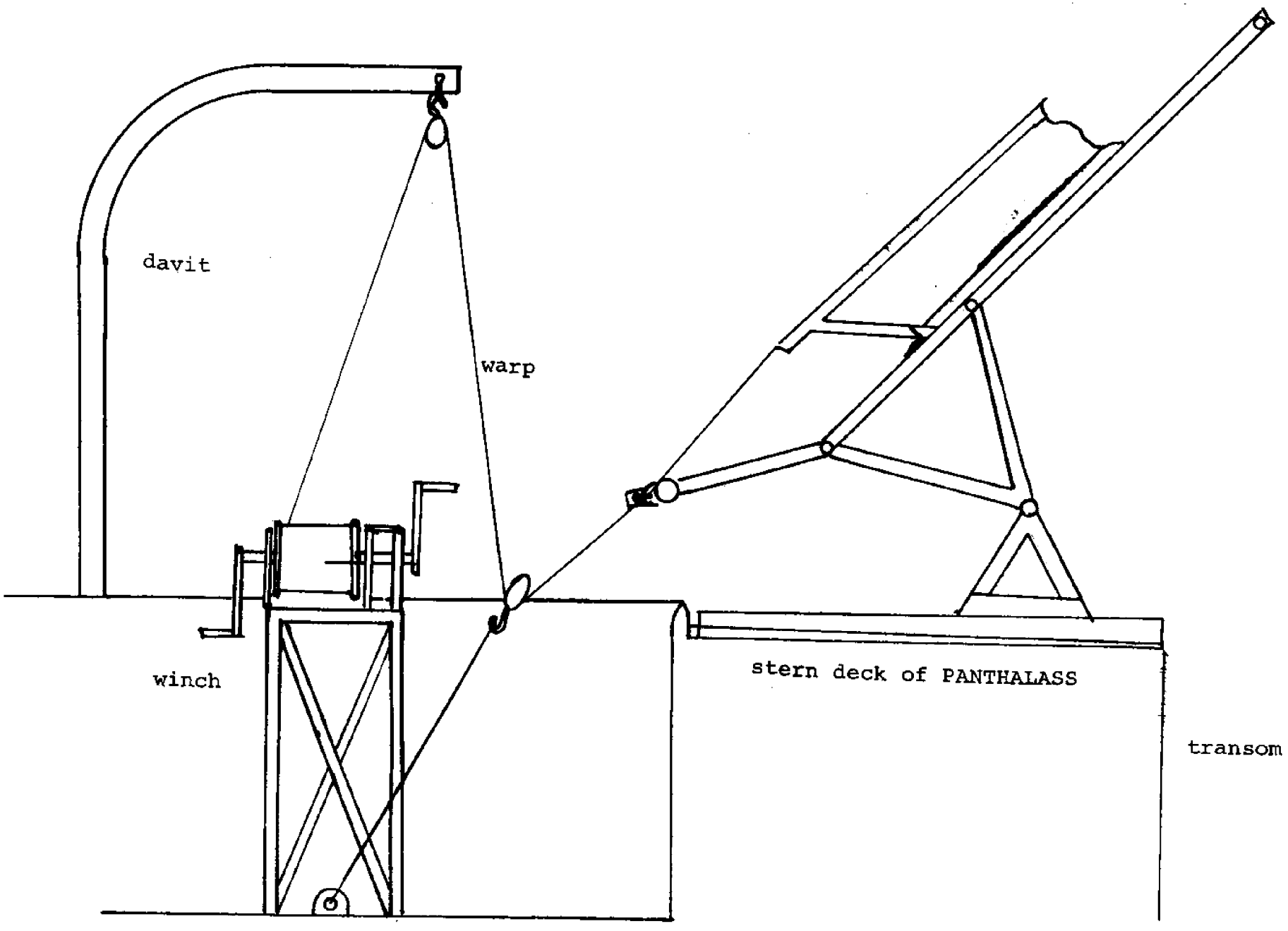

Figure 2.4.2.4

Complete Configuration

ling. The major difficulty was in aligning the dredge on the tipper. The dredge at times came out of the water at an angle so that it hit against and caught on one of the right-angle elbow joints at the bottom of the tipper (Figure 2.4.2.3). This problem could be remedied by placing the elbow joint at a location not likely to catch the dredge. A greater problem was the tendency of the dredge to rotate as it came out of the water so as not to be parallel to the transom of the boat, preventing alignment. This rotation may have been caused by the lay of the wire rope which served as the warp which would twist as passing over a sheave. Since the dredge was stable parallel to the transom while the PANTHALASS was underway, the use of unlaid wire for a warp would probably alleviate this problem, as would a swivel placed between the dredge and warp to prevent the twisting motion of the warp from being transmitted to the dredge.

Less troublesome difficulties were those of operating the tipper with the small hand winch on PANTHALASS, and of objects not emptying from the dredge at a tipping angle of 45 degrees. A greater tipping angle, or a dredge made of finer mesh in which objects could not become lodged may be the answer. The need for more formidable stops on the handler became painfully apparent when the dredge came flying off the tipper toward the deck after having been tipped with too much vigor. There would be a definite danger of the dredge tumbling to the deck were a power winch used, since it could not be so readily controlled as a hand winch.

Conclusions and Recommendations

The problems thus far encountered all appear readily resolvable, given more time which we lacked. With further work, this handler could be developed into a safe, easy method for one man to handle a dredge presently requiring the services of two. Whether any further effort on this particular handling device is justifiable depends on the future of the dredge which was used. Work on this handler has no particular application except for use with this dredge. If it were believed that there was some commercial value in this rigid type dredge in New England either for scalloping or clamming, then developing this handling device would certainly be worthwhile. However, rigid scallop drags are not used in New England waters, and numerous opinions have been received that such dredges are unsuitable for rocky New England ocean bottoms. Further, the fact that clams are dredged in other areas such as Chesapeake Bay, but are hand dug with clam rakes in New England, where labor is comparatively expensive, suggests that dredging for clams is not practical in this area. In this event a more fruitful endeavor would be work on the construction of a handling device for typical Maine scallop dredges. That is a definite need of New England fisheries.

New England scallop dredges are handled from a boom over the side of the vessel amidships. A dredge swinging from a boom can be difficult and dangerous to manage, and working with the

dredge amidships exerts forces along the vessel's least stable axis, giving stability problems. The weight of a large boulder caught in the dredge can cause the boat to heel over to the side from which the dredge is suspended. When the dredge reaches the surface and is no longer buoyed up by the ocean, the sudden addition of force on the already heeling boat may cause it to capsize. What is needed is a handling device on the stern of the vessel which would take advantage of the great longitudinal stability of ships.

Unlike the box-like Australian dredges used over flat sand bottoms, the New England dredge is a flexible metal bag of a construction resembling chain mail attached to a metal frame which can slide over rocky ocean bottoms (see Figure 2.4.2.5). For this type of dredge, a tipper arrangement such as the one built here would not be an appropriate solution. Instead of being inclined in the dumping position used for a rigid dredge, a wire bag must be suspended vertically in order for the contents to fall out of the bag. A Maine dredge bag has a bottom opening which is sealed except for emptying the catch. A good handling device would lift the dredge over the stern and suspend the dredge above the deck so that the bottom could be opened for emptying.

Although no work was done with scallop dredges while in Castine, some thought has been put into designing a handler for these dredges. Two conceptual configurations are shown in Figures 2.4.2.6a and b. In 2.4.2.6b the dredge is hauled over the stern on a ramp until the dredge slips off the ramp into a vertical position for emptying. It is a very simple arrangement, but has the problem of replacing the dredge back on the ramp so that the dredge can be returned to the sea. Lifting a heavy dredge onto the ramp would likely require power machinery. The second design (2.4.2.6a) somewhat resembles the dredge handler which was built at MMA except that the dredge is always in a vertical position. The dredge is lifted out of the water until it hits stops on the handling device, at which time the device swings the dredge on board for emptying. When emptied, the dredge can be lowered back into the sea simply by letting up on the winch controlling the dredge. Hopefully, more work will be done on dredge handlers along these lines.

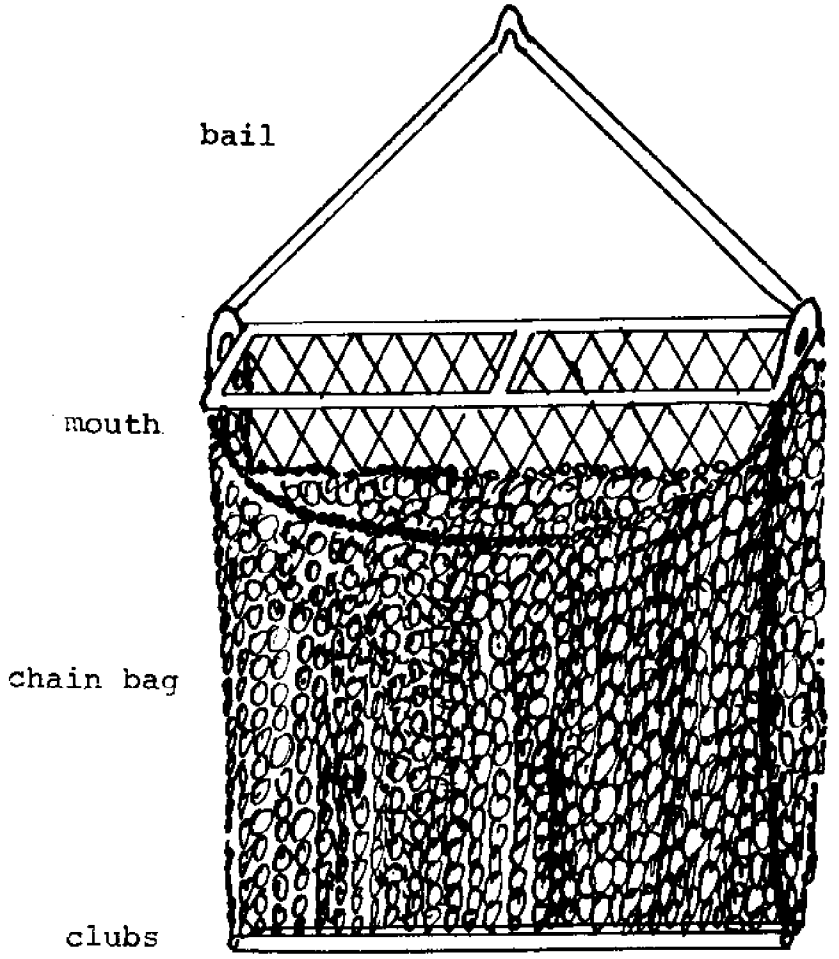

Figure 2.4.2.5

Conventional Scallop Dredge

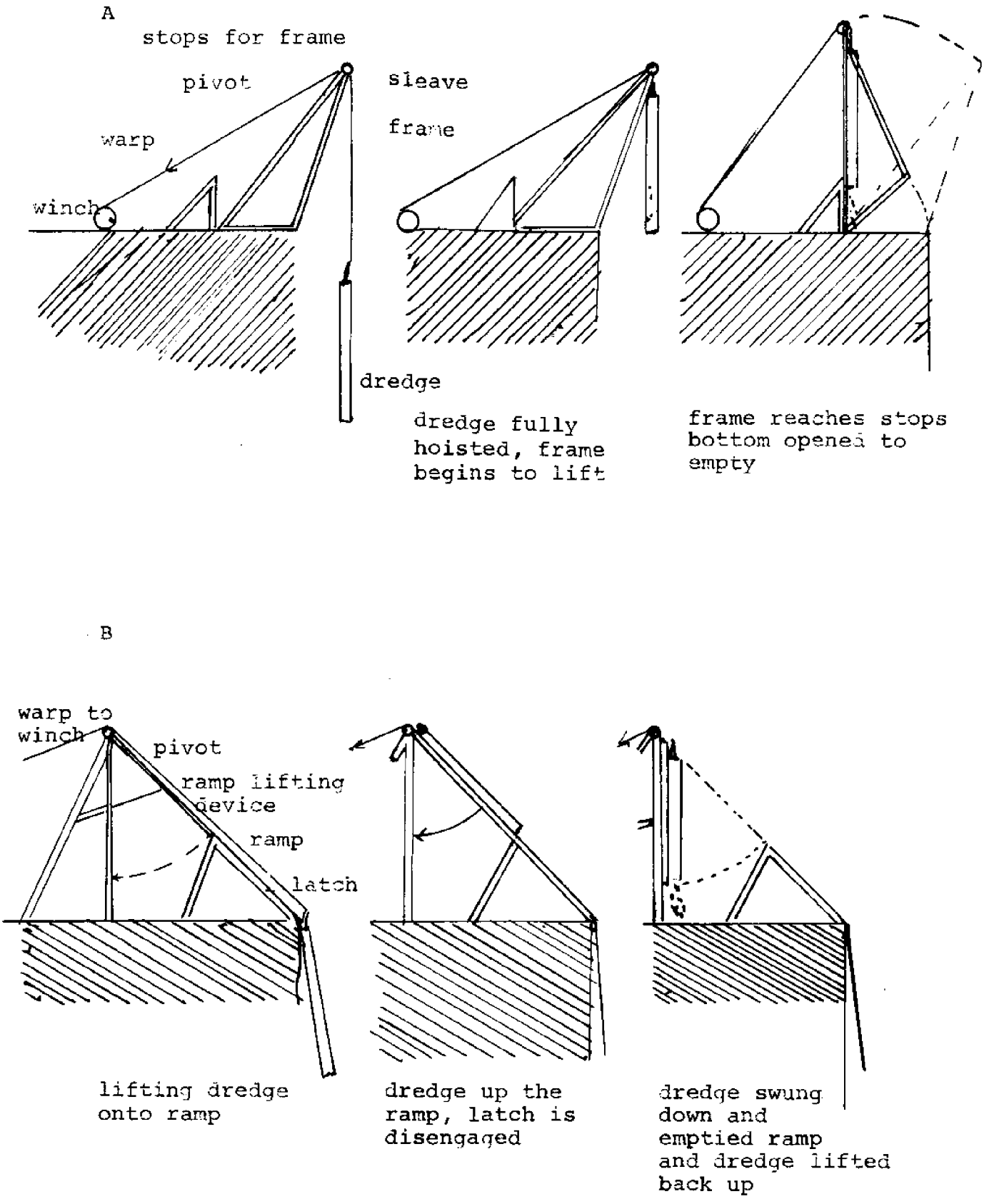

Figure 2.4.2.6

Conceptual Configuration for Dumping a Non-Rigid Scallop Dredge

2.5 CONSTRUCTION AND TEST OF A PORTABLE FLOATING BREAKWATER

2.5.1 THE PORTABLE FLOATING BREAKWATER

The idea of developing a portable floating breakwater was suggested to the academy in 1973 by Dr. Buckminster Fuller, the purpose being a breakwater that was both environmentally safe and portable. The breakwater was to be designed so that it could be easily deployed and retrieved by two or three men in a small boat without any detrimental effects to the environment.

Background

During the first summer a prototype was developed utilizing tire inner tubes three-fourths filled with water and pressurized by air. A plastic covering was then wrapped around the tubes forming a cylinder. After deployment in Castine Harbor, seas ripped the covering. The summer of 1974 brought about a model utilizing six-foot-diameter truck tire inner tubes and a vinyl nylon canvas cover forming a six-foot-diameter cylinder sixty feet long. Due to the tubes' weight (500 lbs each), its limited maneuverability prevented the final assembly. During the summer of 1975 plastic water pipes were substituted to form the hoops. Plastic couplings were used to seal the joints, and weight was placed on the hoop to provide stability. The canvas from the previous year was used. Twelve days after installation several of the hoops crumpled and filled with water.

The plan for 1976 was to construct a breakwater similar to the one of 1975, but with a new set of hoops formed from aluminum tubing sent through a radius-bending machine. The hoops were then welded after a determined amount of concrete was added to each hoop in order to make the breakwater float with three-fourths of its diameter below the surface. The nylon canvas cover from last year was used again, forming a cylinder six feet in diameter and sixty feet long.

Technical Description

In 1975 1-1/2-inch plastic pipe was used to form the hoops for the breakwater. These hoops proved to be not strong enough, and a more rigid type of tubing was recommended for future construction. The pipe we found best suited for our needs was 2"-diameter aluminum tubing with a wall thickness of 0.063". The tubing was sent through a radius-bending machine forming a six-foot diameter.

Weight was added to each hoop in order for it to float with 3/4 of its diameter below the surface of the water.

The weight of the tubes was found as follows:

$$M_{tube} = A \cdot L \cdot D = [\pi(R_o^2 - R_1^2][\pi \cdot 6 \text{ ft}][D_{AL}]$$

$$M_{tube} = \pi((10 \text{ in})^2 - (0.937 \text{ in})^2)(6\pi)(0.98 \text{ lb/in}^3)$$

$$M_{tube} = 8.49 \text{ lbs}$$

The tarp used has a specific gravity of approximately one so only the weight of the tarp being supported by hoops above the water had to be determined:

$$M_{tarp} = \frac{\text{length cut}}{\text{circumference}} \cdot \frac{\text{tarp weight}}{\text{\# of rings}}$$

$$M_{tarp} = \frac{5.26 \text{ ft}}{\pi \cdot 6 \text{ ft}} \cdot \frac{150 \text{ lbs}}{11 \text{ rings}}$$

$$M_{tarp} = 4.02 \text{ for each ring}$$

Next the buoyancy of the tubes was calculated:

$$B_{tube} = A \cdot L_{\text{in water}} \cdot D_{H_2O}$$

$$B_{tube} = (\pi R^2)(\pi \cdot 6 \text{ ft} - 5.56 \text{ ft})(64 \frac{lb}{ft})$$

$$B_{tube} = 18.1 \text{ lbs}$$

From these calculations the weight to be added to each hoop was determined:

$$W + M_{tube} + M_{tarp} = B_{tube}$$

$$W = 18.1 \text{ lbs} - 4.02 \text{ lbs} - 8.49 \text{ lbs}$$

$$W = 5.59 \text{ lbs}$$

In order for the breakwater to float three-fourths underwater, 5.59 lbs of weight had to be added to each hoop. Concrete served as the weight. The concrete was held in place by a dent put in the tubing about 2-1/2 feet from where it was poured in.

Next each hoop was welded in order to make it watertight. Tungsten inert gas (Tig) welding was used.

To construct the breakwater, a line was passed through all of the hoops and strung between two points about 60 feet apart and 8 feet off the ground. The cover was then placed over the line and hoops, and was lashed into place through grommet holes. The D rings (see Figure 2.5.1.1) were lashed to the ends, and the two edges of the cover were lashed together.

Two methods were used for deploying the breakwater. The first method was to secure the breakwater on the beach at low tide with 100 feet of nylon mooring line and a 75-lb mushroom anchor shackled to each end. Once the tide comes in and the breakwater is afloat, it can be towed to its desired location and properly moored. The second method was to make the breakwater into a pile about 3-1/2 feet high by stacking the rings one on top of another. A 75-lb mushroom anchor and 100 feet of nylon mooring line is again shackled to each end. With the

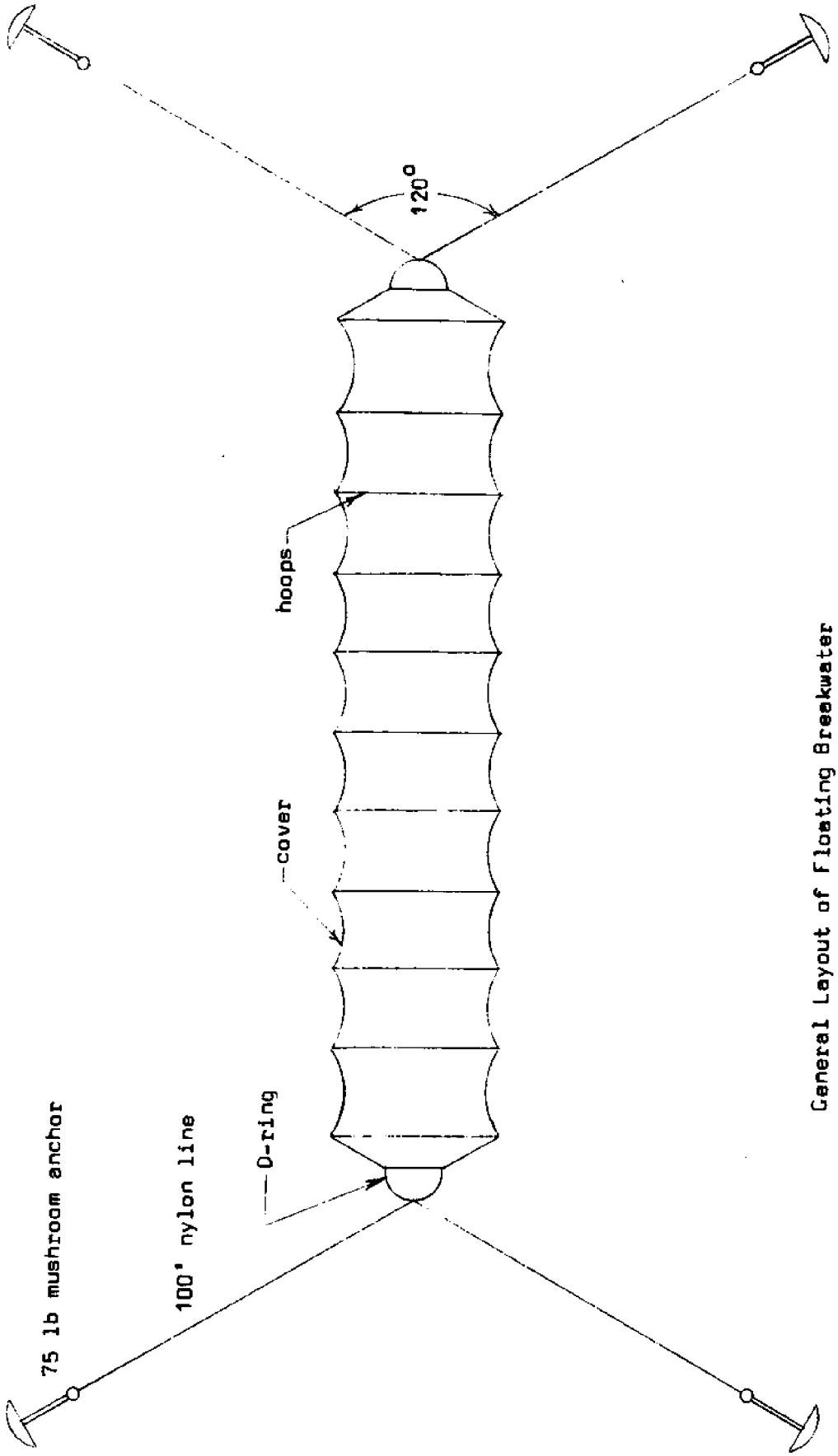

General Layout of Floating Breakwater

Figure 2.5.1.1

breakwater placed in the stern of a boat when at the desired location, the anchor on top is thrown over and the hoops are payed out one at a time by slowly moving the boat forward, and the second anchor is set. Then the other two anchors are set. For retrieval of the breakwater, it was towed close to the shore at high tide and secured. Once the tide goes out and it is beached, the breakwater can be stacked into a pile and carried by four people. The breakwater was also retrieved by the reversal of the second method of deployment. By starting at the downwind end, the hoops are pulled over the stern of the boat one at a time. It is necessary to undo some of the lashing in the stern and the D ring in order to let the water inside to flow out.

Conclusions and Recommendations

The structural problems of the breakwater seem to have been solved this year. The aluminum hoops proved to be of sufficient strength and remained watertight. Our major problem was the mooring system. This mooring system was not strong enough to hold the breakwater across the current. It is recommended that a better mooring system be designed. The same system could be used by substituting more suitable anchors, however; the forces on the breakwater should be estimated and the elements analyzed to ensure that all will withstand the currents encountered in any prospective mooring area.

Table 2.5.1.1

NOMENCLATURE

A = Cross sectional area of metal in the tubes forming the ribs of the breakwater (in^2)

B_{tube} = Buoyancy of a tubular breakwater rib (lbs)

D = Density of aluminum (lb/in^3)

L = Length (circumference) of tube forming the breakwater rib (ft)

M_{tarp} = Weight of canvas covering associated with each breakwater rib (lbs)

M_{tube} = Weight of tubular breakwater rib

2.5.2 MEASURING THE EFFICIENCY OF A PORTABLE BREAKWATER

In 1973 Buckminster Fuller suggested that Maine Maritime Academy (MMA) build a portable breakwater according to a design which he proposed. Over the past three years the Ocean Engineering Summer Laboratory has worked on this breakwater with various improvements. In the summer of 1976 students from MMA completed a 60-foot-long breakwater; a description of the breakwater is elsewhere in this report. This section describes how the efficiency of this breakwater was measured.

Background

Efficiency (h) is defined as:

$$\eta = 1 - \frac{\text{Wave Energy Transmitted Through Breakwater}}{\text{Wave Energy Incident on Breakwater}}$$

By this definition, the efficiency is unity if no waves penetrate the barrier and zero if all the waves get through. It can be shown that the energy in a wave is directly proportional to the square of the wave height. When the incoming waves have components of many frequencies, the significant height ($H_{1/3}$) is used. The significant height of a wave spectrum is the average height of the tallest third of all the waves. So efficiency can be expressed as:

$$\eta = 1 - \frac{(H_{1/3})^2_{\text{transmitted}}}{(H_{1/3})^2_{\text{incident}}}$$

The task is then to measure the wave heights on both sides of the breakwater, to measure $(H_{1/3})_{\text{transmitted}}$ and $(H_{1/3})_{\text{incident}}$.

To measure wave heights, a fixed reference point is needed. The site where the breakwater's efficiency would be measured was several hundred yards offshore and in a water depth of about fifty feet. These conditions prohibited viewing from shore or using reference piling lodged in the bottom. A spar buoy (designed for minimum response to wave excitation of waves having less than 200-foot length) was used as a height reference standard. The spar buoys used were 25 feet long, 3-1/2 inches in diameter, and had a heave damping plate on the bottom.

A record of the waves against the spar buoy was made with a super 8 movie camera. A small power boat was maneuvered to within fifty feet of each buoy where the movie camera photographed the waves. The film was developed, and a special projector was used to show one frame at a time the height of each wave. These data were then analyzed to determine the breakwater's efficiency.

The Buoy

For satisfactory performance of the spar buoy (minimum movement with the waves), several conditions are required:

1) The buoy must float with five feet above the water; 2) the buoy must float upright; 3) the buoy's natural period of heave should be large compared to the dominant period of the waves; 4) the buoy's natural period of pitch should be large compared to the dominant period of the waves.

For a buoy to float with five feet above water, the buoyancy at the corresponding draft must equal the weight. For definition of symbols see Table 2.5.2.1.

$$B = \rho V_u = \rho (V_a + V_p)$$

$$B = 64 \text{ lb/ft}^3 \ (.29 + 1.33)\text{ft}^3 = 104 \text{ lb}$$

$$W = W_p + W_B + W_A + W_E$$

$$W = 37 \text{ lb} + 48 \text{ lb} + 12 \text{ lb} + 7\text{lb} = 104 \text{ lb}$$

$$B = W$$

For the buoy to float upright, the metacenter (in this case it is for all practical purposes the center of buoyancy) must be above the center of gravity. Calculations locate the center of buoyancy 8.1 feet above and the center of gravity 7.5 feet above the sea anchor.

The buoy will tend to move up and down with the waves (heave). This motion must be minimized for the spar buoy to act as a stationary reference point. This requires that the natural heave period of the buoy be much greater than the dominant frequency of the wave spectrum.

$$P_H = 2 \cdot \pi \sqrt{\frac{W_{TH}}{g \cdot K}}$$

$$W_{TH} = W + W_{AH} = (104 + 964) \text{ lb} = 1068 \text{ lb}$$

$$P_H = 2 \cdot \pi \cdot \sqrt{\frac{1068 \text{ lb}}{32 \text{ ft/sec}^2 \cdot 4.25 \text{ lb/ft}}}$$

$$P_H = 17.6 \text{ sec} >> P_W$$

K = buoyancy per foot length of buoy

W_{TH} = total weight in heave

W_{AH} = weight of entrained water

W = weight buoy

P_H = heave period

P_W = wave period

TABLE 2.5.2.1

NOMENCLATURE

ρ	= Density of water	64 lb/ft^3
V_U	= Volume of buoy underwater	1.62 ft^3
V_A	= Volume of sea anchor	0.29 ft^3
V_p	= Volume of pipe underwater	1.33 ft^3
B	= Total buoyant force on buoy	104 lb
W	= Weight of buoy	104 lb
W_p	= Weight of piping	37 lb
W_B	= Weight of ballast	48 lb
W_A	= Weight of anchor	12 lb
W_E	= Weight of extra items	7 lb
P_H	= Natural heave period of buoy	17.6 sec
W_{TH}	= Total weight for heave motion	1,068 lb
g	= Acceleration of gravity	32 ft/sec^2
K	= Buoyancy per length at waterline	4.25 lb/ft
W_{AH}	= Weight of dragged water (heave)	964 lb
P_W	= Dominant period of waves	3 sec
P_p	= Natural pitch period of buoy	9.7 sec
R	= Radius of gyration of buoy	7.3 ft
BG	= Distance between center of buoyancy and center of gravity	0.6 ft

The spar buoy must also be prevented from pitching because of wave action. For this requirement the natural pitch period of the spar buoy must be much greater than the dominant period of the wave spectrum.

$$P_p = \frac{2 \cdot \pi \cdot R}{\sqrt{g \cdot (BG)}}$$

P_p = period in pitch

BG = distance between centers of buoyancy and gravity

Calculations indicate that the radius of gyration (R) is 7.3 feet. In calculating R, the added mass of the entrained water must be taken into account.

$$P_p = \frac{2 \cdot \pi \cdot 7.3 \text{ ft}}{\sqrt{32 \text{ ft/sec}^2 \ .6\text{ft}}}$$

The theoretical predictions were verified by initial calm water tests of the buoys. The spar buoys of this design are cheap, easy to build, easy to handle, and perform well.

The Mooring

Three buoys were used for measurements. One was placed in the shadow of the breakwater (to measure only the transmitted waves). The second buoy was placed immediately in front of the breakwater (to measure the incident plus reflected waves). The last buoy was placed off on one side to measure on incoming waves. From these three measurements, one can see what happens to all the incident energy.

$$E_{incident} = E_{reflected} + E_{dissipated} + E_{transmitted}$$

During measurement, the lazy lines were drawn tight. When no measurements were being made, the lazy lines were loosened to allow for movement of the breakwater to which the lines were attached.

The breakwater presented a large cross section to the current, which created large forces on the mooring lines. This resulted in some polypropylene line snapping and the breakwater's anchors being dragged along the bottom.

The mooring lines to the spar buoys proved to be reliable when subjected to high currents.

Data Reduction

The waves were photographed against the spar buoys on a super eight movie camera from 25-50 feet away. A special analyst's projector was used to read the heights for individual

motion picture frames. From these data, the significant wave height for each run was determined. This allows the efficiency and the rate of the incident energy to be calculated.

Ideally, a power spectrum of the wave trains should be computed. This would then tell the wavelengths in which the breakwater is most effective (and how effective). Due to the inability of the breakwater's anchors to hold the configuration normal to the current, a power spectrum could not be obtained. In the test area, the direction of the current was close to the prevailing wind direction, and consequently the waves. As a result, waves from a boat wake instead of natural waves were used. This eased analysis because a power spectrum was not needed since a boat wake is monochromatic; the wave height is also its significant height. The disadvantage was that the breakwater's efficiency was measured at only one wavelength.

Data

Data from the experiment were recorded in the form of films from a super eight movie camera. These were then developed and viewed through an analyst's projector. Due to adverse conditions, only three runs of the boat by the breakwater were recorded.

The film itself was hard to reduce for several reasons. The film was not able to record colors well enough to easily distinguish the tape markings from one another or the spar. Nor was it easy to distinguish the exact waterline on the spar. Also the white color of the spar was well camouflaged by the light reflecting off the background waves.

The results were:

Run	Buoy	Wave Height	Accuracy
First Run	Incident	15"	$\pm$ 3"
Second Run	Incident	14"	$\pm$ 1"
Third Run	Transmitted	10"	$\pm$ 1"

If the two wave heights of 14" and 10" are adopted, the breakwater's efficiency is:

$$\eta = - \left(\frac{10}{14}\right)^2 = 0.50$$

Choosing the extreme possible values of the second and third run, the efficiency can range anywhere between 0.64 and 0.30.

The height of the reflected waves was too small to be detected so the breakwater decreases the incoming wave energy almost purely by dissipation. This seems to be accomplished by the breakwater's writhing when encountering the wake.

For the sake of better planning in the future, a list of the difficulties encountered while running this experiment follows:

1) The data film was hard to analyze;

2) The boat ran out of gas while making the passes;

3) The camera batteries ran low;

4) The breakwater mooring was too weak for strong current;

5) The breakwater lashing snapped;

6) The initial test site did not receive large enough waves.

Conclusions

The buoy design was a success. The buoy's motion with the waves was small. The buoys were cheap, easy to build, and easy to handle. The mooring system proved sturdy and kept the buoys in their proper location.

The camera recording system idea is basically sound. Minor changes will have to be made to make the data easier to reduce. This method of data recording has the advantage of its great simplicity and reliability. It suffers from the requirement that a cameraman must be on the spot to film the waves.

The efficiency of the breakwater is near 0.5 for boat wakes whose period is around two seconds.

Recommendations

1) A number of minor changes can be made to improve the quality of data on the film. The color code of the tape on the spar should be changed to alternating black and orange. Mark each foot by exchanging an orange stripe for a black stripe. Also have a torus-shaped, orange float around the spar to mark the waterline for the camera. A polarizing lens for the camera will reduce the glare. A 16 mm movie camera will improve resolution.

2) The mooring system for the breakwater will have to be improved. Polypropylene line should not be used for the lashing (or elsewhere).

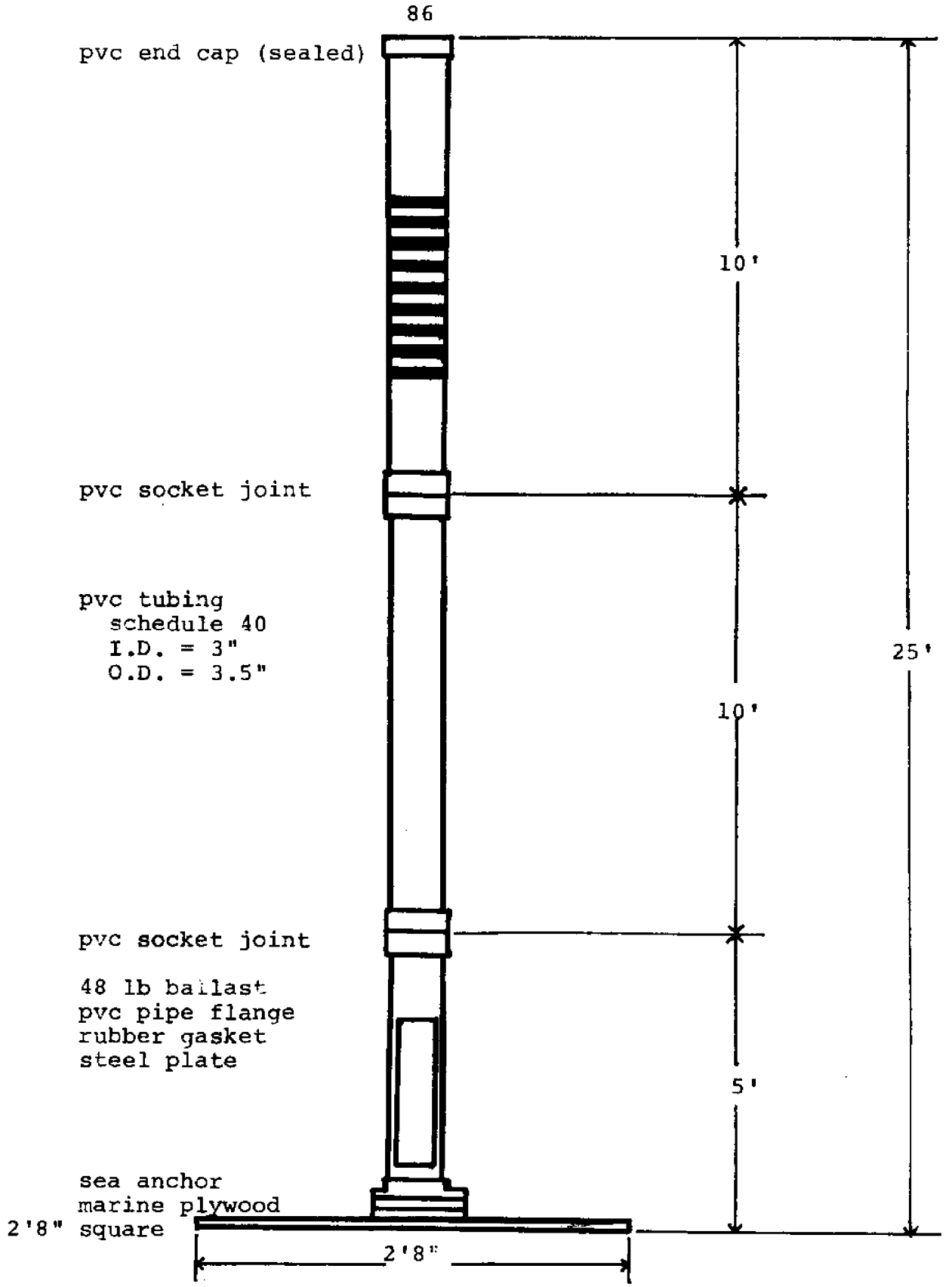

Figure 2.5.2.1

Spar Buoy Construction

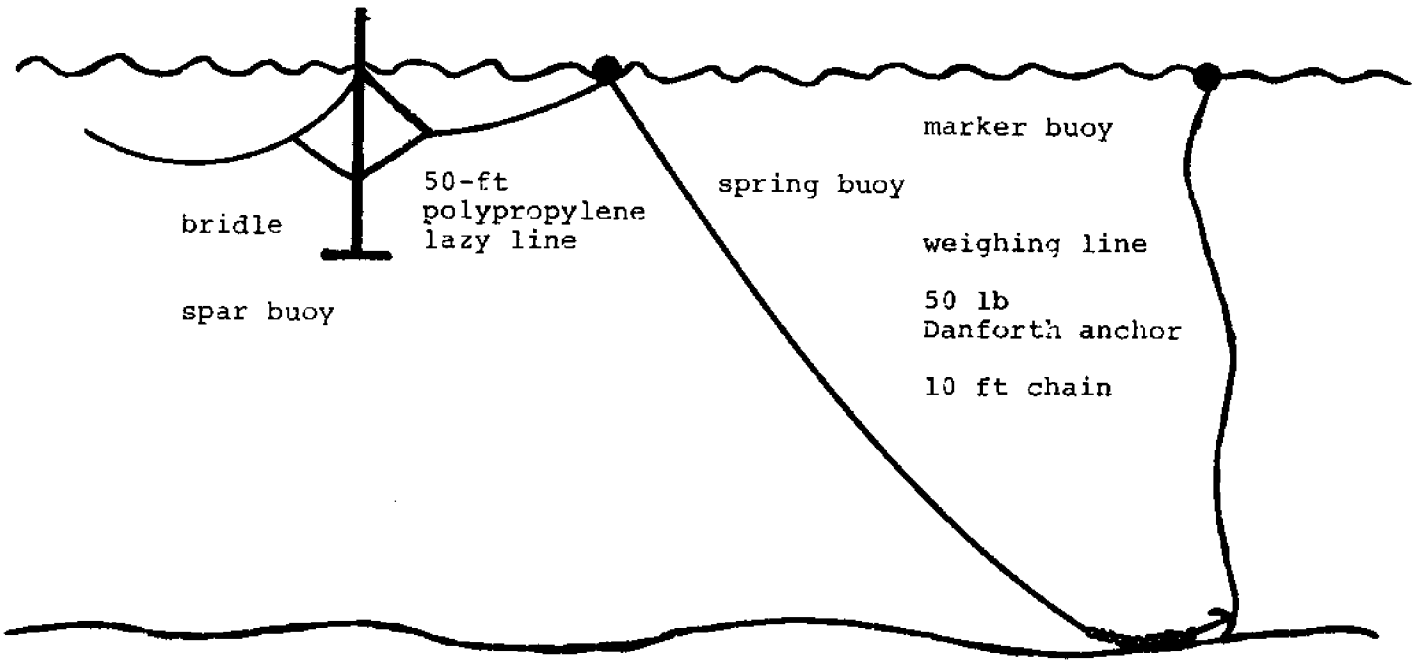

Figure 2.5.2.2 Spar Buoy Mooring System

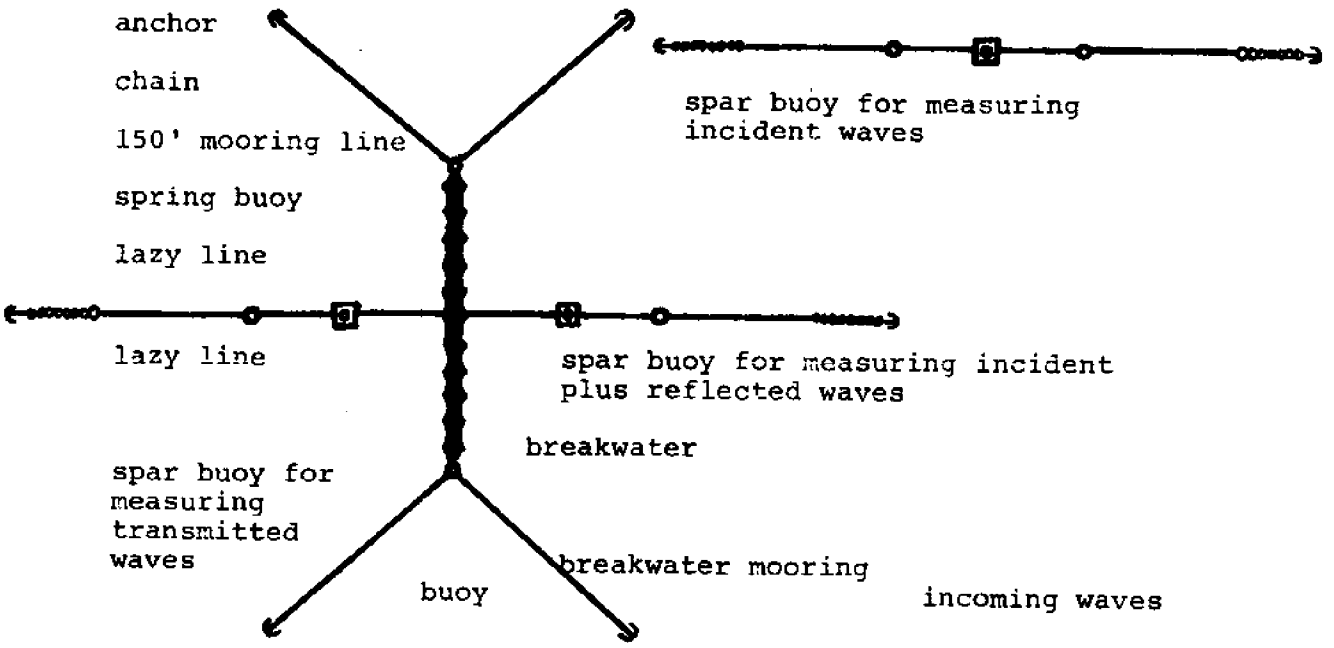

Figure 2.5.2.3 Spar Buoy Placement

2.6 HALL EFFECT ELECTRONIC COMPASS FOR THE ROBOT SUBMARINE

Students of the M.I.T. Ocean Engineering Summer Lab have been developing a robot submarine during the last three years. The robot is approximately 7 feet long and is controlled by an autopilot and computer system. Sensors such as pitch, depth, and roll provide information on the condition of the submarine to the autopilot which adjusts the control fins accordingly. The guidance system is a magnetic compass card which has been modified to produce a voltage readout that varies with magnetic heading. This voltage is used by the autopilot or the computer to control the rudder to maintain or alter course.

Background

The robot's present compass has several drawbacks. The compass consists of a light, a photopotentiometer, and a magnetic card with a spiral scratched on it. As the card rotates, the location on the photopotentiometer where the light hits changes and alters the potential fed to the autopilot. This arrangement has two main problems. The spiral cut on the compass card does not produce a linear readout, which is desirable to facilitate autopilot control. In addition, the magnetic card has a damped oscillation which makes it difficult to provide an accurate measurement of the robot submarine's heading.

These problems are inherent to the design of the compass and can be reduced, but not eliminated, by modifying the construction. An alternate design is required to achieve a more satisfactory compass for the robot's navigation. The requirements are that the compass produce a linear readout with magnetic heading and that the reading be adequately stable in the conditions produced by the moving robot submarine.

Various alternative systems were examined with the emphasis on compasses without moving parts. The most promising system utilized Hall Effect crystals to sense heading. The development of a prototype compass using these devices is described in the following pages.

The Hall Effect

The Hall Effect was discovered in 1789 by E. H. Hall. The Hall Effect is the formation of a small potential difference between opposite edges of a conductor carrying a current and subjected to a magnetic field. This voltage is perpendicular to the direction of the current flow.

The Hall Effect is a result of the Lorentz force; a particle with a charge Q, velocity $\vec{V}$, and moving in a magnetic field $\vec{B}$ will experience a force of $\vec{F} = Q(\vec{V} \times \vec{B}) = Q|V|B| \cos \theta$ where θ is the angle between the direction of the velocity and the direction of the magnetic field. Consider a flat rectangular conductor carrying a current in a magnetic field. The charges in the conductor will experience a Lorentz force in the direc-

tion mutually perpendicular to the current flow and the field direction. This results in an accumulation of negative charge at one edge of the conductor and of positive charge at the opposite edge. This charge distribution between identically opposite points is the Hall Voltage. Since this voltage is directly caused by the Lorentz force, it is proportional to the current, the magnetic field, and also the physical properties of the conductor. This voltage may be generalized as

$$V_H = \gamma IB \cos \theta$$

where

V_H = Hall Effect Voltage

γ = a sensitivity constant of the conductor

I = magnitude of the current

B = magnitude of magnetic field

θ = angle between current flow and magnetic field direction

The Hall Effect Compass

The Hall Effect can be used to make an electronic compass that produces a linear signal. Two Hall Effect Crystals (HEC) are mounted perpendicular to one another in a horizontal plane. The magnitudes of the Hall voltage will vary with changes in magnetic heading and these voltages can be processed to give a compass reading.

The Hall voltage is proportional to the cosine of the angle the earth's magnetic field makes with the Hall Effect Crystal (HEC). However, since the two sensors are orthogonal, one voltage is 90 degrees out-of-phase with respect to the other sensor's Hall voltage. So one voltage is proportional to the cosine and the other voltage to the sine of the incident angle. These HEC sensors are driven by sinusoidal currents each 90 degrees out-of-phase with respect to each other to enable the heading to be determined. The two Hall voltages can be expressed as

$$V_{H1} = K_1 \sin\theta \sin\omega t \quad , \quad \text{from HEC1}$$

$$V_{H2} = K_2 \cos\theta \cos\omega t \quad , \quad \text{from HEC2}$$

where

K_1 and K_2 are the constants of the two crystals

θ = angle between earth's magnetic field and the longitudinal axis of the sensors

ω = frequency of driving current

t = time

The two Hall voltages can be added together if K_2 is made equal to K_1, and using a simple trigonometric identity[2] results in

$$V_{H1} + V_{H2} = K_1 \sin\theta \sin\omega t + K_1 \cos\theta \cos\omega t$$

$$= K_1 \cos(\omega t - \theta)$$

The signal $K_1 \cos(\omega t - \theta)$ represents a phase shift from the driving current. This shift is linearly related to the compass magnetic heading and may be obtained by processing the signal through a phase detector. The output of the phase detector may be calibrated to represent 0 to 360 degrees. A discontinuity occurs at 0 and 360 which represent the same heading. This point may be shifted 90 degrees by comparing the input to phase detector, $\cos(\omega t - \theta)$, against $\sin\omega t$ instead of $\cos\omega t$. This technique, in effect, creates two compass sensors. For operation near zero degree heading, the phase is detected in relation to $\sin\omega t$, and for operation away from zero degree, the signal is compared against $\cos\omega t$. This method provides an overlap of the discontinuity which simplifies autopilot control.

The signals from the Hall Effect crystals are very small. In order to reduce the electronic amplification, it was necessary to increase the magnetic field using metal strips termed flux concentrators.

The Compass Design

The Hall Effect Electronic Compass is composed of several main circuits, each performing a specific function. The output of one circuit becomes the input to the next circuit until the final result is a voltage which the autopilot recognizes as a compass heading. The main circuits are the quadrature oscillator, sensor driver, buffer amplifier, tuned amplifier and adder, phase detector, and interface to the autopilot (see Figures 2.6.1 and 2.6.2).

Quadrature Oscillator: The oscillator provides two sinusoidal voltages, 90 degrees out-of-phase, to the sensor drivers and to the phase detector.

This circuit is composed of two operational amplifiers in a resistor-capacitor network that produces an instability. The feedback network regulates the instability so that a sinusoidal decay is produced.

The initial design for an oscillator was a simple circuit that produced square waves. The tuned amplifier would have filtered the unwanted frequencies in the square wave to produce a sine wave. However, this method produced large voltage spikes on the signal when processed through the sensor driver circuit. The quadrature oscillator was redesigned to remove these spikes by eliminating the sharp rises of the square waves which caused the problem.

FLOWCHART FOR HALL EFFECTS COMPASS

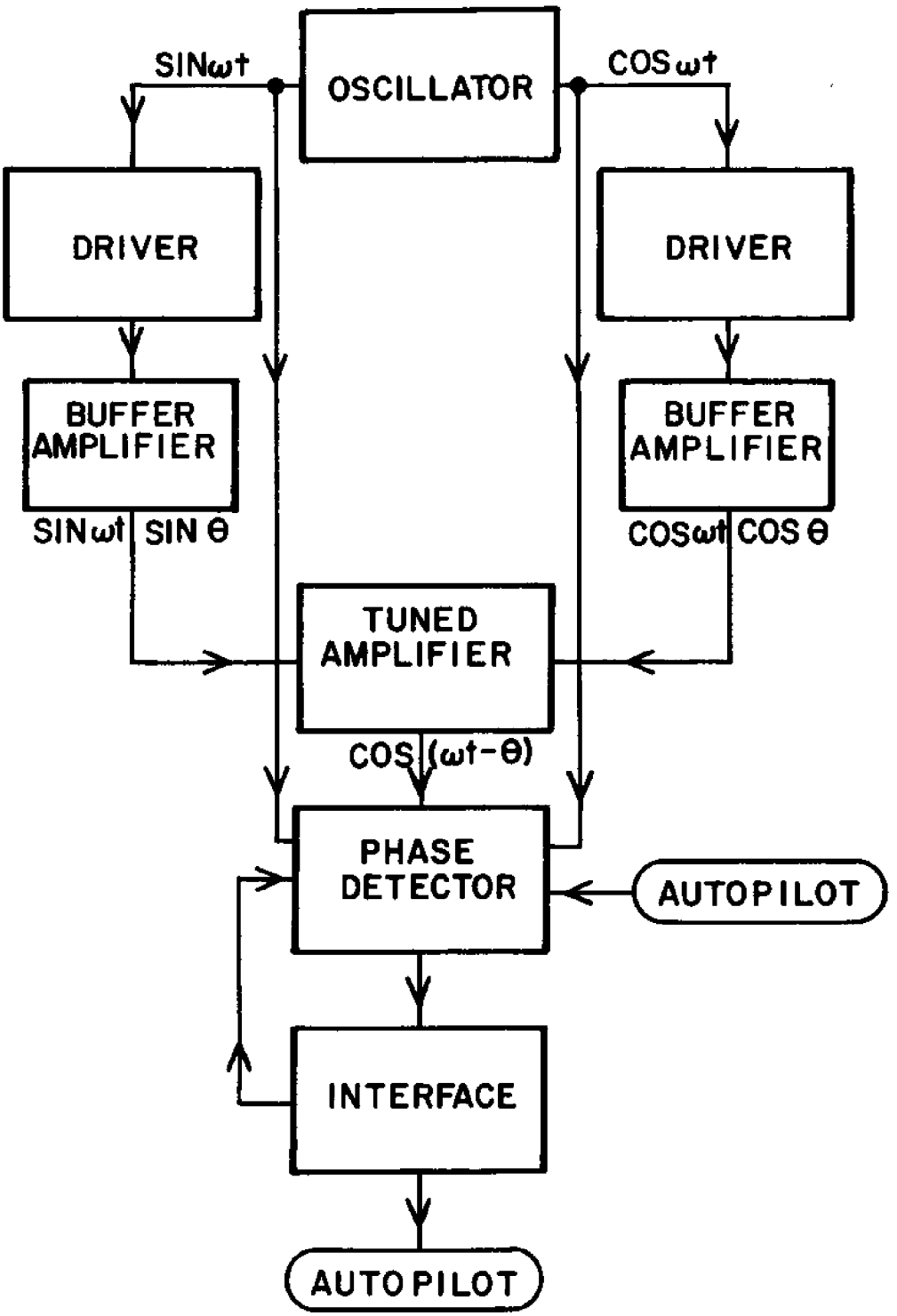

FIGURE 2.6.1

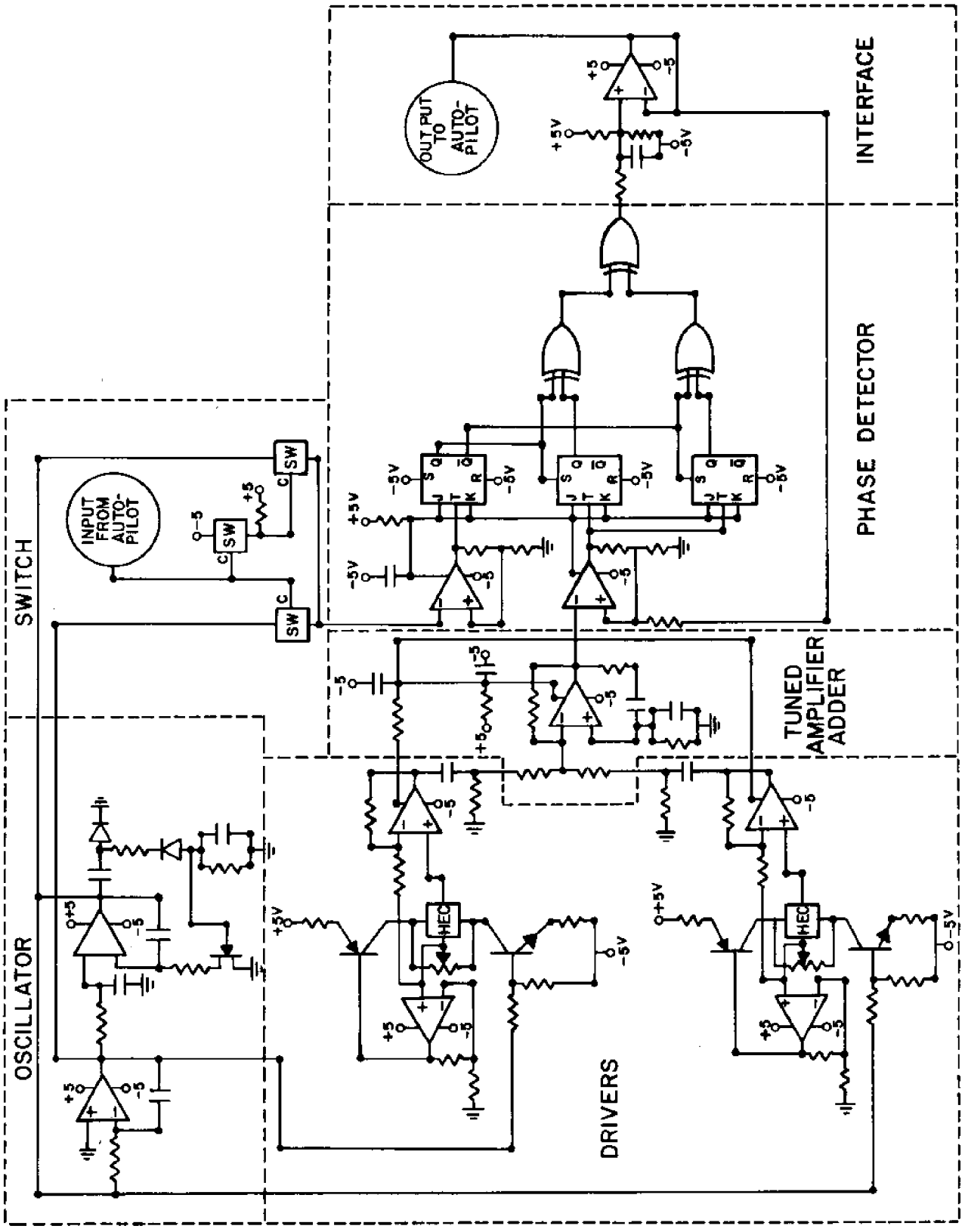
CIRCUIT DIAGRAM FOR HALL EFFECT COMPASS
OSCILLATOR
SWITCH
INPUT FROM AUTO-PILOT
PHASE DETECTOR
INTERFACE
OUT PUT TO AUTO-PILOT
TUNED AMPLIFIER ADDER
DRIVERS
HEC

FIGURE 2.6.2

Sensor Driver: The Hall Effect Crystals require that the Hall output voltage be isolated from the driving current. The crystals have a residual misalignment voltage that in weak magnetic field applications is significant compared to the induced voltage and therefore must be compensated. The driver network is designed to meet these requirements while driving the HEC sensors with sinusoidal current.

Two identical driver circuits are employed, one for each crystal. The HEC is placed between two transistors, a n-p-n and a p-n-p. The output of the quadrature oscillator is used as the base current of the n-p-n which regulates the current flowing through the sensor. Isolation of the Hall voltage is achieved by a feedback network which regulates the p-n-p transistor, keeping the one terminal of the Hall voltage at 5 volts $\pm$ 20 mv. The same terminal is connected to the slider of a potentiometer that is in parallel with the crystal. The residual misalignment voltage is compensated for by adjusting the potentiometer.

Buffer Amplifier: The Hall voltage of each sensor crystal is small, on the order of 1-2 millivolts. This signal is amplified by a negative feedback op-amp with gain of approximately 100. The amplifier also provides the specification output resistance for the HEC.

Tuned Amplifier and Adder: The Hall voltages of the two sensors are added together and further amplified to the same amplitude as the driving current of the sensors. This circuit filters frequencies, other than the driving frequency, that may be on the signal as unwanted noise from the sensors.

The outputs from the buffer amplifiers are a.c. coupled to the tuned amplifier circuit and added together as the negative feedback resistor circuit.

Phase Detector: The phase detector network compares the amplified, added, and filtered signal from the sensor crystals against the sensor driving current and detects any shift in phase of the processed signal. This network consists of three parts: a switch, conversion from analog sine voltages to digital square waves, and digital detection of the phase shift.

The switching circuit determines which driving current, sine or cosine the tuned amplifier output is compared with. The circuit consists of a resistor and a CMOS Integrated Circuit (IC) with four analog multiplex switches, of which only three switches are used. The switching is controlled by the autopilot by providing either a high or low voltage to the IC.

Converting the analog sine waves voltages to digital square waves is achieved by employing two schmitt trigger circuits, one for the output of the switch and the other for the output of the tuned amplifier. The schmitt trigger consists of an op-amp with positive feedback that provides hysteresis to the

circuit. The "zero" crossings of the sine wave are detected and trigger the output to change from a high or low voltage producing a square wave. A small amount of hysteresis is desirable to prevent false triggering from noise. This hysteresis is designed so that a maximum of one percent of phase shift would be introduced by the schmitt trigger circuit. This shift occurs if the amplitudes of the sine voltages being compared are not the same.

CMOS J-K flip-flops and exclusive OR gates are used to detect digitally the phase shift of the square wave outputs of the schmitt triggers. The flip-flops are operated in complement mode. One flip-flop produces an output that is high or low for each period of the driving frequency; the second flip-flop triggers on the falling edge of the shifted sensor signal; and the third flip-flop alternates with the second to provide a 100 percent duty cycle for the output. The outputs of the J-K flip-flops are processed by exclusive OR gates resulting in a pulse every period, the length of the pulse being proportional to the phase shift.

Interface to the Autopilot: The autopilot requires an output voltage between 2.25 volts and 7.75 volts that varies with direction. The interface converts the pulses from the phase detector into a voltage depending on pulse width. Since 0 and 360 degrees represent the same direction, a discontinuity occurs at the maximum and minimum voltage of the output. It is desirable that the output have a small amount of hysteresis to overlap this discontinuity for ease in autopilot control. A feedback circuit from the interface output voltage to the phase detector achieves this goal.

The interface consists of a voltage divider with a capacitor that accumulates a voltage depending on pulse width. A follower op-amp circuit provides the output current to the autopilot.

Hysteresis is produced by providing feedback from the interface output voltage to the schmitt trigger which processes the signal from the HEC sensors. This causes a phase shift of the square wave signal proportional to the interface output voltage. The result is that the output of the interface is proportional to approximately 0 to 370 degrees in the direction increasing output voltage and proportional to -10 to 360 degrees in the direction of declining magnitude.

Power Supply Filtering: Chain RC filtering of the power supplies to the op-amps are used to prevent feedback through the supply lines. This is necessary due to the large amount of amplification that is required because of the small magnitude of the Hall voltage.

Compass Layout

The autopilot of the robot submarine is contained inside a six-inch PVC tube. The compass is provided an area of approx-

imately four and a half inches width inside this tube.

All the electronic components of the compass are placed on a circular backing which stands upright in the horizontal tube. The backing has an inch-square hole cut from its middle along the bottom edge through which the HEC housing is placed. Components are grouped together according to circuit function to reduce connecting wire length and hence noise. Wire wrapping and soldering are the connecting methods.

The Hall Effect Crystals are mounted on opposite sides of a 4" by 4" plexiglass cross. Each crystal is mounted at the junction of the cross in a gap between two metal flux concentrators. The crystals are mutually perpendicular and the face of each crystal is perpendicular to the length of the concentrators. This housing is designed to fit in the autopilot directly beneath the electronic components of the compass.

The compass package has two wires to the autopilot, the compass output voltage and the input to the switching circuit. The power supplies are regulated 10, 5 and 0 volt lines from the autopilot.

The Test Program

The Hall Effect Electronic Compass was bench tested in the laboratory. The sensor was placed on a round turnable tray and 360 degrees marked around the circle in 30-degree increments. The residual misalignment voltage of each crystal was nulled by adjusting the potentiometers. The output voltage of the compass was then measured and recorded at each 30-degree interval. These measurements were placed on a graph and the curve connecting the points was approximated by a straight line. The small deviation of the points from the line indicate a highly linear output. This procedure was repeated several times. However, when the experiment was conducted on different days, the results were less linear until one potentiometer was readjusted. The need to renullify the residual misalignment voltage of one crystal results from drift with temperature. Preliminary tests indicate that the one crystal's residual voltage temperature coefficient is approximately 20 percent greater than the specifications for a typical crystal.

Conclusions

The Hall Effect Electronic Compass produces a linear output when properly adjusted, an improvement over the robot submarine's present compass. The drift of the misalignment voltage with temperature can be eliminated by including a thermistor in the compensation network. This requires that the temperature coefficient be determined experimentally so that the appropriate value for the thermistor is chosen. New crystals should be purchased because of the abnormal drift of one crystal and damage to the leads of the other crystal. With these modifications, the compass is ready to be placed in the submarine and should perform satisfactorily.

Further Developments

The two-axis design of the compass requires that it remain horizontal to give an accurate compass bearing. The compass cannot distinguish between changes in heading or changes induced by roll or pitch of the submarine. The robot is controlled by the autopilot so that roll and pitch are maintained nearly level. Field experiments of the compass will determine whether the error produced by small variations from the horizontal are unacceptable. If this problem develops, a correction technique could be employed. The robot submarine has pitch and roll sensors and their output can be used to compensate the compass reading. Assuming small rotations, the influence of pitch and roll angles could be subtracted from the compass output. This would be accomplished preferably by hardware, but could be done by software for computer control. The compass would then produce a linear reading dependent on magnetic heading and independent of roll or pitch.

2.7 LINE TENSION METER

A line tension meter is a device for measuring the tension in various types of line such as fiber, manila, wire, etc. It is desirable for the operator to be able to install the meter at any point, whether the line be moving or stationary, along the line without having to reeve the end of the line through it. It is also required that the device be unaffected by water, be rugged, and have no external power requirement.

A line tension meter with these characteristics would be useful to fishermen digging for scallops or trawling for fish, yachtsmen, or anyone else needing to know the tension on a working line.

Background

A device of this type was proposed in a previous Ocean Engineering Summer Lab, but was never built. The design described in this report utilizes a coil spring which is deflected by tension on the line in the meter. Deflection is measured on a scale which reads in pounds of tension per inch deflection as shown in Figure 2.7.1.

This type of meter has several advantages over other types. It is simple to build and operate and is inexpensive. It was also unaffected by immersion in water, dirt in the working parts, and rough treatment.

The load range can be varied by replacing the existing spring with another of a different spring constant and changing the scale accordingly.

The primary maintenance requirement is that the spring be protected from corrosion through protective coatings.

During the testing of the prototype meter, some disadvantages became apparent. It is heavy and difficult to read. These problems could be overcome if more appropriate materials were used, which depends upon the amount of money available. Being a prototype model, the meter was constructed of readily available materials.

Technical Description

The prototype tension meter consists of a steel base plate on which is mounted a coil tension spring with a sheave and pointer attached, and two (2) sheaves attached to the base plate. This arrangement is shown in Figure 2.7.1.

The sheaves allow the meter to measure the tension in a slowly moving line. This feature is useful to fishermen dragging for scallops or trawling for fish, yachtsmen, or anyone else needing to know the tension in a working line.

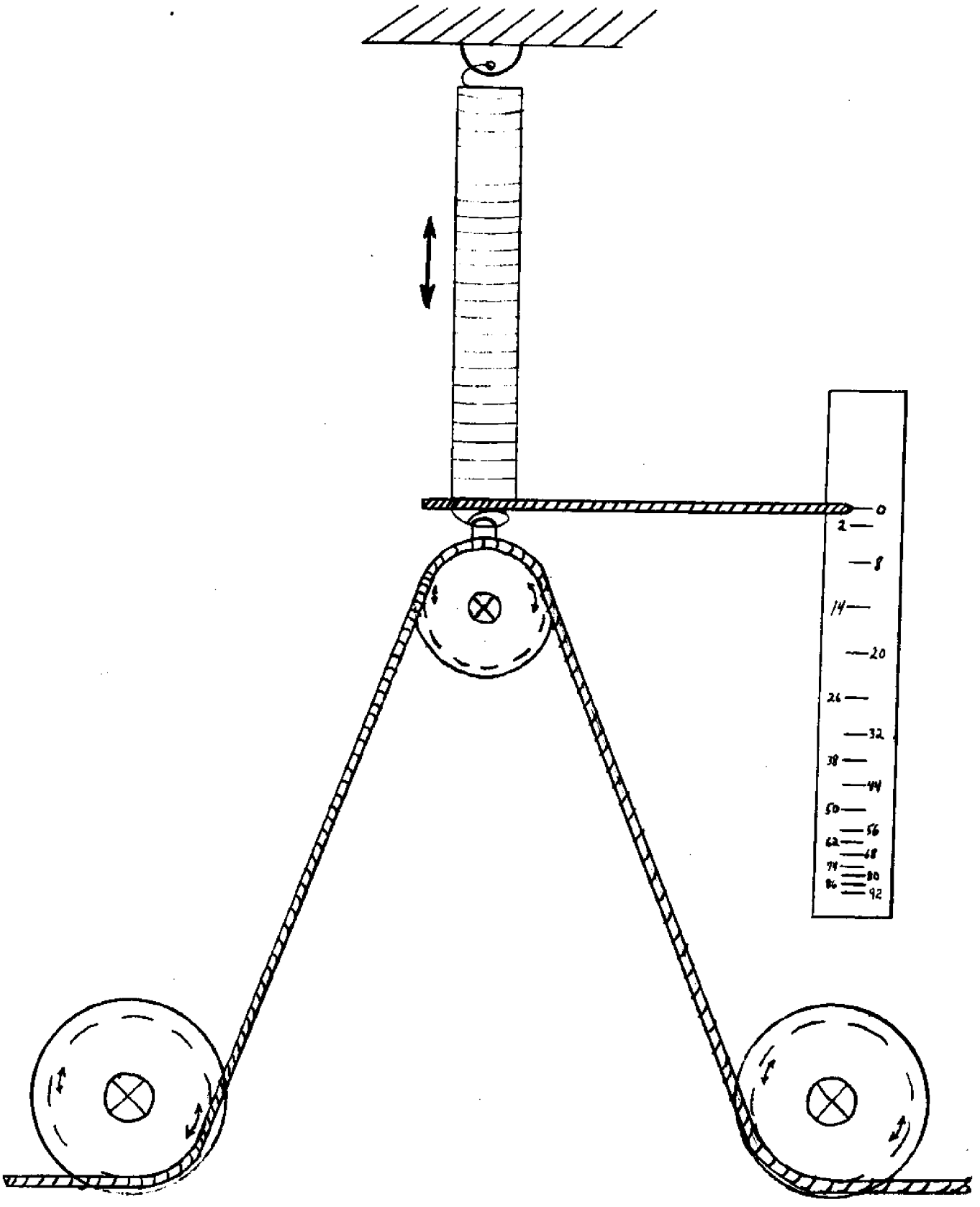

Figure 2.7.1

Friction in the sheaves must be kept to a minimum to provide accurate readings. This was accomplished by providing the fixed sheaves with roller bearings packed with hard grease. Conventional roller bearing grease proved unsatisfactory because it formed an emulsion with sea water and washed away. After exposing the meter to sea water, no difference in test results was noticed. A simple, well-greased pulley was used on the spring in order to keep costs down.

The fixed sheaves were attached to the base plate by studs threaded on either end. The sheaves bore on the smooth part of the stud, as shown in Figure 2.7.2.

The movable pulley was attached to the spring by cutting and bending the ring on the pulley through the ring on the end of the spring.

Once the load-carrying parts of the meter were in place, the spring was fixed to the base plate. An upright was welded to the base plate and drilled to receive a stud threaded on one end. This stud was bolted to the upright. The other end of the stud was drilled, and the ring on the end of the spring was passed through the hole. This arrangement proved reliable and enabled the spring to be removed easily. A U-bolt was welded to the base plate, straddling the spring to hold the spring in place when not carrying a load. The U-bolt and upright were designed so that the spring could deflect freely while the meter was in operation.

A pointer was attached to the spring to allow the spring deflection to be read on a scale. The pointer was first attached with epoxy cement. This proved satisfactory during testing, but did not hold up under actual use of the meter in sea water. Then an attempt was made to tack-weld the pointer to the spring. The type of steel in this tension coil spring was found to break under the heat of arc welding. The final method of attaching the pointer to the spring proved satisfactory in actual use and was used to solder the pointer to the spring.

The spring constant was determined by hanging the spring and suspending known weights, cylinders of lead shot with a mean weight of 6 pounds each, from it and measuring the increased deflection of the pointer. The spring constant was found to be approximately 10.5 pounds per inch of elongation (see Figure 2.7.3). It was noticed that this constant did not hold true over the first 25 pounds of load.

When the spring was installed on the meter, spring deflection was not in a linear relationship to the tension in the line. This was due to the changing geometry of the sheaves and line angles. A simplified sketch of the layout is shown in Figure 2.7.4.

From Figure 2.7.3 the relation between spring extension and total downward force on the spring is approximately

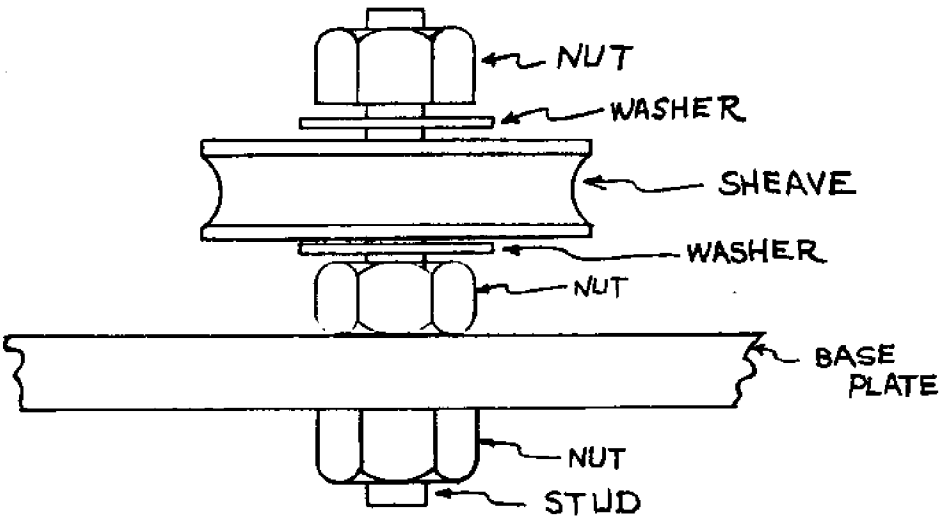

Figure 2.7.2

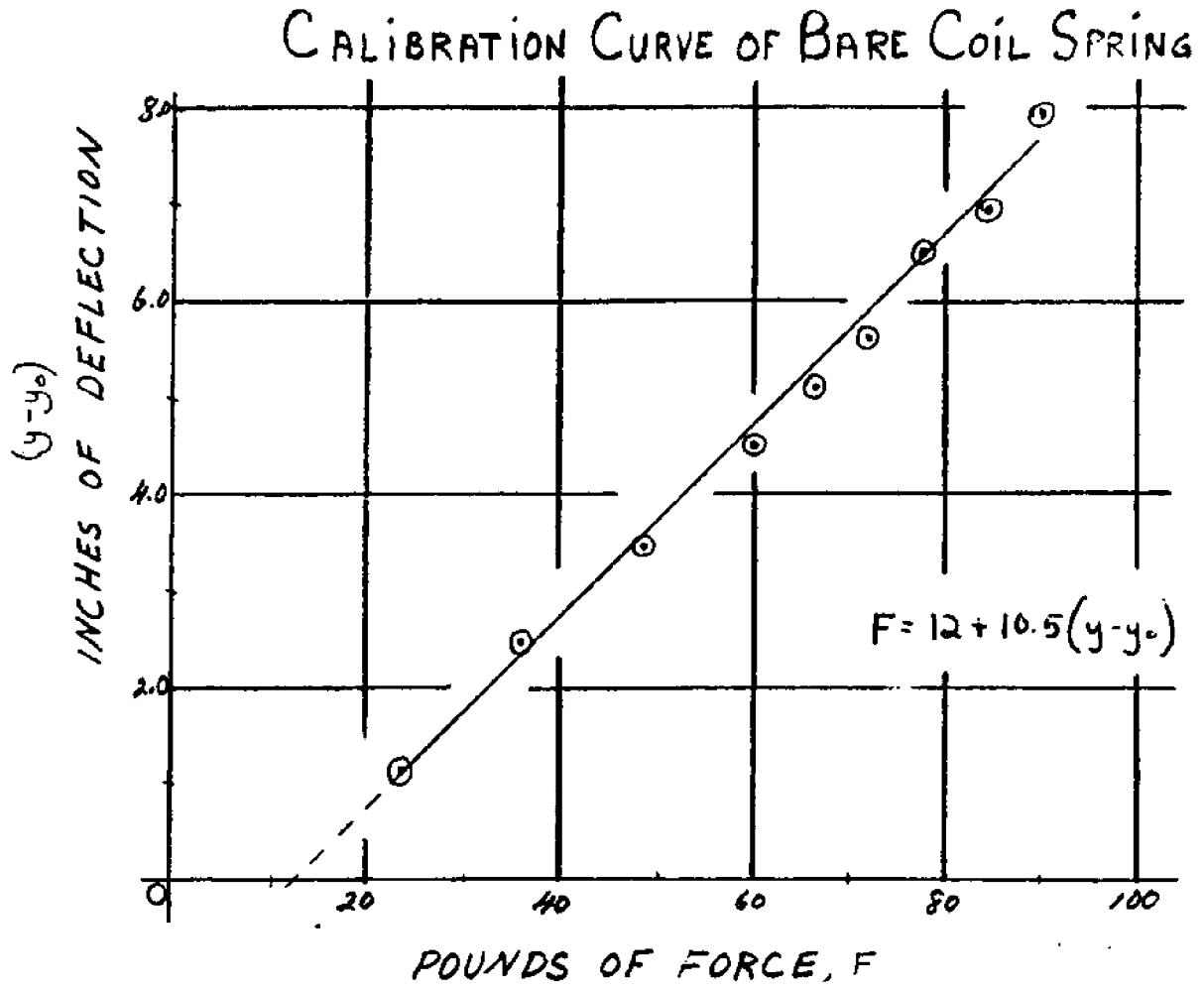
CALIBRATION CURVE OF BARE COIL SPRING
INCHES OF DEFLECTION (y-y₀)
8.0
6.0
4.0
2.0
0
20
40
60
80
100
POUNDS OF FORCE, F
F = 12 + 10.5(y-y₀)

Figure 2.7.3

$$F = 12 + 10.5(y-y_o)$$

where the "12 lbs" value refers to the force required to overcome the residual stress in the spring.

From the sketch in Figure 2.7.4 it can be seen that

$$T = \frac{12 + 10.5\ (y-y_o)}{2\ \cos\ \theta}$$

where $\theta = \tan^{-1} \frac{X/2}{h_i - (y-y_o)}$

The predicted relation between T and $(y-y_o)$ is the solid curve in Figure 2.7.5. As is shown in the curve, at high tensions the relative sensitivity of the meter to small changes in tension is reduced. This could be made more linear by raising the mounting point of the spring so that the angle would be smaller for a given deflection. While such a change would improve the accuracy of the meter, it would not make it more useful because of the extra size and weight of the meter that would result.

The meter was tested in two (2) different attitudes, shown in Figure 2.7.6. No significant difference in test results was noticed between a hanging attitude and a fixed attitude. In operation, however, it is recommended that the meter be bolted in place along the line of pull of the line to be measured.

The meter was also tested using different sizes of line and wire. As seen in Figure 2.7.5, this introduced little difference in test results. In all of the tests made, the error between indicated and true tension did not exceed 5-1/2% of the load capacity of the meter, or 5-1/2 pounds for the prototype. The maximum error was observed at the high end of the meter scale. This was mainly due to the friction between the pulley and the line. If the load were jostled, the error would decrease and the meter would read accurately again.

Conclusions and Recommendations

A line tension meter built on the principle described in this report is feasible. This type of meter has the following advantages:

- It is easy to handle.
- It is not affected by typical exposure to salt water or rough treatment.
- It can measure the tension in a moving line (the prototype was used successfully in the setting of scallop culture traps).

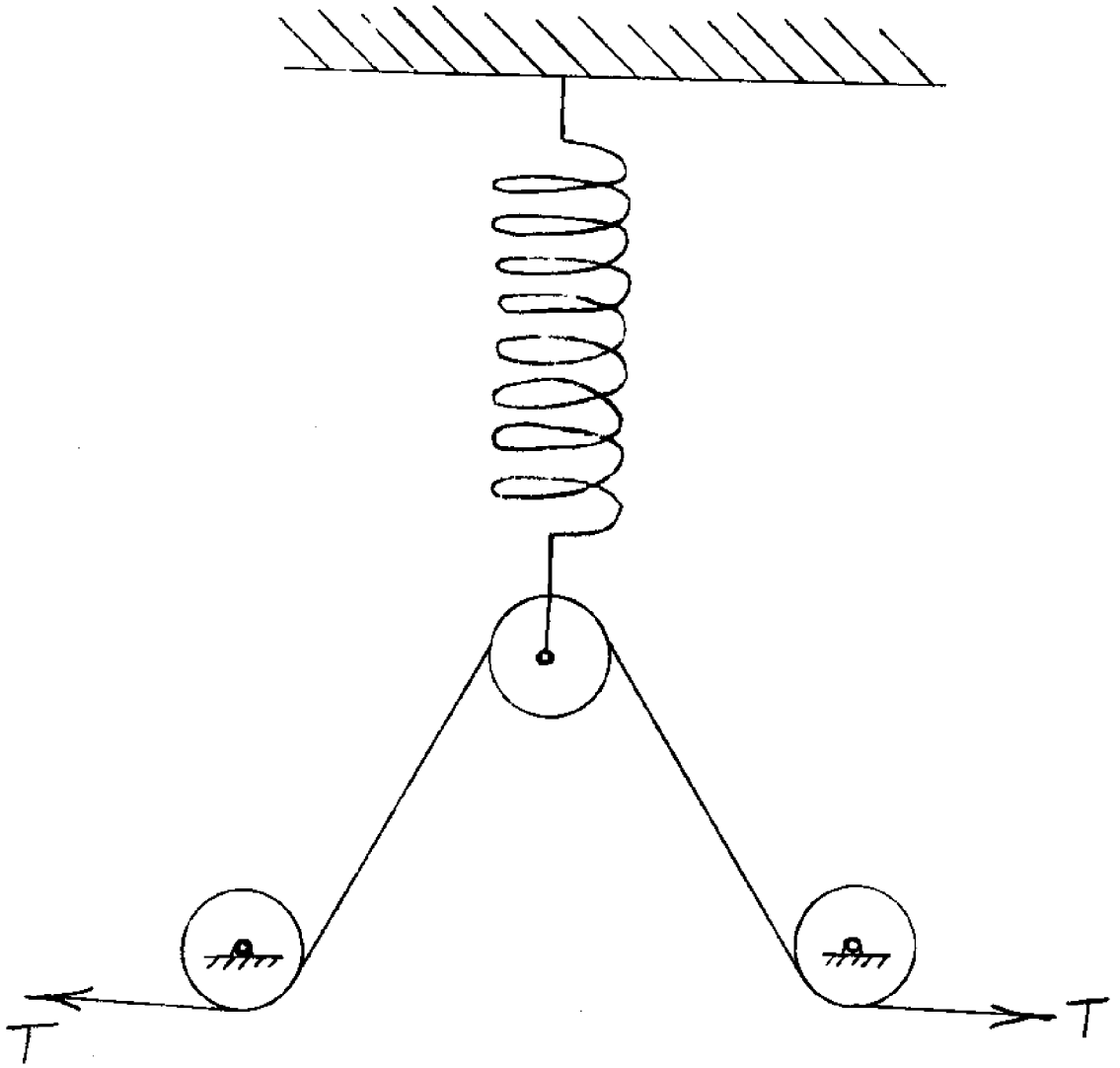

X = horizontal distance between fixed sheaves

$y-y_o$ = extension of spring from its zero load position

h_o = height of apex in tension line (above fixed sheaves) with zero tension

h = height of apex in tension line under tension

θ = apex half-angle

Figure 2.7.4

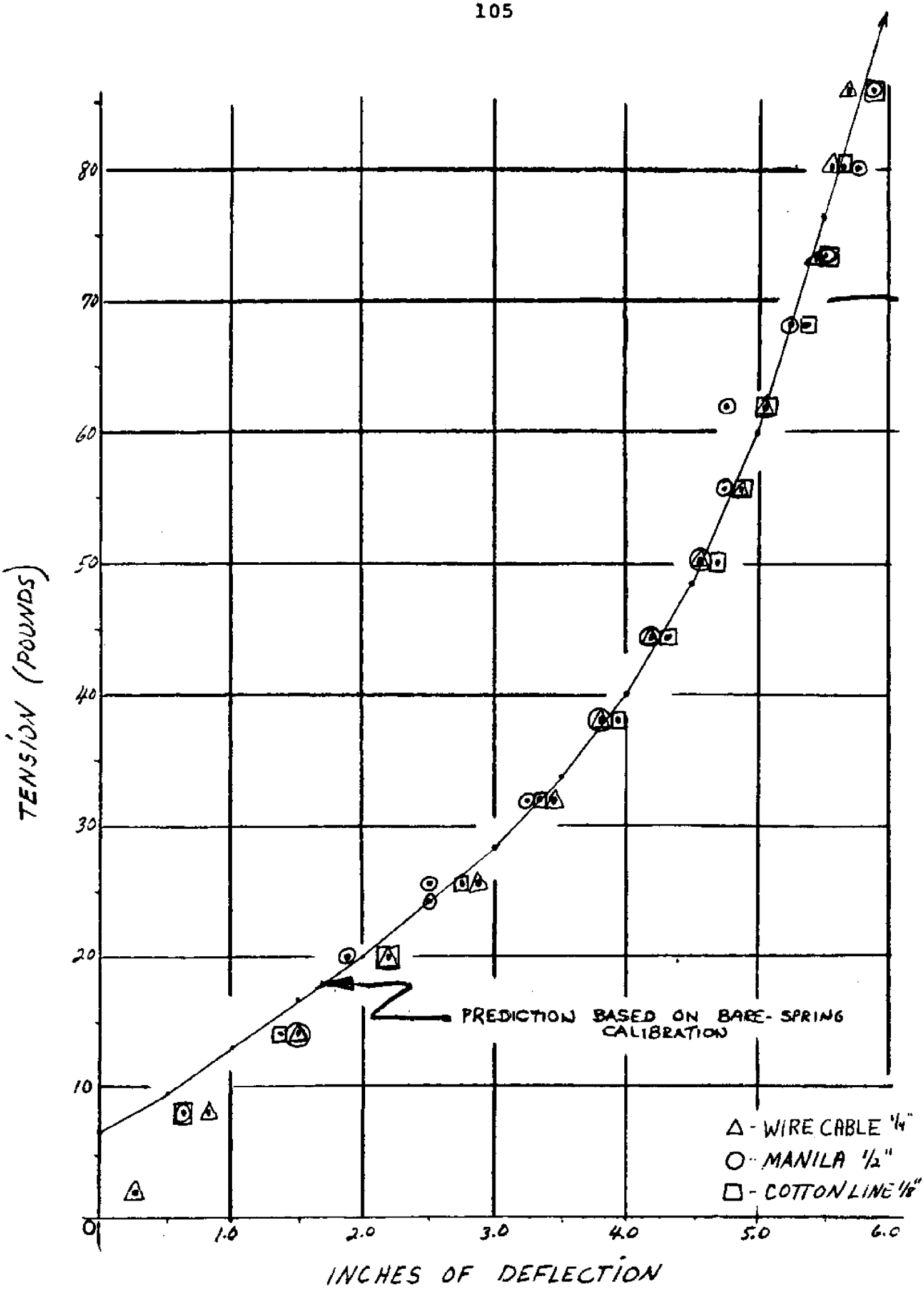
TENSION (POUNDS)
80
70
60
50
40
30
20
10
0
1.0
2.0
3.0
4.0
5.0
6.0
INCHES OF DEFLECTION
PREDICTION BASED ON BARE-SPRING CALIBRATION
△ - WIRE CABLE 1/4"
○ - MANILA 1/2"
□ - COTTON LINE 1/8"

Figure 2.7.5

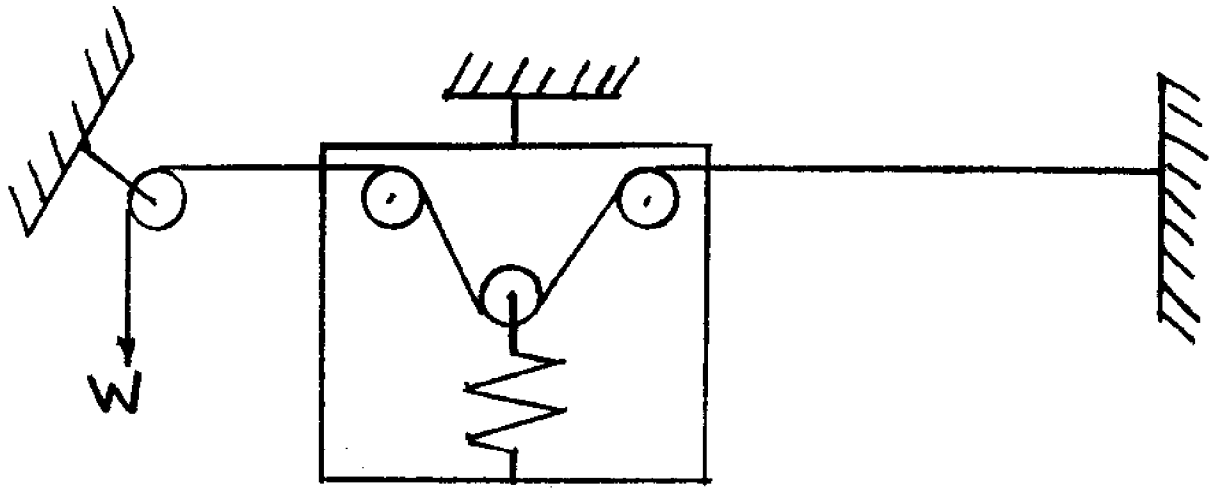

(a)

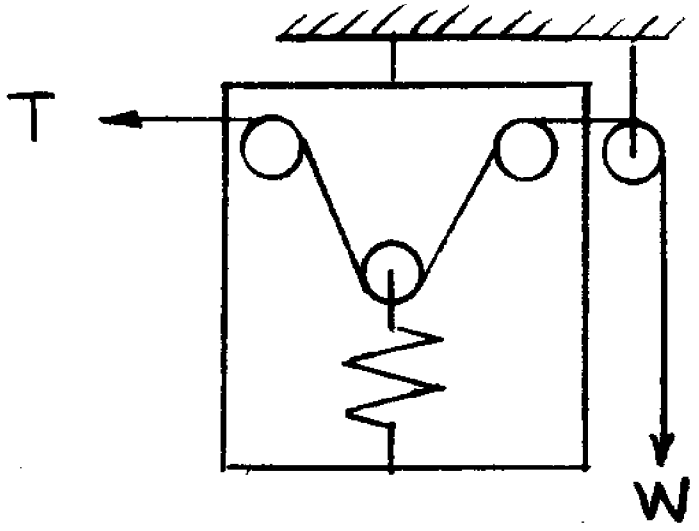

(b)

Figure 2.7.6

- It does not require the line to be broken along its length to be placed in the meter.

- It is inexpensive. (The retail price of the parts for the prototype was $6.89.)

With some changes in construction and design the meter can be improved. If the base plate were made of lighter metal, the meter would be easier to handle. The same effect can be obtained by cutting weight reducing holes in the mild steel plate used.

Near the upper end of the tension range the meter becomes nonlinear due to geometric effects, and the accuracy of the readings is decreased. This problem could be minimized in one of two ways: a) either by placing the fixed sheaves closer together or b) by mounting the spring higher on the base plate thus reducing the apex angle θ for a given tension. The first alternative reduces the range of tensions which can be measured with a given coil spring, while the latter increases the weight and size of the meter system.

The limited tests performed on the prototype suggest that it is reliable and easily used. It is recommended that it be given more extensive testing in actual service on a larger scale.

2.8 MOORING RESEARCH PROJECT

Purpose

The purpose of this project was to obtain experimental data on a compound catenary utilizing a clump and two separate scopes of mooring line (see Figure 2.8.1). This is an area of ocean engineering where experimental information is very sparse. The process involved measuring the horizontal force versus horizontal displacement of a test model compound catenary.

Background

A computer program was available to supply theoretical data. Information such as scope and weight of lines, depth of water, and size of clump was fed into the computer to obtain the most discernible discontinuity in the characteristic horizontal force versus horizontal displacement curve (see Figure 2.8.2).

As the force on the system increases, the distance between the source of pull and the anchor increases resulting in a curve resembling a parabola when plotted. The slope of the curve increases until there is a sudden decrease in slope (this is the point at which the clump is lifted), then continues with another parabolic-like curve. The slopes of the curve and the position of discontinuity depend on the characteristics of the mooring mentioned above.

Method and Materials

In this experiment there were two quantities to be measured. The first was the horizontal distance from the boat generating the force to the anchor, and the second was the force generated. To measure the horizontal force, a load cell using strain gauges was constructed. It was then shackled into the towing cable which connected the boat to the mooring. The towing cable was connected to a large spring buoy which opposed the vertical force produced by the weight of the lifted line and clump. To measure the horizontal distance, a buoy with a long vertical pole was placed above the anchor. Then, by measuring the angle subtended by a known distance marked on the pole with a sextant, the horizontal distance from the boat to the anchor was calculated. This buoy was moored over the anchor by a triple point moor to insure its horizontal position. A float attached to the anchor marked its position. The line from the anchor was then pulled taut for accurate positioning.

One of the first jobs at Castine was testing the available boats to see if they could produce the force which the computer models predicted would be needed. This was accomplished by conducting a bollard pull test. The towing cable from the boat is tied to an immovable object. The boat then pulls on the cable while the force exerted by the boat is measured with the load cell. It was found that PANTHALASS, the boat assigned to the Summer Lab, was adequate for the job.

SETUP AND MATERIALS

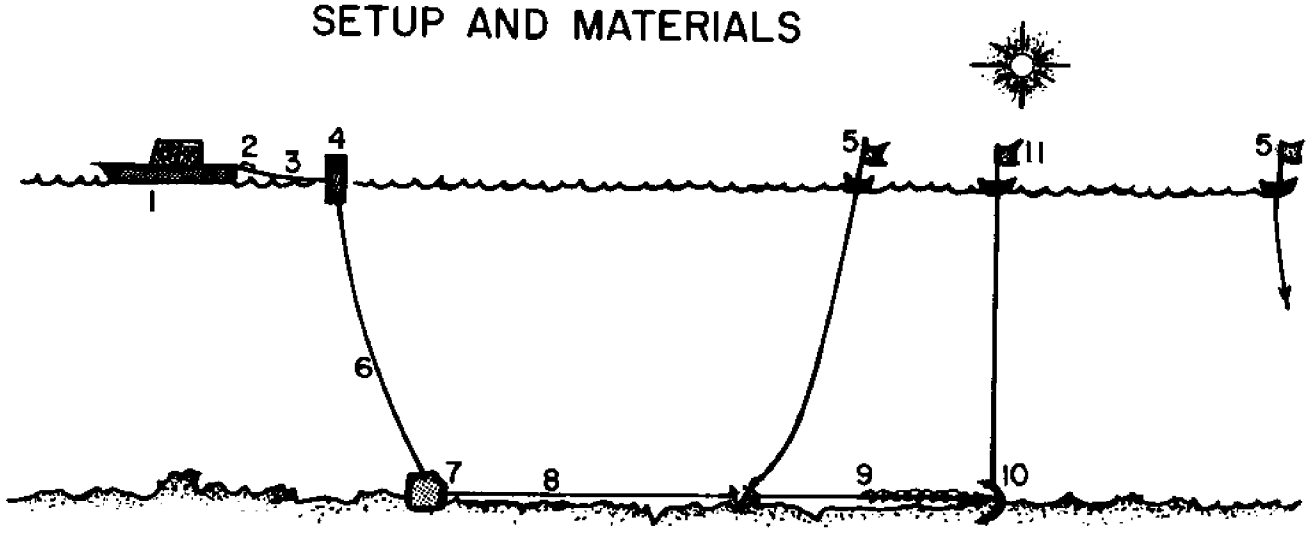

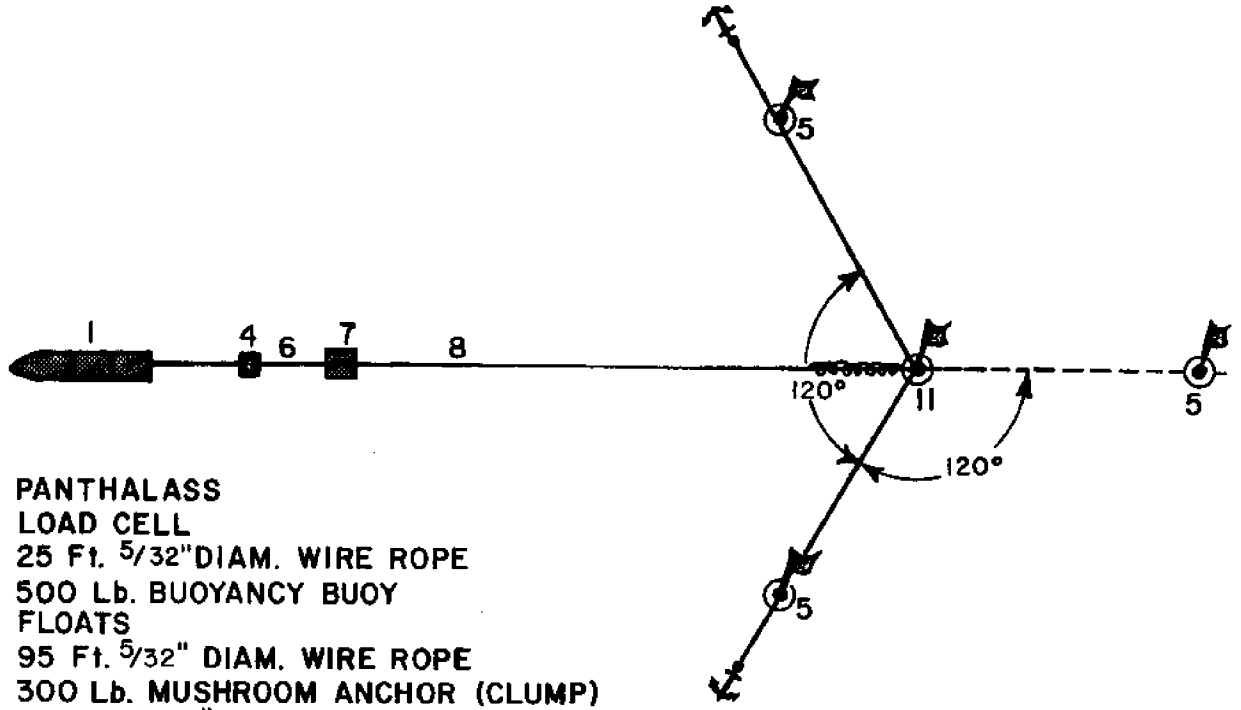

1 PANTHALASS
2 LOAD CELL
3 25 Ft. 5/32"DIAM. WIRE ROPE
4 500 Lb. BUOYANCY BUOY
5 FLOATS
6 95 Ft. 5/32" DIAM. WIRE ROPE
7 300 Lb. MUSHROOM ANCHOR (CLUMP)
8 105 Ft. 5/32" DIAM. WIRE ROPE
9 65 Ft. CHAIN
10 75 Lb. STOCK ANCHOR
11 MARKER BUOY WITH RANGING ROD

FIGURE 2.8.1

TYPICAL CURVE FOR COMPOUND CATENARY

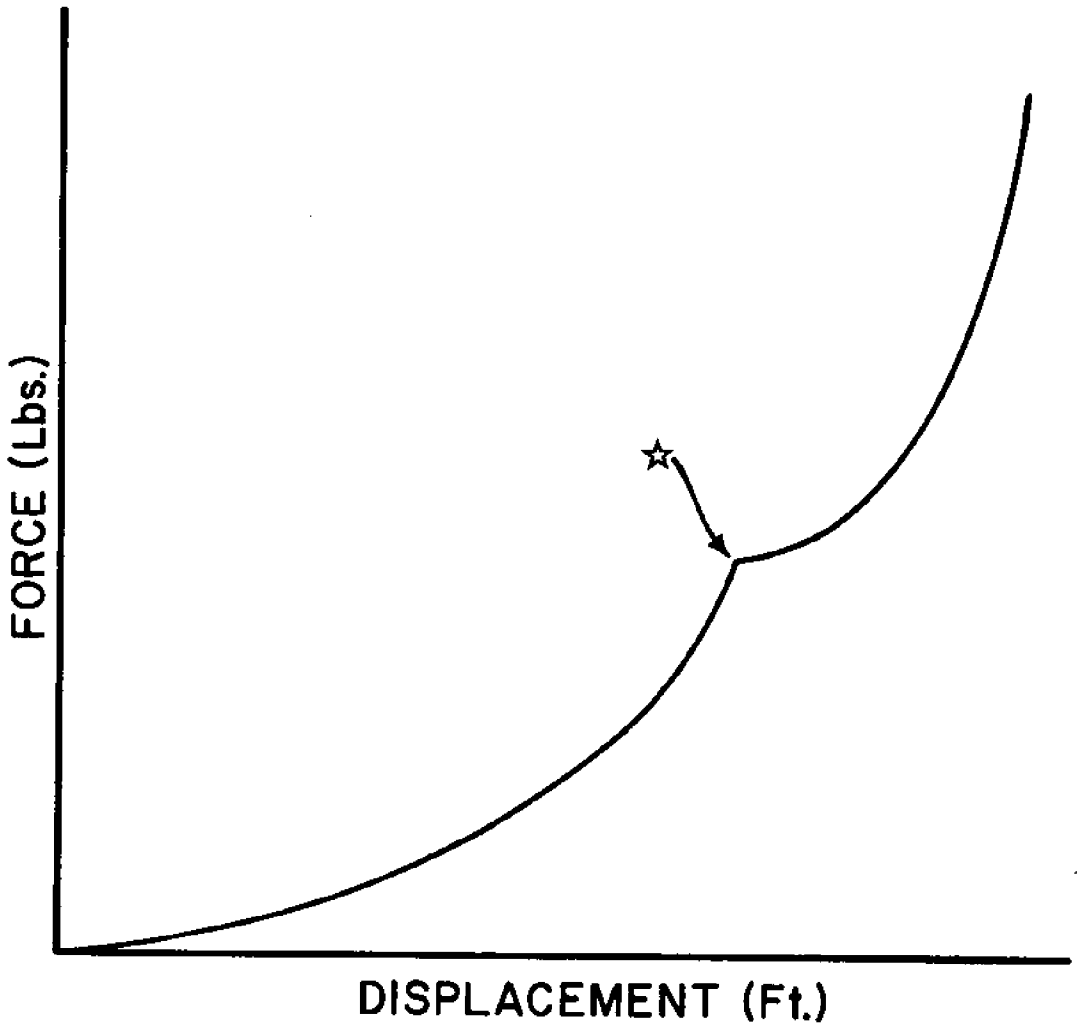

☆ AT THIS POINT THE CLUMP WAS LIFTED
IT IS A DISCONTINUITY IN THE CURVE

FIGURE 2.8.2

The next task was collecting and preparing the materials for the moor such as numerous shackles, thimbles, lines, etc.

Distance

The angle measured by the sextant was subject to parallax error. This is due to the fact that a sextant is designed to be used with objects at nearly infinite distances--stars, not objects at close range. This produces an error at 4.2 to 4.6 minutes of arc at 100 feet. This error is caused by the distance between the eye piece and the upper mirror. This distance, 2.25 inches, causes the sextant to measure the angle subtended the measured distance on the pole on the marker buoy minus 2.25 inches.

Table 2.8.1

Test to Determine the Accuracy of the Sextant for Measuring Distance on Dry Land at One Hundred Feet

Measured Angle	Calculated Distance
3°55.1'	100.36
3°56.7'	99.67
3°54.2'	100.75
3°59.8'	98.37
3°54.4'	100.66
3°57.3'	99.42
3°57.0'	99.55
3°55.9'	100.02
3°54.6'	100.58
3°54.7'	100.53
3°56.1'	99.93
3°54.8'	100.49
Average Angle 3°55.9'	100.02

With the correction factor of 6.5' added to sextant measurements, this method of measuring distances was accurate to within one foot at one hundred feet on dry land.

Measuring Horizontal Force

In the process of devising a method for measuring horizontal force, there was the major problem of isolating the components of the horizontal and vertical forces. The first method considered was the use of a combination of sheaves to provide a horizontal lead to the tow line. Another method was measuring the total force in this manner, determining the angle formed, and then using known data to calculate the horizontal force.

A better solution was to add a large spring buoy to the system to absorb the vertical force, leaving only the horizontal force to be measured.

SOURCE OF PARALLAX ERROR IN SEXTANT

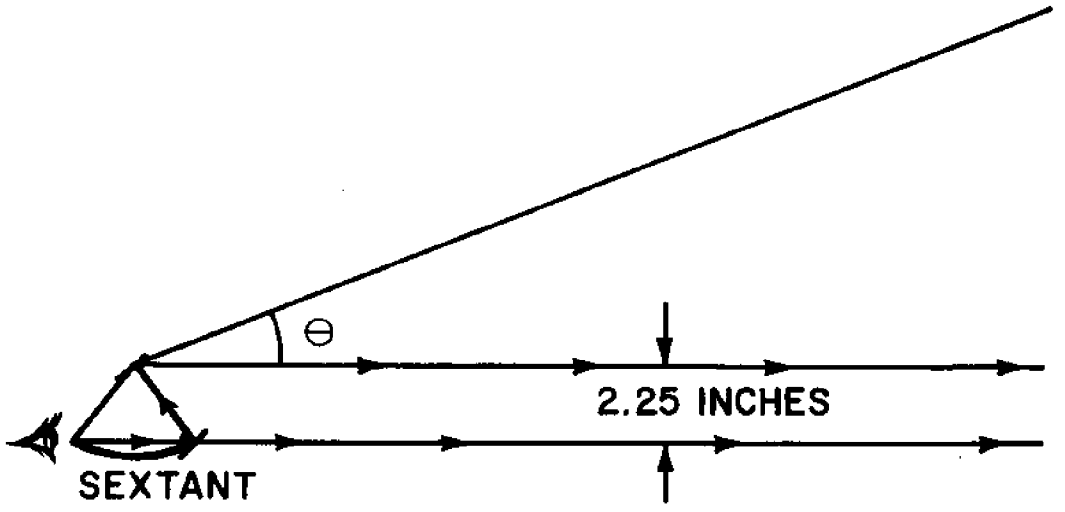

FIGURE 2.8.3

A practical means of measuring force is first to measure strain with a load cell, then calculating force based upon that strain. The load cell is based on the principle of the Wheatstone Bridge, a device used for measuring small changes in resistance.

Figure 2.8.4 shows the actual Wheatstone Bridge circuitry of the load cell used in the experiment. R3 and R4 are the internal resistors of the Vishay 1011 Strain Gauge Reader. When all four resistors are equal, or when R1 + R2 = R3 + R4, there is no potential difference across points C and D, so there is no current flow and the meter reads zero. Any change in the resistances of R1 and/or R2 results in a deflection of the meter.

In a load cell small resistors called strain gauges are carefully attached to a surface. When the surface expands the sensitive wires in the strain gauge stretch, resistance is increased. Knowing the resistance of the gauge and its gauge factor from change in resistance, one can determine the strain to which the surface was subjected. The Vishay meter can be set for resistance and gauge factor and reads out directly.

In the actual experiment four gauges of 120 ohms each with gauge factors of 2.9 were joined to an aluminum bar with a carrying capacity of 1,000 lbs and a maximum load limit of 5,000 lbs.

The strain gauges were placed on the bar, two on either side for purposes of temperature compensation and cancellation of any bending effects. When the bar is bent, two strain gauges parallel to one another and on opposite sides act as one resistor (R1). While one side is being compressed by bending, the other side is being stretched; therefore, the decreasing resistance on one cancels the increasing resistance of the other.

The cell was waterproofed by applying layers of M-Coat F and M-Coat D supplied by Micro Measurements. The cell was then tested for temperature compensation and calibrated using a hydraulic load device with known loads. The calibration curve (see Figure 2.8.5) was very linear except for the curved portion between zero lb and 125 lbs of load. This characteristic appeared to be caused by the elasticity of the protective coating which absorbed some of the force since the curve was linear before the coating was applied. The gauge had an accuracy of ± 5 lbs and was also used for weighing equipment used in the experiment.

Results

Readings were taken on two days, Friday, July 30, and Wednesday, August 4. On July 30 the readings were taken at 1430 hours EDT which was near high tide. For specific tide information refer to the addendum to this section. The water depth was approximately 87 feet as determined by Fathometer. The sky was overcast and thus accurate sextant readings were

WHEATSTONE BRIDGE

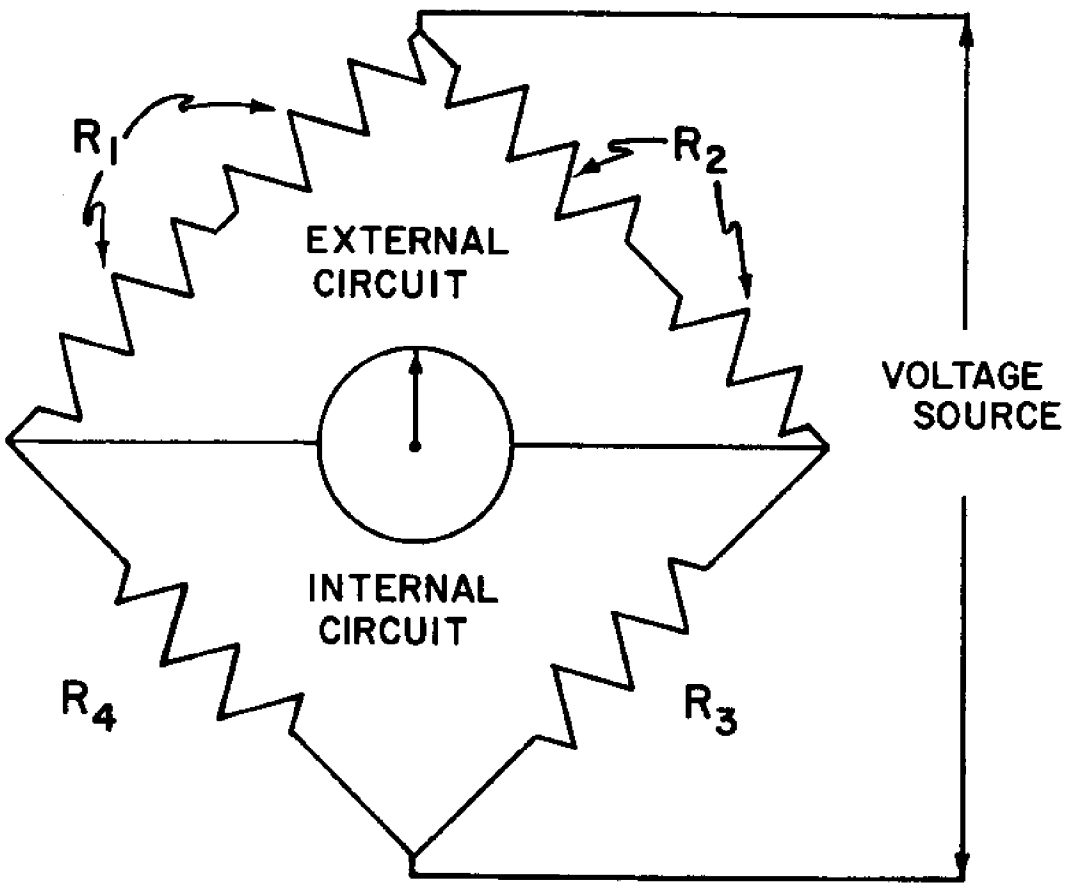

FIGURE 2.8.4

CALIBRATION FOR THE LOAD CELL

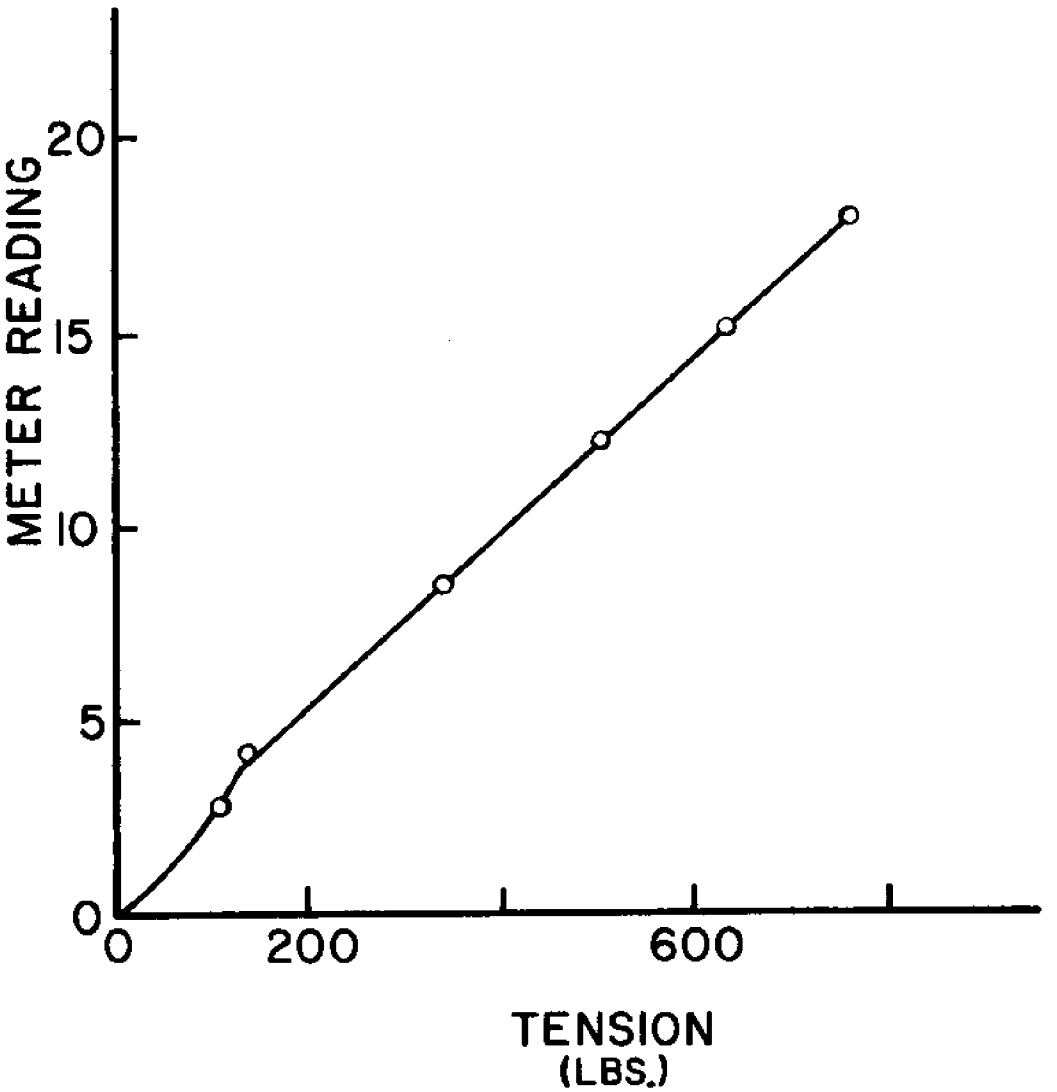

FIGURE 2.8.5

difficult to take. The electronic strain meter was not isolated from the engine vibrations of PANTHALASS. This decreased the accuracy of the third run and ruined the fourth run. Since it was late in the day, the wind had picked up. This made it difficult to keep PANTHALASS positioned correctly as the wind tended to push her out of alignment. Had the tow line been attached nearer amidships, the boat might have been able to maintain alignment. As a result of the force of the wind, extraneous forces came into play which caused the clump to lift early. The loss of position of the boat caused the distance measured to be less than the actual distance (see Figure 2.8.6). However, the wind was only enough of a factor to change the quantitative measurements, and not enough to affect the shape of the graphs. Thus the first day yielded good qualitative results.

Since fine adjustments in the boat's throttle were difficult to make, multiple runs were made. Figure 2.8.7 contains the first day's results. For numerical data see the addendum to this section.

The second day was an improvement over the first. Although not as sunny a day as was hoped for, it was sunnier than the first. A towel was used as a cushion to isolate the strain meter from the engine vibrations. The readings were taken much earlier in the day (between 0630 hours EDT and 0700 hours EDT) when the wind was practically nonexistent. A small power boat, SEA SPIDER, was attached to the bow of PANTHALASS to help keep her positioned correctly. The depth was 89 feet. The curves of the second day's results are contained in Figure 2.8.8. The numerical data are in the addendum.

As can be seen in both sets of graphs, not all sets of points represent the characteristic curves drawn between the points. These curves are drawn to show the probable curves which would have resulted had more data points been taken. The graphs also show a significant difference in the amount of horizontal force required to lift the clump. This was probably due largely to the drag force on the spring buoy resulting from the wake of PANTHALASS. This force could have been 80 to 100 pounds or more at higher throttle settings.

The suction of the ocean bottom on the clump was undetermined, but almost certainly was second order to the drag force on the spring buoy.

Conclusions

Based upon the qualitative results, the shape of the experimental curves of horizontal force versus horizontal distance support the theoretical results. Quantitatively the values of force and distance vary substantially from theory. This appears to result from the following sources of experimental error:

Distance was distorted by the uncontrollable leaning of the vertical staff and by the difficulties encoun-

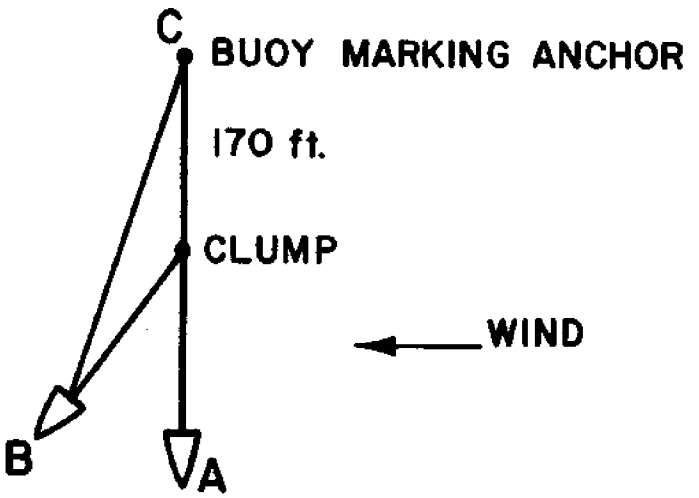

WITH NO WIND THE MEASURED DISTANCE IS FROM A TO C
WITH WIND THE MEASURED DISTANCE IS FROM B TO C

FIGURE 2.8.6

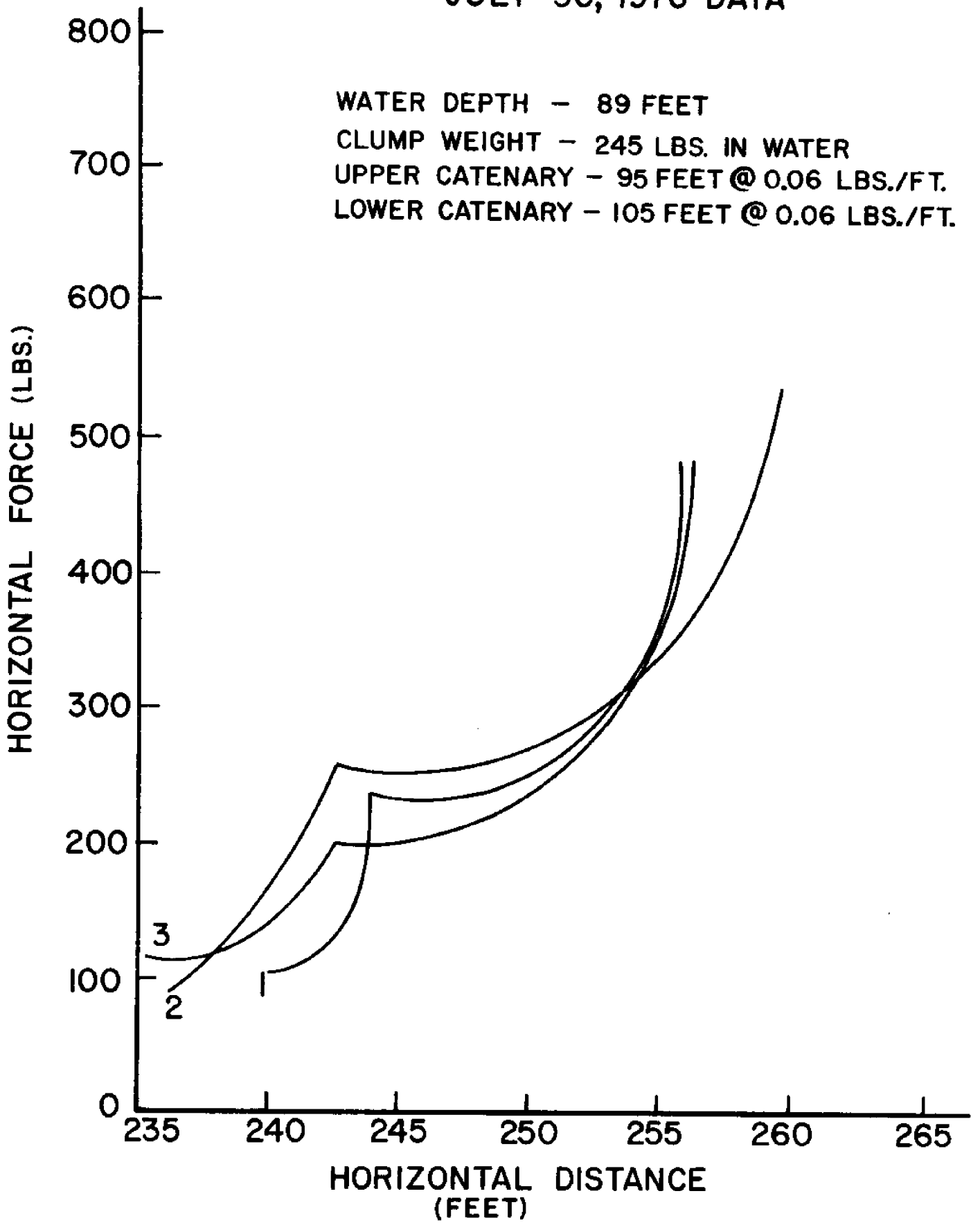
JULY 30, 1976 DATA
WATER DEPTH – 89 FEET
CLUMP WEIGHT – 245 LBS. IN WATER
UPPER CATENARY – 95 FEET @ 0.06 LBS./FT.
LOWER CATENARY – 105 FEET @ 0.06 LBS./FT.
HORIZONTAL FORCE (LBS.)
800
700
600
500
400
300
200
100
0
235
240
245
250
255
260
265
HORIZONTAL DISTANCE
(FEET)
1
2
3

FIGURE 2.8.7

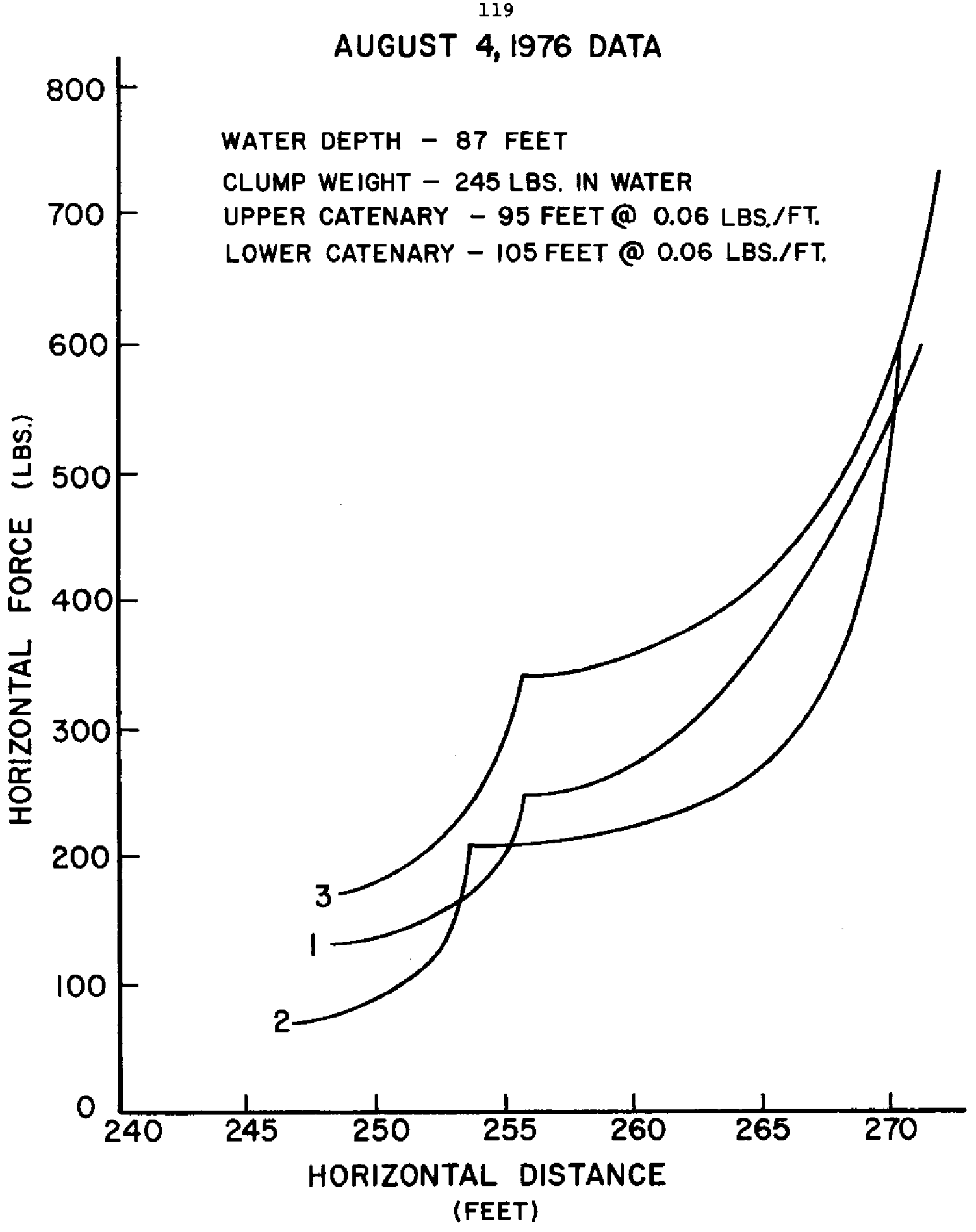
AUGUST 4, 1976 DATA
WATER DEPTH – 87 FEET
CLUMP WEIGHT – 245 LBS. IN WATER
UPPER CATENARY – 95 FEET @ 0.06 LBS./FT.
LOWER CATENARY – 105 FEET @ 0.06 LBS./FT.
HORIZONTAL FORCE (LBS.)
800
700
600
500
400
300
200
100
0
240
245
250
255
260
265
270
HORIZONTAL DISTANCE
(FEET)
1
2
3

FIGURE 2.8.8

tered in maintaining alignment of the boat, spring buoy, and anchor marker.

Force was influenced by the propeller wash (and it is estimated that it may have increased the higher values of horizontal force by as much as 80 to 100 pounds) and the soft bottom which may have varied the breakout force of the clump on various tests.

Recommendations

It would certainly be worthwhile to do this experiment again, benefiting from the knowledge gained here. To this effect many things could be changed. While any new method entails new problems, it is possible that most of the problems encountered here in measuring horizontal distance could be overcome by using a winch mounted on a stable surface (i.e., the dock or land) to apply the horizontal force. The change in distance might be measured by measuring the amount of line reeled in. This would eliminate three of the biggest problems--measuring the distance, lack of boat control, and the drag force on the spring buoy. By choosing a site with a hard bottom, the problem of suction could be overcome. If the sextant method were decided on, improvements could still be made. A better sighting buoy could be devised, and research into better colors for contrast on the sighting pole should be considered. It would also help to position the sighting buoy closer to the boat rather than directly over the anchor. A bright sunny day should be considered mandatory. For measuring horizontal force, the load cell worked great and should be seriously considered.

ADDENDUM TO SECTION 2.8

NUMERICAL DATA FOR JULY 30

Group Number	Meter Reading	lbs of Force	Sextant Reading (degrees)	Distance (feet)
	3.7	117	1.780	241.9
	4.1	134	1.775	242.5
1	6.3	230	1.765	243.6
	6.2	225	1.742	246.7
	7.3	273	1.723	249.3
	9.1	351	1.680	255.3
	2.6	98	1.818	237.0
2	5.8	208	1.783	241.5
	8.8	338	1.683	254.8
	4.8	168	1.775	242.5
3	5.75	206	1.742	246.7
	9.9	385	1.683	254.8
	9.2	355	1.617	264.5
4	9.2	355	1.613	265.1
	11.5	455	1.600	267.2
	12.7	506	1.635	261.7

NUMERICAL DATA FOR AUGUST 4

Group Number	Meter Reading	lbs of Force	Sextant Reading (degrees)	Distance (feet)
	4.1	134	1.733	247.9
	4.8	165	1.698	252.9
1	7.2	268	1.650	259.7
	9.9	385	1.620	264.0
	12.2	485	1.658	258.5
	14.6	589	1.552	274.7
	1.7	75	1.735	247.6
	2.3	85	1.225	249.0
2	3.8	121	1.698	252.7
	5.6	199	1.658	258.5
	7.4	277	1.610	265.6
	10.5	411	1.605	265.4
	14.0	563	1.580	270.4
	52.0	182	1.712	250.8
	68.0	251	1.690	253.8
3	88.0	338	1.677	255.7
	109.0	429	1.607	266.0
	139.0	558	1.586	272.0
	182.0	745	1.585	272.0

2.9 AIRLIFT BAGS

Background

The idea of attaching a deflated bag to a submerged object and then inflating it to lift the object has been used by others with varying degrees of success. The main problem with this method is that as the bag rises the pressure decreases, the air expands, the buoyant force increases, and as a result the object accelerates at an increasing rate. This unstable situation is dangerous to the divers and surface craft, and also may damage the object being salvaged. The method chosen to solve this problem was to build a lift bag with a valve at the top. A diver swimming alongside can control this valve and thus control the rate of ascent.

Technical Description

Very little written material was found on lift bags, but Professor Edgar Biggie of MMA and Mr. Herman Kunz helped a great deal with ideas for this project.

Two bags were built. The first, one-third the size of the second, was a trial bag. It is made of canvas and, when inflated, has the shape of a pear. There is a 2-inch hole in the top with a soft rubber diaphragm across the opening. There is also a plexiglass backing plate for the diaphragm to sit against.

There were a number of trials with the small bag in the indoor swimming pool at the Maine Maritime Academy. The first was unsuccessful because the rubber used for the diaphragm was not flexible enough for a tight seal. The second trial was unsuccessful, but we found out that, even with a flexible rubber diaphragm, the rubber would not seal to the plexiglass that we had used for backing on the orifice. At the third trial, we glued another piece of rubber to the plexiglass and then put on the rubber diaphragm. This seemed to work significantly better.

The way the diaphragm works is that there is a line attached to the diaphragm hanging down inside the bag and out of the bottom low enough so that the diver can pull it at any time. The lifting capacity of the small bag was found to be approximately 100 pounds.

The second bag was made out of rubberized nylon material and canvas. The canvas was used for the top of the bag. The diaphragm was doubled in diameter, making it four (4) inches across. The lifting capacity of the second bag is approximately 650 pounds.

Conclusions and Recommendations

The airlift bags that were built seemed to work very well. In particular, the orifice diaphragm valve was effective in re-

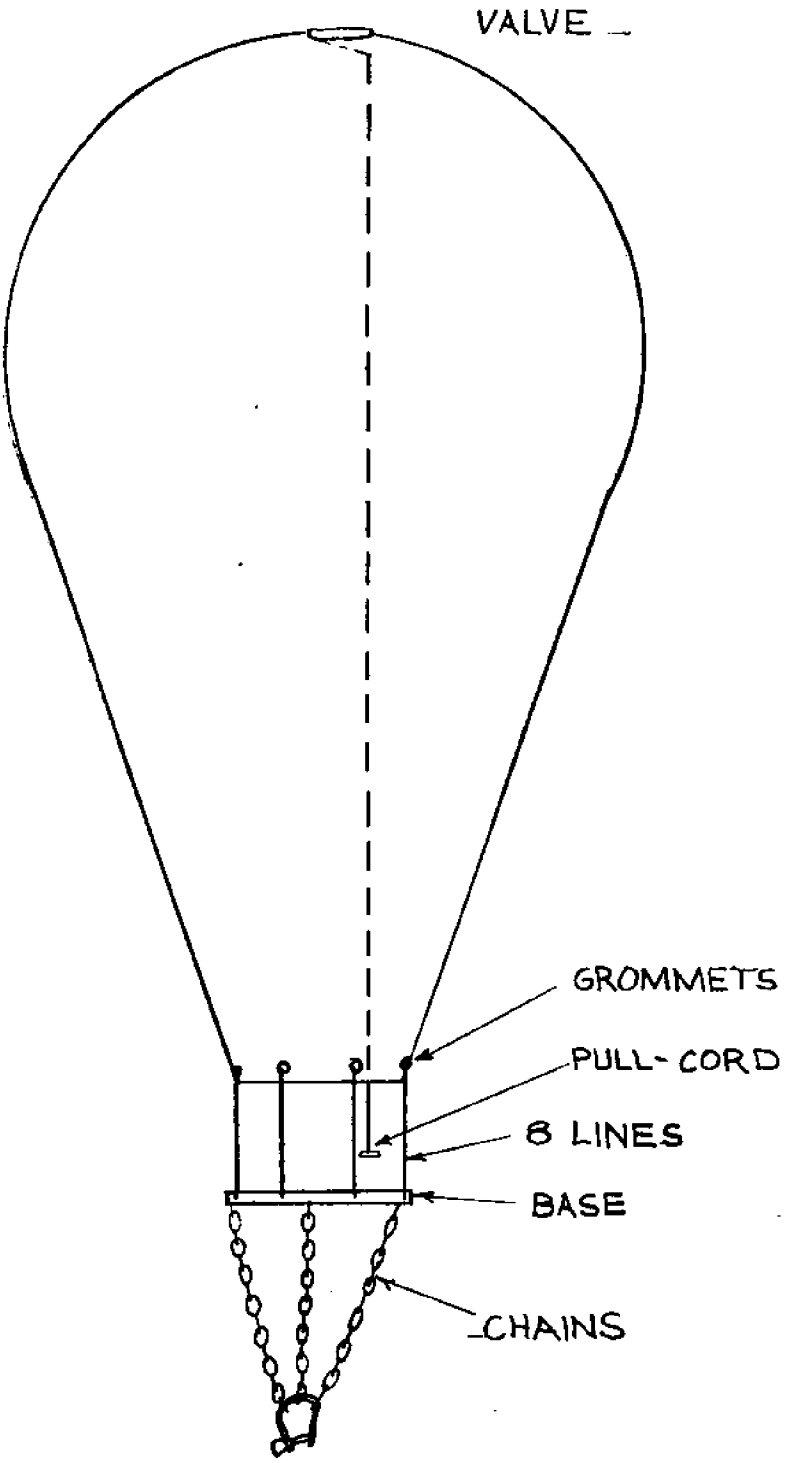

Fig. 2.9.1 Lift Bag

Fig. 2.9.2 Construction of Bag

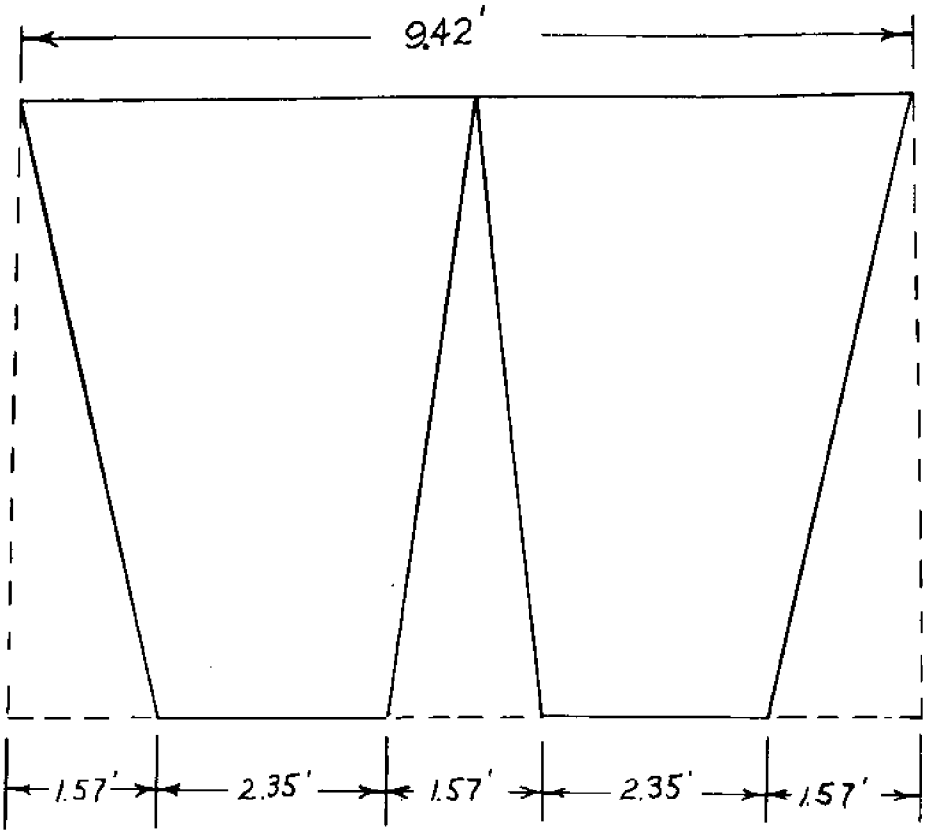

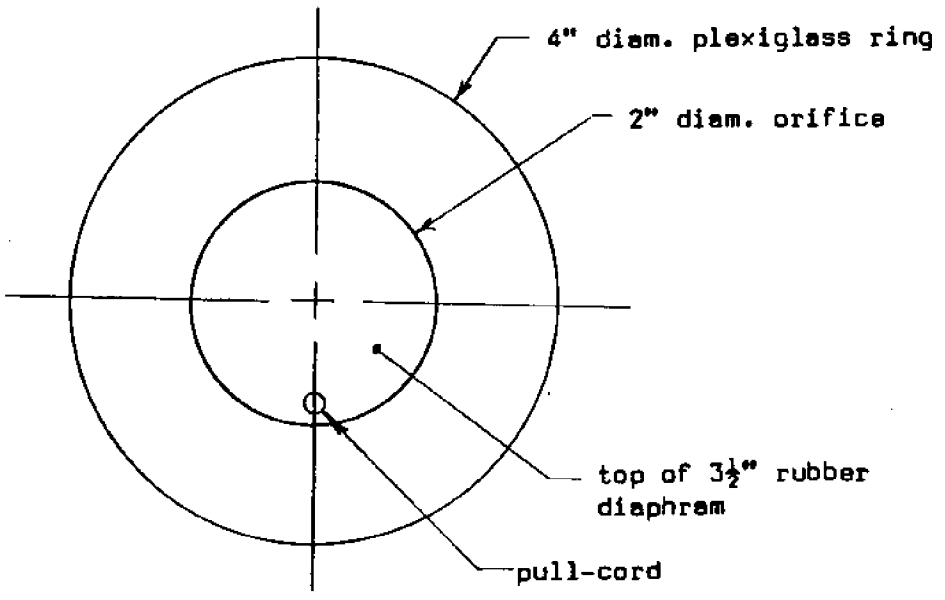

Fig. 2.9.3 Bleed-Off Valve

leasing air. Time and weather did not allow a complete test. It is recommended that this be completed before the left bag is used for salvage work.

3.0 OCEAN SCIENCE PROJECTS

3.1 AN EEL SURVEY OF THE BAGADUCE RIVER

The purpose of undertaking this project was to evaluate the Bagaduce River as a commercial source of eels. In the process the eel life cycle was studied; trap designs and bait that are used in various parts of the world were considered, and several eel traps were built for use in this study.

Most of the eel fishing done today is in northwestern Europe and the Far East. Eel meat is a popular food in both locations, and is commonly fried, smoked, or broiled. Eel is also in demand in many of the large cities of North America. An eel fishery in Maine has the potential of commercial importance to the state's fishing industry.

Background

The North American eel, *Anguilla rostrata*, begins life in the Sargasso Sea, some 300 miles northeast of Bermuda. The young drift north with the Gulf stream and enter rivers, streams and lakes all along the east coast of North America. They stay for five to ten years growing from the elver stage (several inches long) to adults several feet long. At the end of this time they return to the sea to spawn.

Commercial fishing is usually concerned with the adults before they leave to spawn. During this time they may be found in fresh water, salt water estuaries, and possibly even the ocean near the coast. They are active (feed) during the night and hide in dark crevices or bury themselves in mud during the day. Eels both hunt and scavenge, but for the latter are interested only in fresh food. Thus, an eel trapper should bait his traps with fresh bait in late afternoon and haul the traps shortly after daylight. The kind of bait to be used depends on what is available locally, but all of the following have been used successfully: herring, squid, alewives, mackerel, caplin, perch, catfish, smelts, salmon gut, lobster bodies, worms, crabs, clams, shrimp, fresh or salt water mussels, and others.

Sampling Method

In the State of Maine the law requires a license to trap eels and this is stated as a $10 charge for one person or a $25 charge for a person and crew. Since the group was doing a survey on eel trapping in the Bagaduce River, a special permit was granted by the Maine Department of Marine Resources, but the project was limited to twelve traps and was not able to take the eels caught beyond the Bagaduce River or Castine.

The trap design selected was the cone type (see Figure 3.1.1). This includes a cone made out of 1/4" mesh galvanized wire or nylon net which has a large opening at one end and a very small opening at the entrance of the trap.

Four traps were made in the first week, three of which were

Figure 3.1.1. Design of Eel Traps and Pots

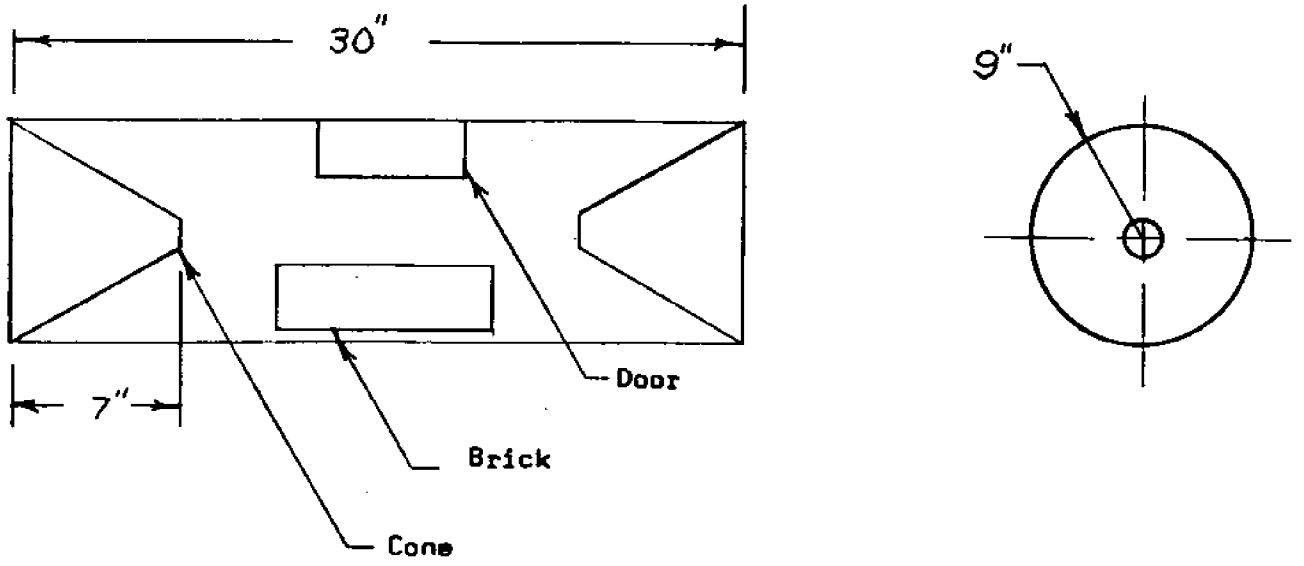

(a) Cylindrical-type Trap, all wire mesh

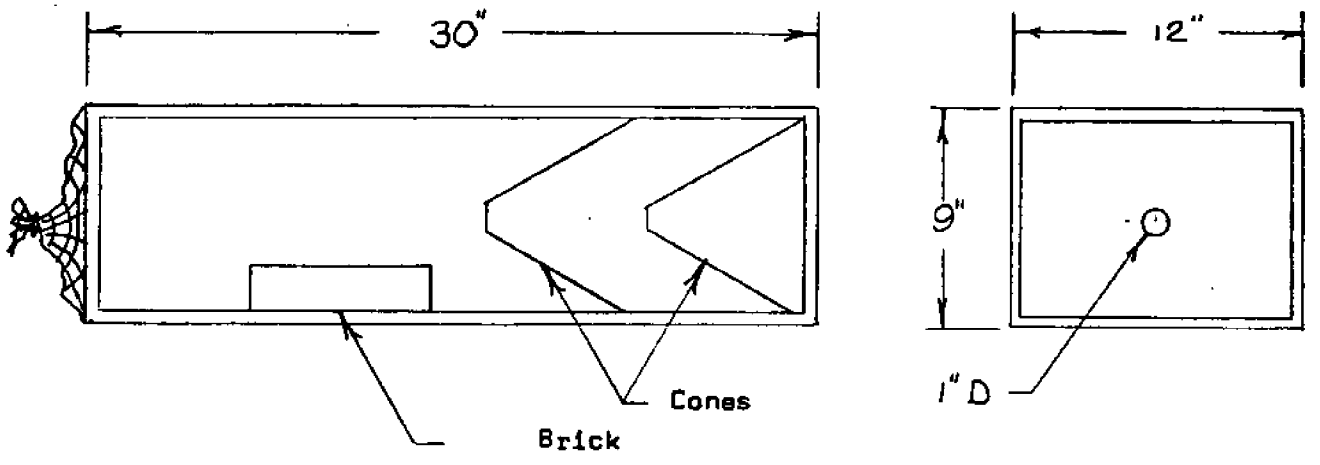

(b) Box-type Trap, wooden frame, wire mesh cover, nylon cones and opening

of the cylindrical type, and the last was a box-type pot (see Figure 3.1.1 for trap design and Table 3.1.1 for materials used. The construction of the cylindrical trap was to take a 30" square of 1/4"-mesh galvanized wire, coil it up and tie off the ends with wire, then to make two cones out of the same material, and attach the cones to the ends of the cylinder.

The box-type pot construction was a rectangular box of 2"-wood straping and 1/4"-mesh galvanized wire tacked to the sides of the box. Then place two nylon cones, one inside the pot and the other at one end (see Figure 3.1.1). Finally, all the traps were tied off to 25' of polypropylene line and a half gallon milk container was used for a buoy. Also bricks were placed in the traps for weight.

The locations of the traps are shown in Figure 3.1.2. The group went upstream as far as the Red Nun buoy past Young Island and by Johnsons Point. The trap set nearest the mouth of the river was in Smith Cove near the millpond. The bait used included clams and crabs.

Results

No eels were caught in any of the traps; however, it is not believed that this is conclusive evidence that there are no commercial-size eels in the river. One local fisherman was of the opinion that the trap cones were too shallow and the opening too large, allowing the eels to freely swim in and out again. Traps were hauled and baited at the same time (usually in the morning) which, as was previously mentioned, is not ideal. One eel about seven inches long was caught in a sampling drag in Smith Cove, and a very large school of elvers was observed in Castine Harbor. Several people living in Penobscot and Brooksville have successfully fished for eels in the Bagaduce, although they have trapped only in the portion of the river above the bridge beyond Johnson Point, an area not investigated. These ideas, taken together, indicate that the trapping results may not be valid. On the other hand, it is understood that one of the local eel fisherman did try trapping in the Young Island-Northern Bay area without success. This could not be verified.

Conclusions and Recommendations

It is the author's opinion that the Bagaduce River needs more research to determine if the river is a good place for eel fishing.

Attempts were made to capture eels in all the places shown in Figure 3.1.2 with no success. One possible reason for the lack of success may have been that the traps were too new. Eels seem to detect smells given off by the trap and they will not enter. Another possible cause for not catching any eels could be the bait that was used, or that the cone opening may have been too large. Trap designs should be further researched, and a successful design chosen for use.

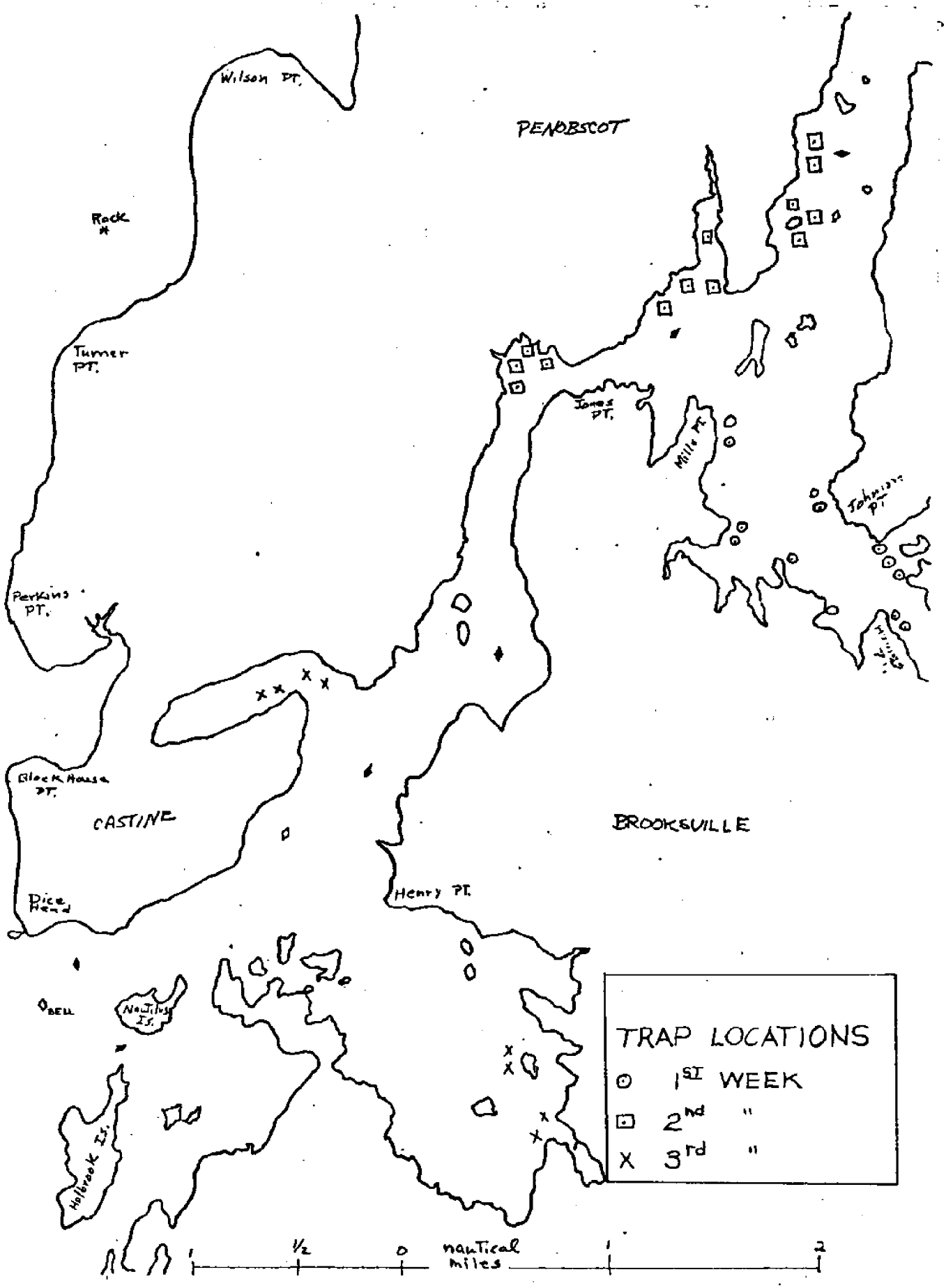
Wilson Pt.
PENOBSCOT
Rock
Turner Pt.
Jones Pt.
Mills Pt.
Perkins Pt.
Block House Pt.
CASTINE
BROOKSVILLE
Henry Pt.
Rice Head
Nautilus I.
Holbrook I.
TRAP LOCATIONS
1st WEEK
2nd "
3rd "
1/2
0
nautical miles
1
2

Figure 3.1.2

Table 3.1.1

Material for Traps

Equipment	Amount	Cost or Place Found
1/4" square galvanized wire	12'	$10
1" wood straping	6'	$2
Bricks	4	Summer Lab
Line	100'	Ship
1/2-gallon milk containers	4	Ship
Small wire	10'	Summer Lab

The traps should be set as late in the afternoon as possible and checked as early the next morning as possible. This is because eels almost never feed during the day. They go after live or freshly killed bait at night.

Market research should be undertaken to determine where eels can be sold, and if the price makes the fishery worthwhile. Part of this study might be the possibility of selling elvers to eel farms in Europe.

Bibliography

1. Forrest, David M., Eel Capture, Culture, Processing, and Marketing, 1976.

2. Perlmutter, Alfred, Guide to Marine Fishes, New York University Press, 1961.

3. Marshall, N. B., The Sea Life of Fishes, The World Publishing Co., Cleveland & N.Y., 1966.

4. Eales, J. G., Eel Fisheries of Eastern Canada, FRB Bulletin 166, 1968.

3.2 THE FEASIBILITY OF COMMERCIALLY GROWING THE DEEP SEA SCALLOP (*Placopecten magellanicus*)

Due to the increase of aquaculture of species in the area we decided that the sea scallop could have a great potential if adapted to an aquaculture setting. As far as can be determined, there has been no attempt to grow this species to a size suitable for commercial use. Due to the success of the Japanese in growing the *Patinopecten yessoinsis*, it was decided to try to adapt some of their methods for use with the deep sea scallop. Also taken into consideration are the methods used for growing oysters in the Penobscot Bay area.

The adolescent form of the scallop was used since the spawning takes place from August until October and no spawn could be obtained in the one-month period of the project.

Background

Scallops have been reared from spat by Dr. Culliney[1] in 1973, and also by Dr. Robert Dow, a director of the Department of Marine Resources of the State of Maine.[2]

The Japanese have achieved a great deal of success in raising their native scallop (*P. yessoensis*). The Oyster Research Institute begins their culture by hanging loose plant fiber in 0.3m x 1m rectangular metal frames covered with nylon mesh. The spat sets in the layers of fiber and is removed when it reaches significant size and is placed in larger mesh nylon cages. Another method used on juveniles is to drill through the ear of the shell, fasten a nylon line to the scallop and fasten these to a line that extends from the surface to the bottom and leaves the scallops suspended. This suspension above bottom approximately halves the growing time and gives marketable shellfish in about two years.[3]

The spawning of the deep sea scallop is controlled by water temperature and food supply. They usually release the spat from late August to October. One can tell when a scallop begins to spawn because the orange (female) or white (male) gonads begin to lose color. Under controlled conditions scallops can be made to release their spawn in July if held in warm water (65° - 66°F). However, either the male or the female will spawn. They both will not spawn together under these controlled conditions. Understandably, further work is needed to successfully and economically obtain scallop larvae.

The spat is released into the water and free-floats until it comes into contact with a smooth clean object such as a shell or a certain seaweed, called eucretea, a bryazoan, a light brown branching moss. The spat will stay attached to this shell or seaweed until approximately 10mm in size. After the spat reaches the 10mm size, it disengages itself and becomes a bottom dweller. Until the scallop reaches the three-inch size, it is

active up to six months per year. The inactive period is during spawning time (August to October) when they also may attach themselves to an object again, and during the winter from January to March.

The deep sea scallop has a life span of approximately ten years. Ratio of meat to size increases in a straight-line relationship.

Their main natural enemies are starfish, parasites and boring sponges.

Technical Description

The larval stage of the scallop is defined as approximately through the first growing season when they are about 4mm in size and have completed their involvement with the bryazoan. The juvenile stage is defined as from the first growing season to the third growing season, or from when they leave the bryazoan until they stop their constant byssal attachment.

Dr. John L. Culliney has successfully cultured spat[1] of the deep sea scallop. Sexually mature scallops collected late in September were stimulated into spawning by raising the temperature of their water by 3 - 5°C. The larvae were reared in glass jars containing seawater filtered to one micron and at 32 parts per thousand salinity. The seawater was changed every two days. The flagellate *Isochrysis galbana* was used to feed the larvae. A combination of this flagellate and *Chroomonas salina* has also been used successfully. Young spat were fed concentrations of approximately 10,000 cells per milliliter. When the larvae reached the pediveliger stage the antibiotic Sulmet (sodium sulfamethazine) was added at 60 ppm to arrest an apparent necrotic disease.

Two groups were reared, one at 15°C and the other at 19°C. Development was rapid with little apparent difference in growth rates. However, after the fifteenth day excessive mortalities occurred in the larvae held at 19°C. After the nineteenth day the 19°C culture mortality rate was almost 100%.

The larvae were separated and held in salinities from 10.5 to 30 ppth for 42 hours. No mortalities were observed. Initial shock was observed at the lower salinities. The first spat was found 35 days after spawning, spat being the metamorphosed larvae. Experiments show that metamorphosis took place more readily with a material such as shells or pebbles available for settling. The larvae appeared very reluctant to settle in culture containers which were bare.

In regard to the mortality rate of the larval population at 19°C, Dickie (1958) found the lethal temperatures for adult scallops ranged from 21° to 23.5°C.[1] Gruffydd and Beaumont (1972) found temperatures of 18°C and above favored bacterial and ciliate growth that decimated their *Pecten maximus* well before metamorphosis.[4]

It may be feasible to collect the spat after metamorphosis rather than culturing the larvae in the laboratory. The spat has been observed naturally attached to the bryazoan eucratea. It may be possible to collect this bryazoan and separate the spat by washing in sea water. The spat could then be contained in cages of 0.5mm mesh (spat-rearing bags).[5]

Another possible method of collecting spat is to place bags of 3 - 4mm mesh filled with monofilament line in areas where scallops are known to exist during and after the spawning season. The spat may collect on the line, thus substituting for the natural settling place of the bryazoan.[5]

After the first growing season (4mm) the scallops leave the bryazoan and begin their byssal attachment to clean, smooth surfaces such as rocks and shells. This lasts until approximately the third growing season or up to about 10mm size. Scallops then begin their nonattachment period of filter-feeding on the bottom. However, some scallops of this size (10mm) have been observed entering oyster trays.[2] This could be another good source of obtaining the scallops to cultivate, planting trays and gathering scallops to work on.

Scallops of the 3 - 4mm size could be taken from the fine mesh bags (spat-rearing bags) and placed in growing trays of a mesh slightly smaller than the size of the scallops. The scallops should be sorted with growth. The scallops should be placed in the largest mesh tray possible to eliminate fouling of the trays' mesh. Commercially available plastic mesh trays such as are now being used in oyster farming seem practical for this purpose. It may be feasible economically to build one's own trays out of wood and plastic or nylon mesh. These trays would be stacked in floating rafts, being kept several feet below the water surface. The Japanese have been growing their native scallops (*Pecten yessoensis*) in trays very successfully.[6]

Temperature plays a major part in the development of scallops. Since a scallop born in a certain year becomes valuable commercially six years later, there seems to be a direct relationship between highs and lows of temperature and scallop landings. As seen in Table 3.2.1, the best temperature seems to be around 46°F. As found by Dickie, low temperatures prolong the pelagic stages when the scallop is most vulnerable to plankton feeders and to wide dispersal by water currents. High temperatures, conversely, are favorable to larval survival, as are low rates of water exchange. Studies have indicated that the number of larvae which settle on their parent bodies is inversely proportional to the prevailing rate of water exchange.[7]

The best situation that can be constructed from the table is that the water should be of approximately average (30 - 33 pp thousand) salinity and at a constant temperature of 46°F plus or minus 0.3°F for the rearing of the juvenile and adult scallop. The area should have good tidal exchange and possibly a discharge of treated sewage to increase the food supply.

Table 3.2.1

Relationship Between Sea Water Temperatures Six Years Earlier and Highs and Lows in Maine's Scallop Landings

Seawater Temperature Year	°F	Scallop Landings Year	(Meats Only) 000 lbs
1913	47.4	1919	73
1927	46.2	1933	1,073
1938	45.1	1944	101
1944	46.5	1950	512
1954	50.2	1960	72

Encyclopedia of Marine Resources, edited by Frank E. Firth, p. 622, Sea Scallop Fishery, Robert L. Dow. Van Nostrand Reinhold Company, New York, N.Y, 1969.

Table 3.2.2

Baird has constructed the various tables to show approximate size and meat yield.

Growth Season	Age	Size	Size	Meat Yield in Ounces
1	1/2 yr	2mm	2.0 in.	.092
2	1-1/2	5-12mm	2.4	.15
3	2-1/2	2.2 in.	2.8	.25
4	3-1/2	2.9	3.1	.36
5	4-1/2	3.5	3.5	.62
6	5-1/2	4.1	3.9	.67
7	6-1/2	4.4	4.3	1.02
8	7-1/2	4.7	4.7	1.23
9	8-1/2	4.9	5.1	1.50
10	9-1/2	5.1	5.5	1.90
			5.9	2.07
			6.2	2.38

The most probable size to harvest would be after the sixth growing season if the scallops grew as they do in natural conditions. However, Baird in 1954 (see Table 3.2.2) shows the results that he obtained in his study, and one could assume that the meat yield as compared to shell size will increase steadily into the eleventh or twelfth growing season, a straight line ratio. This would give a very slow return on the initial investment.

Holding scallops in confinement would have no effect on them. The deep sea scallop has little or no urge to migrate.[8] Since they are filter-feeders, they would not have to move to find food as long as there was good water circulation. If a method of suspension, 6' to 8' above bottom, were used, the threat of starfish, their main enemy, would be eliminated. However, some mortalities were encountered after ten days in this experiment. These could be due to thermal or salinity inconsistencies, as will be explained later in the paper.

The summer program being only a month in length left little time to do truly objective experimental research on scallops. Several methods of experimentation were suggested by very prominent men in the field of marine biology. Dr. John Caddy of the Fisheries Research Board of Canada Biological Station in St. Andrews, New Brunswick, suggested the possibilities of taking sample scallops of the sixth to seventh growing season every week during spawning season (August-September) and opening them to examine their gonads. The gonads should be an orange (female) or white (male) color, and when they begin to lose their color, they are starting to spawn. (It seems that one would have to be very careful because a scallop will often spawn in a bucket or holding tank when taken from its natural environment due to the increasing water temperature.) Three weeks after the gonads begin losing their color, one should set spat bags (described in the introduction). After collection the spat could be placed in growing trays to see if any success will be achieved in this raising technique. Dr. Caddy also suggested the collection and washing of eucratea, the bryazoan that the scallops of one growing season attach themselves to. This would yield scallop spat that one could try to cultivate. Another project suggested by Dr. Caddy was measuring the water intake of the scallop after spawning as *Pecten magellicanus* does increase the percentage of water in its body after October or whenever it does spawn. Dr. Dow of the Maine Department of Marine Resources suggested an experiment to determine the effects of salinity on the native scallops' growth rate. He suggested monitoring scallops in the Penobscot River (by Sears Island) and comparing them with scallops placed in Penobscot Bay where the salinity would be higher. Dr. Dow also suggested setting small mesh trays in hopes of catching the scallops of two to three growing seasons, as one local oyster farmer gets a lot of this size scallops in his oyster trays.

Experimental Technique

Due to the time available as compared to the six years it takes for the development of the scallop, the project was set simply to measure the success of three objectives: 1) to see if scallops could live in confinement; 2) to measure the growth rate (if observable) of the scallops at four different depths; 3) to try to see how the factors affecting the environment (temperature, salinity, storms and fouling) would affect the growth rate.

Sample scallops were about the seven-centimeter size and were obtained from the mud bottom at the mouth of the Bagaduce River where it empties into Penobscot Bay. Four trays were used. Three of the trays held nine scallops each. Each scallop had 25 square inches of room with the vertical sides of each pocket made of spruce, and the horizontal large sides made of approximately 1/8" nylon mesh. Each scallop was separated from one another. The fourth tray contained only six pockets. The trays were set attached to a large piece of granite with the first being about 8' from the bottom, the second 8' above that, the six-pocket tray 8' above that, and the next nine-pocket tray about 8' above that, or 20' below the surface at mean high water and approximately 10' below the surface at an average low water. A small segment of line with a piece of styrofoam was attached to the top tray to keep the trays horizontal. Another buoy and line was attached to the granite block to allow checking the trays while not pulling on them as it would distort them (see Figures 3.2.1 and 3.2.2).

The trays were placed in a horizontal fashion to keep the scallops as they are found naturally. The trays were separated to try to determine which depth was best suited for the scallops. There was a total of 33 scallops in the project. They were located about 300 yards from a treated sewage outlet with a variable 0-2-knot current.

Initial measurements of the scallops were taken when they were set in the trays (see Table 3.2.3). Fifteen days later measurements were taken again.

After the first five days of captivity, the trays could not be located. Four days later they were located approximately a quarter mile upriver. They were then relocated about half a mile from the original site and the gear and the scallops were checked for damage. The racks were numbered from closest to the bottom being #1, next #2, next #2A (the six-scallop rack), and the next #3. Rack #1 had two mortalities, rack #2 had one, rack #2A had none, and rack #3 had one. Also on rack #3 a coating of brown algae was noticed on the nylon mesh and was not noticeable on the others.

The new site was away from any sewage outlet and, when the tide changed, there would be an approximate 1/2-knot current. The depth was approximately 50 feet at mean high water.

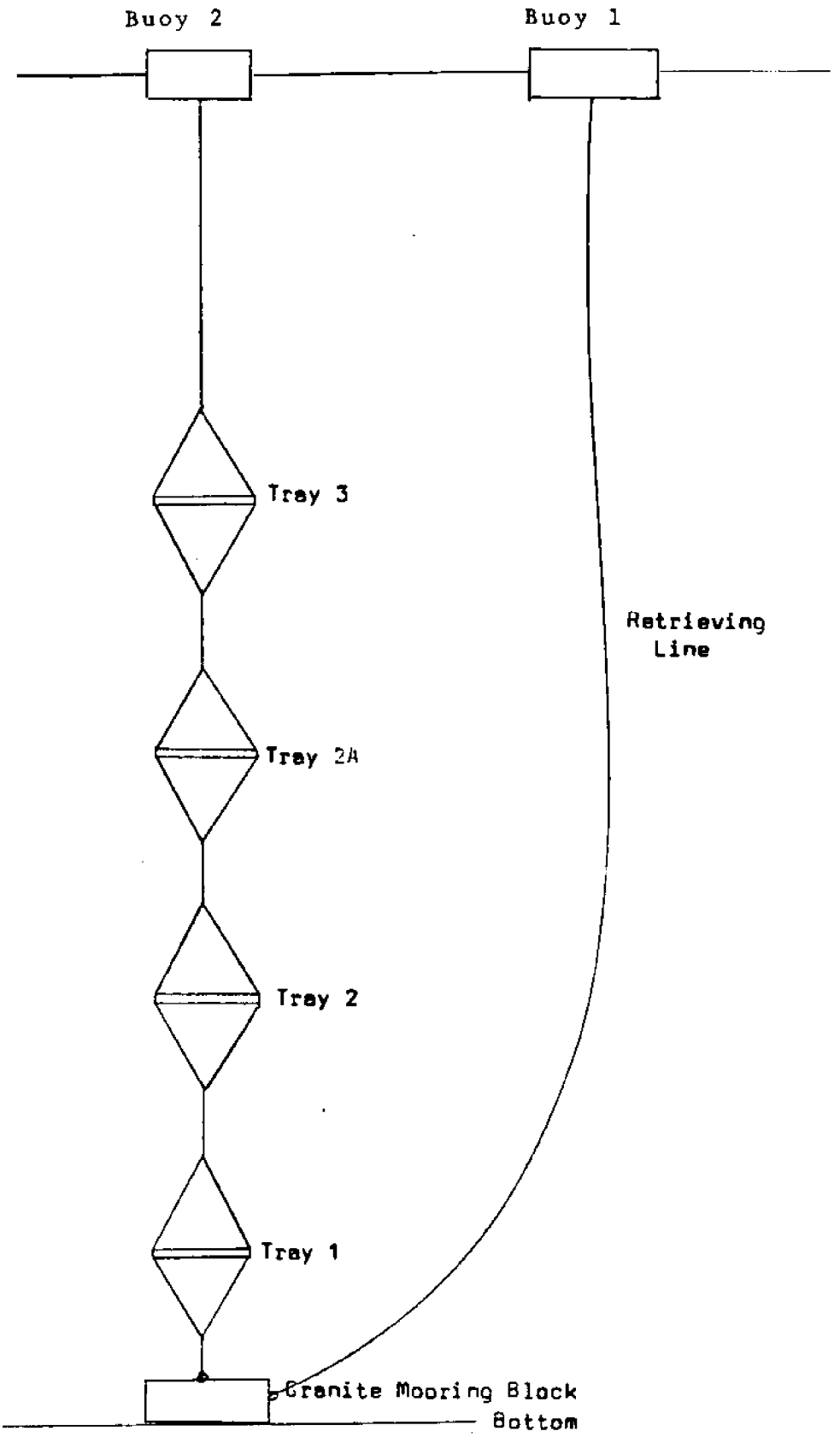

Figure 3.2.1. Scallop-Culture Tray Mooring System

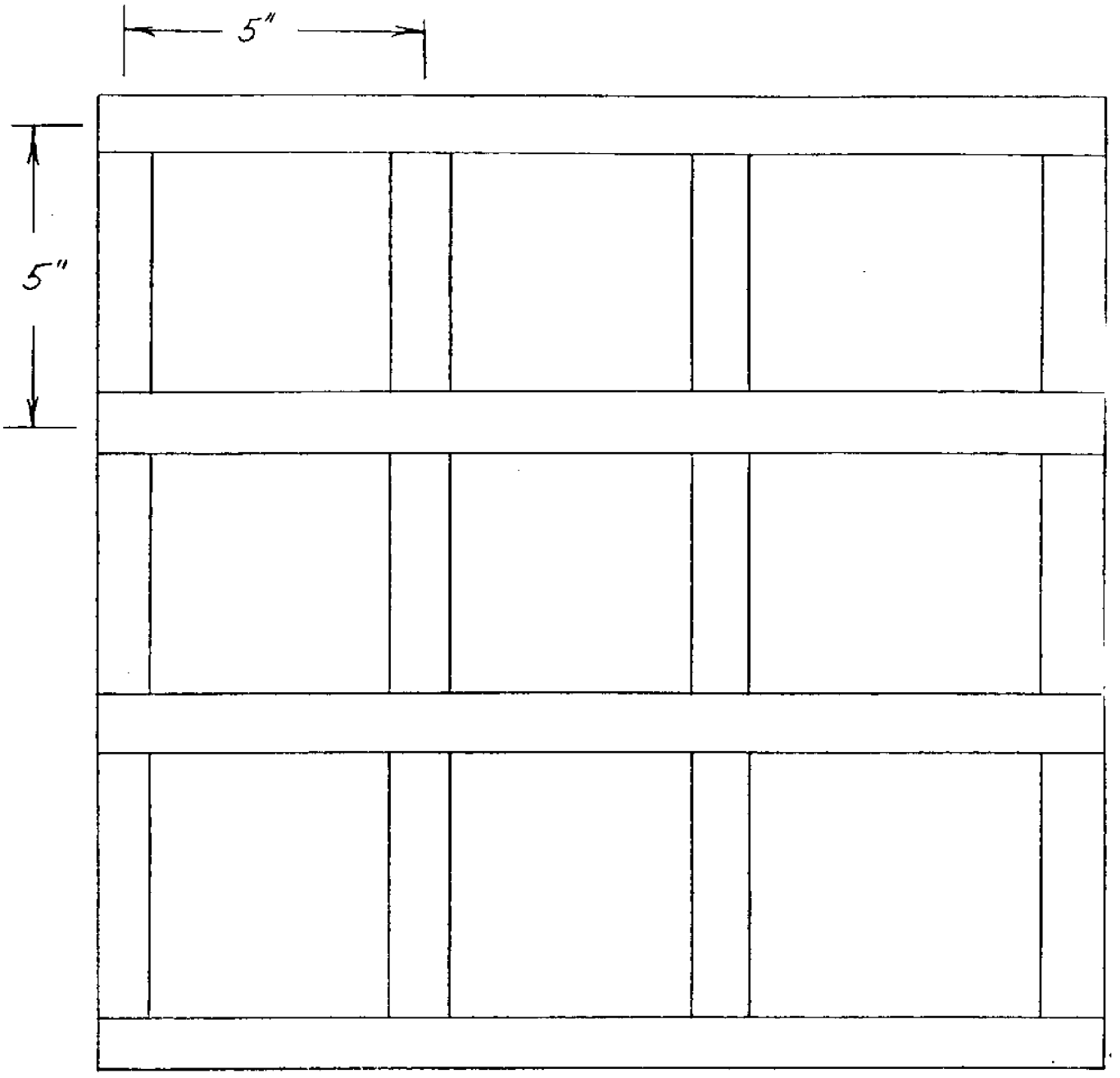

Figure 3.2.2. Frame for Scallop Culture Tray
Constructed of 1" x ½" wood strips, two layers, and covered with nylon mesh

Table 3.2.3

TRAY 1

Scallop	July 21 L x W	August 4 L x W
1	7.5 x 7.4	7.4 x 7.4
2	6.6 x 6.75	6.7 x 6.9
3	6.85 x 6.85	7.0 x 6.9
4	7.50 x 7.25	deceased
5	6.55 x 6.4	6.7 x 6.4
6	7.7 x 7.55	7.7 x 7.6
7	6.85 x 6.7	6.6 x 6.9
8	6.5 x 6.35	deceased
9	7.5 x 7.1	7.4 x 7.2

TRAY 2

Scallop		
1	7.2 x 7.05	7.2 x 7.0
2	6.8 x 6.55	6.85 x 6.8
3	6.35 x 6.15	6.4 x 6.2
4	6.7 x 6.7	deceased
5	6.65 x 6.7	6.5 x 6.7
6	5.95 x 5.75	6.0 x 6.0
7	7.1 x 6.9	7.1 x 7.0
8	7.0 x 7.1	7.15 x 7.15
9	7.4 x 7.5	7.5 x 7.5

TRAY 2A

Scallop		
1	7.55 x 7.2	7.6 x 7.48
2	6.2 x 6.35	6.7 x 6.42
3	6.6 x 6.75	6.8 x 6.92
4	7.0 x 6.95	7.0 x 7.0
5	7.2 x 7.3	7.35 x 7.5
6	7.5 x 7.3	7.35 x 7.32

TRAY 3

Scallop		
1	7.2 x 7.2	7.3 x 7.28
2	5.7 x 5.5	5.7 x 5.55
3	6.95 x 7.0	7.28 x 7.3
4	6.95 x 7.0	7.05 x 7.08
5	7.7 x 7.55	7.7 x 7.3
6	5.5 x 5.45	5.5 x 5.7
7	6.3 x 6.1	6.2 x 6.2
8	6.5 x 6.35	deceased
9	4.2 x 3.99	4.3 x 4.1

Economic Analysis

If a person or a group were to go into the process of growing scallops commercially, the scallop market would have to improve with higher prices. As things stand now, the commercial fisherman must bring in 10 - 12 gallons to make a day's pay (as considered by the fishermen). Using the meat age ratio developed by Baird (see Table 3.2.2) and assuming, as does the Maine Department of Marine Resources, that the average harvested scallop is at least six growing seasons old, the average commercial fisherman shucks approximately 1,440 scallops to get, say, ten gallons per day. (16 oz. per pound x 1 oz. meat per scallop = 16 scallops per pound x 9 pounds per gallon = 144 scallops per gallon x 10 gallons = 1,440 scallops per 10 gallons.) Using an arbitrary price of $14 per gallon, one would make $140 per day before expenses. Let us assume that the commercial scalloper and the scallop farmer have expenses that approximately equal each other. (A dragger's boat, gear, fuel and sternman could offset the cost of the farmer getting the scallop spat, his trays and boat and his helpers.) Say these expenses average $50 a day. This means that the scallop farmer, if he fishes 100 days a year, must shuck approximately 150,000 scallops per year. If he shucks them when they attain the sixth year, that means, when he has his first harvestable crop, he has 900,000 scallops on his farm. In order to get 150,000 per year, he must allow for some mortality, say, 10%, possibly a lenient figure as it could be much more, and he would have to get 165,000 scallop spat per year. The labor alone in obtaining the spat for one year would be enormous.

The market must improve in price to make scallop farming economically feasible, which probably means a decrease in quantity brought in, even with overfishing, will decrease appreciably because scallops from 1 - 3 years old are very quick and, even if small drag mesh size were used, they could escape because of their speed. Also the scallop drag as used today is only 5 - 15% efficient. Only a disaster concerning the deep sea scallop could bring down the quantity appreciably enough to get the price up to where it would be feasible to grow them.

Another major problem is that *Pecten magellicanus* (Gmelin) spat is not available commercially as is the European oyster and the Bay scallop. This is probably the major drawback in the whole operation.

Assuming one could buy scallop spat for $6 per thousand (the price of oyster spat today), it would cost him $1,000 the first year for his spat. Let us assume some things using arbitrary values being as close to realistic as possible, and see how a scallop farmer would venture.[9]

FIRST YEAR

$165{,}000 \times \frac{6}{10}$ cents per spat = $1,000 for spat
Assume each spat $4mm^2$, let him have 10 times his size

for room = $40mm^2$. A square yard (size of tray) = $93,025mm^2$ allows 2,300 scallops per tray and 72 trays. Assume \$2 per $yard^2$ for plastic mesh and \$1 for wood per tray = \$3 per tray x 72 = \$216.
Assume \$20 per stack for 4 stacks = \$80. 20 trays per stack.

SECOND YEAR

165,000 spat x $\frac{6}{10}$ cents per spat = \$1,000.
Assume second year scallops $144mm^2$ in size; let him have 5 times his size for room = 580^2 tray = $93,025mm^2$.
Allow 160 scallops per tray minus 2% mortality = 162,000 scallops. 1,013 trays. Assume \$2 per $yard^2$ plastic mesh and \$1 for wood = \$3 per tray = \$3,039 for trays. Need 51 stacks x \$20 per stack = \$1,020 for stacks.

THIRD YEAR

165,000 spat @ $\frac{6}{10}$ cents per spat = \$1,000 for spat.
Assume third year scallops are 4.84 $in.^2$ in size. Let him have 3 times his size for room = 14.52 $in.^2$. A square yard tray has 1,296 $in.^2$ so that 89 scallops per tray. Minus mortality = 158,760 scallops. 1,784 trays at \$3 per tray = \$5,352 = 90 stacks x \$20 = \$1,800.

FOURTH YEAR

165,000 spat @ $\frac{6}{10}$ cents per spat = \$1,000 for spat. Assume fourth year scallops are 8.41 $in.^2$ in size. Let him have 2 times his size for room = 16.82 $in.^2$. A square yard tray has 1,296 $in.^2$ so that is 77 scallops per tray, minus mortality = 155,585 2,021 trays. However, since one can start using bigger mesh trays, assume mesh cost \$1 per square yard versus \$2. Cost of tray = \$2 per tray. Total cost of trays = \$4,042. Cost of stacks = 102 stacks x \$20 = \$2,040.

FIFTH YEAR

165,000 spat x $\frac{6}{10}$ cents per spat = \$1,000. Assume fifth year scallops are 12.25 $in.^2$ in size. Let him have 1.5 times his size for room = 18.4 $in.^2$. A square yard tray has 1,296 $in.^2$ so that 71 scallops per tray, minus mortalities = 152,473 = 2,148 trays @ \$2 per tray = \$4,296. Cost of stacks 108 stacks x \$20 = \$2,160.

SIXTH YEAR

165,000 spat x $\frac{6}{10}$ cents per spat = \$1,000. Assume sixth year scallops = 16.8^2. Let him have 1.5 times his size for room = 25.2 $in.^2$. A square yard tray has 1,296 $in.^2$ so that is 51 scallops per tray. Minus mortalities = 149,423 = 2,930 trays @ \$2 per tray = \$5,860 = 147 stacks @ \$20 = \$2,940 for stacks.

FIRST YEAR

spat	$1,000	
trays	216	
stacks	80	
labor: 1 man 40 hours @ $3 = $120 x 52	6,240	
interest @ 7%	527.52	$8,063.52

SECOND YEAR

spat	$1,000	
trays	3,039	
stacks	1,020	
labor	6,240	
interest @ 7%	790.93	$12,089.93

THIRD YEAR

spat	$1,000	
trays	5,352	
stacks	1,800	
labor	6,240	
interest @ 7%	1,007.44	$15,399.44

FOURTH YEAR

spat	$1,000	
trays	4,042	
stacks	2,040	
labor (2 men)	12,480	
interest @ 7%	1,369.34	$20,931.34

FIFTH YEAR

spat	$1,000	
trays	4,296	
stacks	2,160	
labor (2 men)	12,480	
interest @ 7%	1,395.52	$21,331.52

SIXTH YEAR

spat	$1,000	
trays	5,860	
stacks	2,940	
labor (2 men)	12,480	
interest @ 7%	1,559.60	$23,839.60

Six-year total investment $101,628.35
Sixth year yield
$14 per gallon 144 scallops per gallon
149,423 scallops = 1,038 gallons x 14 = $14,532.00 or
14% gross yield on investment

After six years, in debt $87,096.35.
But trays are paid off.
After 20 years

spat	20,000	
labor (2 men)	249,600	expenses
	269,600	

Assume 1,038 gals/yr for
20 yrs @ 14 per/gal 290,640
credits 269,600
21,040 after 20 years

So, after 26 years, the farmer still owes $59,433.

Also many things have been ignored here. We are assuming that for 26 years he takes nothing from the company for personal expenses. Also prices have been assumed to be constant. We feel that any increase in the price paid for scallop meats would be offset by an increase in the price paid for his gear and labor.

Labor is the major expense in the operation. After paying his two men, he is left with only $2,100 for other expenses. If the farmer could harvest 500,000 scallops per year (a farm of 3,000,000 scallops), he might make a profit, but he would still have to keep his labor cost down. With all the cleaning of trays and shucking to be done, he might be able to get by with two men. Let us assume he can.

Expenses for 6 yrs	$233,079	
First yr crop	49,000	
After 6 yrs in debt	$184,079	
Average income minus labor and spat per yr		$ 33,520
For 20 yrs		670,400
less debt		184,069
		$486,079

For 26 years $18,704.65 per year.

This would be the only feasible way to do it: a farm of three million scallops, two men for help and buying the spat which cannot be done today. If one could successfully use spat bags, this would be an alternative to buying commercial spat, but we feel sure the cost of buying the bags and collecting the spat would be discouraging.

If one were to try to grow scallops, one would have to apply for a permit from the Maine Department of Marine Resources. As the law now reads, no person may have in his possession more than 10% of the total number of scallops on board less than three inches in size. There would be a public hearing before issuance of the permit, and possibly the permit would be denied because of the commercial fishermen's reaction. One would also

have to obtain permission from the state and the municipality to set out these trays and moorings in the water.

Conclusions and Recommendations

Out of a total of thirty-three scallops held, there were four mortalities, for an average mortality of 12.1%. For a fourteen-day period this is very high, but these four mortalities were found after the scallop trays were lost for four days. They could have been beached or the mortalities could have occurred because of temperature or salinity shocks to the scallops as the trays moved upriver. It was also noticed on the first day they were found that the dead scallops had only the aductor muscle left in the shell and this muscle (meat) had a clear, slimy mass surrounding it. This could have been a result of deterioration. The rim and all organs of the scallops were gone.

There were never any starfish or visible predators found on the trays. It was also observed that it seems to make no difference to the survivability of the scallops if they are placed in the tray with the round, dark shell toward the surface or if the flat, white shell is towards the surface.

The three objectives in this experimental project were: 1) to see if scallops could live in confinement; 2) to measure the growth rate of the scallops; and 3) to see how environmental factors affect the growth rate.

Although there were some mortalities, it is concluded that scallops can be grown in confinement. The growth rate, however, did provide a problem. The measurements were not accurate enough to measure the small growth achieved by these scallops. The only conclusion can be made from the inclusive measurements (see Table 3.2.3) is that the scallops in the upper two trays seemed to have done better than the scallops in the lower two trays. The measurements for the upward growth for the bottom two trays were that seven of the eighteen scallops increased their size or stayed the same. In the top two trays ten scallops of the fifteen increased their size or stayed the same.

As was stated earlier, the top tray had accumulated a brown algae (unfortunately not the same algae as the scallops utilize in their first growing season). To keep the cost of maintenance lower, it is suggested that the trays be kept about twenty feet below the surface to avoid this fouling.

It is believed that a scallop farm could be economically feasible only if the price of scallop meats went up substantially. A person with a large farm (and a large investment) could be successful if he could get the money for capital and could provide himself with the means for support for six years.

This person should hang his trays about twenty feet below

the surface; have an average water temperature of approximately 46°F; an average salinity (30-33 parts per thousand), an area with a good tidal exchange; and an area with a treated sewage outfall to increase the food supply.

It is recommended that further investigation be made into the growth rate of scallops in suspension. If the growth rates increase, as found by the Japanese, the farming of scallops would be much more feasible. Another possibility would be the growing of the bay scallop as the time required to reach maturity is only three years. Local conditions could play an important part in the success of any aquaculture attempt.

REFERENCES

1. Culliney, J. L., "Larval Development of the Giant Scallop *Placopecten magellanicus (Gmelin)*," Biological Bulletin 147: 321-332 (October 1974).

2. Personal conversation with Dr. Robert Dow, Research Director, Maine Dept. of Marine Resources, July 27, 1976.

3. Milne, F. H., "Fish and Shellfish Farming in Coastal Waters," Fishing News, Ltd., 23 Rosemont Ave., West Byfleet, London, England, 1972, pp. 137-138.

4. Gruffydd, L. L. D. and A. R. Beaumont, 1972, "A Method for Rearing *Pecten Maximus* Larvae in the Laboratory."

5. Personal conversation with Dr. John Caddy, St. Andrews Biological Station, New Brunswick, July 14, 1976.

6. Progress in Fishery and Food Science, p. 182.

7. Dickie, L. M., "1955 Fluctuations in Abundance of the Giant Scallop *Placopecten magellanicarus (Gmelin)* in the Digby Area of the Bay of Fundy," Journal of Fisheries Research Board of Canada, Vol. 12, No. 6, 797-857.

8. Baird, F. T., Jr., "Migration of the Deep Sea Scallop *Pecten magellanicanus*," Maine Dept. of Sea and Shore Fisheries, Fisheries Circular No. 14, p. 8.

9. Average sizes and meat yields used are from tables taken from the Encyclopedia of Marine Resources, Sea Scallop Fisheries by Robert L. Dow, Van Nostrand Reinhold Company, New York, 1969.